U.PORTO

FEUP FACULDADE DE ENGENHARIA UNIVERSIDADE DO PORTO

LNEC LABORATÓRIO NACIONAL DE ENGENHARIA CIVIL

Indirect assessment of railway track vertical stiffness

Studies on the application of a recent approach

PEDRO GUILHERME DA SILVA CAMPOS

A Dissertation submitted in partial fulfilment of the requirements for the degree of

MASTER OF SCIENCE IN CIVIL ENGINEERING — SPECIALIZATION IN GEOTECHNICS

Advisor: Professor Doctor Eduardo Manuel Cabrita Fortunato

Co-Advisor: Doctor André Luís Marques Paixão

JULY, 2017

INTEGRATED MASTER IN CIVIL ENGINEERING 2016/2017

DEPARTMENT OF CIVIL ENGINEERING

Tel. +351-22-508 1901

Fax +351-22-508 1446

✉ miec@fe.up.

Edited by

FACULTY OF ENGINEERING OF THE UNIVERSITY OF PORTO

Rua Dr. Roberto Frias

4200-465 PORTO

Portugal

Tel. +351-22-508 1400

Fax +351-22-508 1440

✉ feup@fe.up.pt

http://www.fe.up.pt

Reproduções parciais deste documento serão autorizadas na condição que seja mencionado o Autor e feita referência a *Mestrado Integrado em Engenharia Civil - 2014/2015 - Departamento de Engenharia Civil, Faculdade de Engenharia da Universidade do Porto, Porto, Portugal, 2015*.

As opiniões e informações incluídas neste documento representam unicamente o ponto de vista do respetivo Autor, não podendo o Editor aceitar qualquer responsabilidade legal ou outra em relação a erros ou omissões que possam existir.

Este documento foi produzido a partir de versão eletrónica fornecida pelo respetivo Autor.

Dissertação elaborada no Laboratório Nacional de Engenharia Civil (LNEC) para obtenção do grau de Mestre em Engenharia Civil pela Faculdade de Engenharia Civil da Universidade do Porto (FEUP) no âmbito do Protocolo de Cooperação entre estas duas entidades.

To my parents and my brother,
The reason I am who I am.

All great truths begin as blasphemies
George Bernard Shaw

Acknowledgement

This thesis was made at LNEC (Laboratório Nacional de Engenharia Civil – Portuguese National Laboratory of Civil Engineering) under the guidance of Professor Eduardo Manuel Cabrita Fortunato as advisor and Doctor André Luís Marques Paixão as co-advisor.

In this modest acknowledgement, I present my most sincere thanks to the persons and institutions without whom this Thesis would not be possible:

To my advisor, Professor Eduardo Fortunato, for the opportunity provided on the development of this theme and the interaction and collaboration with other professionals of the area at LNEC. For his guidance, constructive critics and lessons he taught me I am thankful, and finally for the teachings and dedication to all of his students.

To my co-advisor, Doctor André Paixão, for the availability and patience showed through the hours of work along this process. For the opportunity to work closely with an amazing person and professional in the area, with high standards of performance.

To LNEC, in the name of its President Eng.º Carlos Alberto de Brito Pina and to LNEC's Transportation Department, in the name of its Director, Eng.º António Lemonde de Macedo, for all the conditions and means provided during my time in LNEC.

To FEUP and the Civil Engineering Department for all the conditions and teachings provided along the years passed, in the name of its President, Professor João Falcão e Cunha, and its Director, Professor António Silva Cardoso.

To Margarida Milicic for her motivation and support while sharing the same office along this path which led to a thriving friendship.

To my all of my teachers, because they guided me on this path. A special note to the professors António Topa Gomes, Manuel de Matos Fernandes and António Viana da Fonseca for guiding me towards Geotechnics.

To my all my LNEC friends, for their support, motivation and joyful moments, especially Vitor, Daniel, Vânia, Anabela and Ayke.

To all of my friends and especially to Sara, Gabriela, João Teixeira, João Ferreira and Inês for the share, support and amazing moments lived.

To Karen Reinders for her incredible support and sharing through all this journey and for being part of this path.

At last, but not least, to my close family to whom I owe everything and who I am. Especially to my parents who guided and keep guiding me through life and for being my model as Humans and to my brother and best friend for all the share and moments ever lived.

Abstract

It is commonly accepted by the scientific community that the track system modulus has a significant influence on its behaviour and on the control of the deterioration of its geometric quality. Hence, it is important to improve our methodologies to determine the track system modulus, especially where the stiffness changes brusquely, due to the problems that usually appear in these areas.

In the last few decades, new techniques have been developed, however, some are quite difficult to apply, require assumptions regarding the track behaviour and axle loading, thus can lead to different results.

This thesis focuses on a very recent methodology developed at the University of Southampton. This methodology eliminates the necessity to determine the axle loads which is a huge improvement from the previous methods. To do so, it is necessary to use the Fourier Transform to analyse displacements, velocities or accelerations in the frequency domain. However, it is still necessary to increase our knowledge towards this method, to have a solid data basis that helps with the comprehension of the method and its performance in several cases, which can be achieved by studying its application to other case studies.

It was on this context that this thesis was developed, to analyse in greater depth the applicability of this method and to identify strong and weak points it may have. To do so, it was developed a MATLAB script to run this method quickly and efficiently. Firstly, to verify its applicability, the results obtained by the original authors of the method were recalculated, so it was possible to compare the two approaches.

In order to test the method further, it was applied to other case studies, consisting of two transition zones to underpasses where track measurements were carried out in earlier studies. These transition zones were selected aiming at testing a wider range of track stiffness situations with the method. With that objective, an important aspect of these case studies is that one of the transitions zone had under sleeper pads (USP) and the other did not.

KEYWORDS: stiffness, track system modulus, frequency, axle loads, transition zones.

Resumo

A importância que a rigidez vertical tem no comportamento e controlo da deterioração da qualidade da via férrea é reconhecida pela generalidade da comunidade cientifica. Daí a importância de desenvolvimento de metodologias para determinação de parâmetros de rigidez vertical, em especial em locais onde ocorram bruscas alterações de rigidez, devido aos problemas característicos destes locais.

Nas últimas décadas surgiram novos métodos e propostas para a determinação da rigidez vertical da via; no entanto, alguns são de difícil execução e requerem a assunção do comportamento da via e das forças aplicadas pelos comboios aquando da sua passagem, o que pode levar a diversas interpretações.

Esta tese foca-se num método, desenvolvido pela Universidade de Southampton, que elimina a necessidade de determinação das cargas aplicadas pelo comboio às vias, uma evolução significativa relativamente aos métodos anteriores. Para tal, o método requer a transformação de dados de deslocamento, velocidade ou aceleração através da Transformada de Fourier para o espectro das frequências. No entanto, é ainda necessário aumentar o conhecimento relativo ao método em causa, criando bases de dados sólidas que ajudem a compreender a sua adaptabilidade em diversos casos, o que pode ser conseguido com a análise de diversos estudos de caso.

É neste contexto que a tese foi desenvolvida: para analisar com maior profundidade a aplicabilidade do método e no sentido de encontrar as suas limitações e pontos fortes. Para tal, foi desenvolvido um *script* em ambiente MATLAB, capaz de aplicar o método de forma rápida e eficaz. Inicialmente, para verificar a validade do *script*, foram recriados os resultados obtidos pelos autores originais do método, os quais foram comparados com os obtidos a partir do *script*.

De forma a proceder a uma análise mais profunda, o método foi aplicado a outros estudos de caso sobre zonas de transição, em que já tinham sido efetuadas medições para estudos anteriores. Estas zonas foram selecionadas com o objetivo de testar o método numa grande gama de diferentes rigidezes. Nesse sentido, é importante salientar que, nestes estudos de caso, uma das zonas de transição possui travessas com palmilhas e a outra não.

Os estudos são apresentados com recurso a teoria, não só relativa ao método, mas também à forma como os dados foram recolhidos, assim como quaisquer informações consideradas relevantes.

PALAVRAS-CHAVE: rigidez, rigidez vertical da via-férrea, frequência, força aplicada por eixo, zonas de transição.

Résumé

L'importance de la rigidité verticale au niveau du comportement et contrôle de la détérioration de la qualité de la voie ferrée est reconnue par la communauté scientifique en général. D'où l'importance de développement de méthodologies pour déterminer les paramètres de rigidité verticale, en particulier dans des locaux où ont lieu des changements brusques de rigidité, ceci dû aux problèmes spécifiques de ces lieux.

De nouvelles méthodes et propositions pour la détermination de la rigidité verticale de la voie sont apparues ces dernières décennies ; cependant, certaines sont d'exécution difficile et exigent que l'on assume le comportement de la voie et des forces appliquées par les trains, lors de leur passage, ce qui peut amener à diverses interprétations.

Cette thèse se focalise sur une méthode, développée par l'Université de Southampton, et qui élimine le besoin de détermination des charges appliquées par le train sur les voies, une évolution significative par rapport aux méthodes précédentes. Pour cela, la méthode exige la transformation de données de déplacement, vitesse ou accélération à travers la Transformée de Fourier pour le spectre des fréquences. Cependant, il est encore nécessaire d'augmenter les connaissances concernant cette méthode, en créant des bases de données solides qui permettent de comprendre son adaptabilité à divers cas, ce que l'on peut réussir à partir de l'analyse de diverses études de cas.

C'est dans ce contexte que la thèse a été développée, pour analyser plus profondément l'applicabilité de la méthode et afin de découvrir ses limitations et points forts. Pour cela, a été développé un *script* MATLAB, capable d'appliquer la méthode de façon rapide et efficace. Au départ, pour vérifier la validité du *script*, ont été recréés les résultats obtenus par les auteurs originaux de la méthode, qui ont été comparés à ceux obtenus à partir du *script*.

Afin de s'adonner à une analyse plus profonde, la méthode a été appliquée à d'autres études de cas portant sur des zones de transition, où des mesures avaient déjà été effectuées pour des études antérieures. Ces zones ont été sélectionnées avec l'objectif de tester la méthode sur une grande gamme de différentes rigidités. Dans ce sens, il est important de souligner que, dans ces cas d'étude, l'une des zones de transition possède des semelles sous traverse et l'autre non.

Les études sont présentées avec recours à la théorie, non seulement concernant la méthode, mais également la façon comme les données ont été recueillies, ainsi que toute information considérée importante.

MOTS-CLES : rigidité, rigidité verticale de la voie ferrée, fréquence, force appliquée par essieu, zone de transition.

Table of Contents

Acknowledgement v

Abstract vii

Resumo ix

Résumé xi

1. Introduction 1

1.1 Background and Motivations 1

1.2 Main objectives and contributions to achieve 5

1.3 Organization of the work 6

2 Evaluating Support Stiffness 7

2.1 Railway Track Structures 7

2.1.1 The Track Superstructure 9

2.1.2 The Track Substructure 10

2.2 Mechanical Behaviour 11

2.2.1 Beam on elastic foundation 11

2.2.2 Zimmermann-Timoshenko Equations 12

2.2.3 Railway track parameters related to the vertical stiffness 14

2.3 Track dynamics 18

2.3.1 Excitation Sources 20

2.3.2 Dynamic Loads 21

3 Evaluating Support Stiffness 23

3.1 Introduction 23

3.2 Mathematical theory behind the method 23

3.2.1 Beam on an elastic foundation 23

3.2.2 Fourier Transform 24

3.2.3 Calculation example 25

3.2.4 Determination of the track stiffness 28

3.3 Calculation using field data 29

3.3.1 General aspects of the case study 29

3.3.2 Field measurements and data post-processing 31

3.4 Estimation of track support stiffness 34

3.4.1 Interpretation using frequency evaluation 34

3.4.2 Calculation of the track stiffness using the “traditional method” 36

3.4.3 Influence of the railpads 37

3.4.4 Comparison of results 37

3.4.5 Comparison between methods 43
3.4.6 Final Considerations 44
4 Case study: application to two transition zones 45
4.1 Introduction 45
4.2 The railway tracks 45
4.3 The Traffic 46
4.4 The transition zones to underpasses UP1 and UP2 48
4.5 Track support stiffness in UP1 and UP2 53
4.5.1 MATLAB script input data 53
4.5.2 Discretization of the problem 55
4.5.3 Determination of the track support stiffness with displacement data 59
4.5.4 Determination of the track support stiffness with acceleration data 69
5 Conclusions and Final Remarks 81
5.1 Main Conclusions and recommendations 81
5.2 Future works 84
6 References 85
7 Annex A 91

List of Figures

Figure 1-1 – Evolution of the passenger and freight transport in the EU-28 between 1995 and 2014 (EC, 2016) 2
Figure 1-2 - Evolution of the CO2 emission relatively to the year 1990 (EC, 2016) 3
Figure 1-3 - Percentage of CO2 emissions per transportation mode (EC, 2016) 3
Figure 1-4 - Share of the total investment and expenditure on the railways in the USA in 2013 (AAR, 2013). 4
Figure 2-1 - Schematic cross-section of a ballasted track (Selig and Waters, 1994) 8
Figure 2-2 - Representation of the stress transfer system (Esveld, 2001) 8
Figure 2-3 - Superstructure of a ballasted track (Paixão, 2014) 10
Figure 2-4 - Substructure of a ballasted track (Paixão, 2014) 10
Figure 2-5 - Aspect of the track completed (Paixão, 2014) 11
Figure 2-6 - Schematic of the displacement curve on a track over an elastic foundation (T., 2003) 13
Figure 2-7 - Forces and bending moments over an elementary part of the rail 13
Figure 2-8 - Winkler model for rails on baseplates (Teixeira, 2003) 15
Figure 2-9 – Typical load/displacement diagram for the railway track under a static load (Berggren, 2009) 18
Figure 2-10 - Typical track receptances when the rail is loaded with a sinusoidal force (Load between two sleepers - full line, and above one sleeper - dashed curve) versus loading frequency (De Man, 2002) 20
Figure 2-11 - Infinite beam on elastic foundation model considering dynamic loads (Le Pen [et al.], 2016) 22
Figure 3-1 - Rail deflections for different system modulus 26
Figure 3-2 - Displacement amplitude in frequency spectrum for different track system modulus 26
Figure 3-3 - Loading function at a speed of 23.9m/s 26
Figure 3-4 - Displacement amplitude in the frequency spectra 27
Figure 3-5 - Velocity Amplitude in the frequency spectra 27
Figure 3-6 - Acceleration amplitude in the frequency spectra 27
Figure 3-7 – Calibration Curves (CC) obtained with the velocity amplitude (a) using the MATLAB script developed and (b) by Le Pen et al.(2016) 31
Figure 3-8 - - Geophones at the end of the sleepers, (Le Pen [et al.], 2016) 32
Figure 3-9 - Geophones orientation to measure vertical and lateral velocities, (Le Pen [et al.], 2016) 32
Figure 3-10 - Measured deflection data from the Supervoyager at site 1 representing the bogie deflection 33
Figure 3-11 - Numerical FFT obtained for velocity data from a Electrostar at site 4a 33
Figure 3-12 - Numerical FFT obtained for velocity data from a Javelin at site 3a 33
Figure 3-13 - Numerical FFT obtained for velocity data from a Turbostar at site 2 34
Figure 3-14 - Numerical FFT obtained for velocity data from a Pendolino at site 1 34
Figure 3-15 - Numerical FFT obtained for velocity data from a Supervoyager at site 1 34
Figure 3-16 - Calibration curves created with the MATLAB script with the same assumptions than the ones made by (Le Pen [et al.], 2016) 40
Figure 3-17 - Calibration Curves made by (Le Pen [et al.], 2016) 40
Figure 3-18 – Velocity amplitude in the frequency domain for the Pendolino train at: a) 200km/h and b) 80km/h 42

Figure 3-19 – Velocity amplitudes for the first four harmonics of the Pendolino train a) with the base FFT and b) with a high discretization achieved with the introduction of zeros 42

Figure 3-20 – Comparison between frequency and traditional methods 43

Figure 4-1 - Schematic representation of the standard track cross section on embankment (Paixão, 2014) 46

Figure 4-2 - The Alfa Pendular train: a) general aspect and b) schematic representation of the axle spacing and respective axle load estimation (Paixão, 2014) 47

Figure 4-3 - Intercity Express (IE) - a) General aspect and b) schematic representation of the IE and respective axle position and loads estimation (Paixão, 2014) 47

Figure 4-4 – Coal Freight Train (CFT) - a) General aspect and b) schematic representation of the CFT and respective axle position and loads estimation (Paixão, 2014) 48

Figure 4-5 - UP1 (a) and UP2 (b) view (Paixão, 2014, Paixão [et al.], 2015) 49

Figure 4-6 - Schematic representation of the sites UP1 and UP2 and its main characteristics 50

Figure 4-7 - Track cross-section scheme of sites S1 to S4 (Paixão, 2014, Paixão [et al.], 2015) 51

Figure 4-8 - Location of the measurements at sites UP1 and UP2 (Paixão [et al.], 2015) 52

Figure 4-9 – View of the track instrumentation: a) displacements transducers along the studied zone; b) detail of the PSD on the rail web; c) MEMS accelerometers placed on the track and d) Piezoelectric accelerometer. 53

Figure 4-10 - Container freight trains displacements measured with PSD 54

Figure 4-11 - Calibration curves for IE and standard velocity of 160 km/h: a) dx velocity divided by 5000 (df=0.0954); b) dx velocity divided by 500 (df=0.0763); c) dx velocity divided by 500 and introduction of zeros to improve discretization (df=0.0191) 56

Figure 4-12 – Discretization of the 7th harmonic for the AF: a) dt =1/ 5000; b) zeros were added to the previous plot introduced through the Fourier Transform to increase the discretization; c) dt =1/500; d)) zeros were added to the previous plot introduced through the Fourier Transform to increase the discretization. 58

Figure 4-13 – Discretization of the 7th harmonic for the CFT: a) (df = 0.0763) in the dx, the velocity was divided by 500; b) (df=0.0191) to the discretization achieved in a) it was introduced zeros through the Fourier Transform. 58

Figure 4-14 - Calibration curves: a) Alfa Pendular (AP) and Intercity Express (IE) for different number of cars and b) for Coal Freight Trains (CFT) 59

Figure 4-15 - Average values of track system modulus at UP1 65

Figure 4-16 - Average values of track system modulus at UP2 65

Figure 4-17 – Displacement Amplitude Ratios in the frequency spectrum for a) all cars in the CFT and b) the last 7 cars in the CFT. 66

Figure 4-18 – a) Displacements amplitude ratios per section and respective b) Track System Modulus per site for the Alfa Pendular (AP) at UP2 67

Figure 4-19 – CC for acceleration data for the AP, IE and CFT: a) regular shape, b) with inverted axis 70

Figure 4-20 – Accelerations data recorded for: a) AP with piezoelectric accelerometers, b) AP with MEMS, c) IE with piezoelectric accelerometers, d) IE with MEMS. 72

Figure 4-21 – Track system modulus according to the distance to the box culvert for: a) AP, b) IE and c) CFT at UP1 73

Figure 4-22 - Track system modulus according to train type and data provenience at UP1 75

Figure 4-23 – Track system modulus for AP(a), IE(b) and CFT(c) services at UP2 78

Figure 4-24 - Track system modulus according to train type and data provenience at UP2 79

List of Tables

Table 2-1 - Relations between stiffness-related parameters (Teixeira, 2003) 17
Table 2-2 - Overview of the division in frequency range, adapted from (De Man, 2002) 19
Table 3-1 - Train and track data for Pendolino simulation adapted from (Le Pen [et al.], 2016) 25
Table 3-2 - General characteristics of sites (Le Pen [et al.], 2016) 30
Table 3-3 - Characteristics of sites (Le Pen [et al.], 2016) 30
Table 3-4 - Train characteristics (Le Pen [et al.], 2016) 30
Table 3-5 - Amplitude ratios (seventh/third harmonics) 35
Table 3-6 – Track system modulus 36
Table 3-7 – Coefficients of the calibrated 7th order curves 36
Table 3-8 - Average results for system and track bed support modulus 38
Table 3-9 - Absolute differences between both frequency methods amplitude ratios 38
Table 3-10 - Absolute error between the Frequency Method Results obtained by (Le Pen [et al.], 2016) and the Frequency Method Results obtained in this work 39
Table 3-11 - Absolute error between the Sleeper Displacement Method obtained by (Le Pen [et al.], 2016) and the Frequency Method Results obtained in this work 39
Table 3-12 - Ratio of Results between the different methods 39
Table 4-1 - Characteristics of the under sleeper pads, provided by manufacturer, CDM (Paixão [et al.], 2015) 51
Table 4-2 - Main track characteristics 54
Table 4-3 – Main train characteristics (excluding locomotives) 55
Table 4-4 – df according to the number of cars per train for the IE service at 160 km/h 57
Table 4-5 - Results obtained via Traditional method with PSD data (PSD) and Receptance method (R) for UP1 60
Table 4-6 - Results obtained via Traditional method with PSD data (PSD) and Receptance method (R) for UP2 60
Table 4-7 - Track system modulus (k) and track bed system modulus (k_{tb}) obtained with Intercity Express data at UP1 (corresponding to trains 1 to 7) 61
Table 4-8 - Track system modulus (k) and track bed system modulus (k_{tb}) obtained with Alfa Pendular data at UP1 (corresponding to trains 1 to 5) 62
Table 4-9 - Track system modulus (k) and track bed system modulus (k_{tb}) obtained with Coal Freight Trains data at UP1 62
Table 4-10 - Track system modulus (k) obtained with Intercity Express data at UP2 63
Table 4-11 - Track system modulus (k) obtained with Alfa Pendular data at UP2 63
Table 4-12 – Track System modulus (k) obtained with CFT data at UP2 64
Table 4-13 - Errors between the frequency method and the conventional method and the receptance method at UP1 68
Table 4-14 - Errors between the frequency method and the conventional method and the receptance method at UP2 68
Table 4-15 – Coefficients used to construct the inverted CC 70
Table 4-16 – Track System Modulus values for AP, CFT and IE services at UP1 71
Table 4-17 - Ratios between the average results according to train type at UP1 75

Table 4-18 – Track system modulus for AP, CFT and IE services at UP2 77
Table 4-19 - Ratios between the average results according to train type at UP2 80

List of Symbols

Latin symbols

b	width of baseplates
C	ballast coefficient
d	distance between sleepers
d_c	car length
d_n	axle locations
E	Young's modulus
F_n	point load
f	Frequency
f_p	first harmonic frequency
f_q	second harmonic frequency
$\dot{f}$	Fourier Transform
H(x)	Heaviside function
I	moment of inertia of the cross section
i	imaginary number = $\sqrt{-1}$
K	vertical stiffness coefficient
k	track system modulus
k_b	ballast vertical stiffness
k_{bp}	base plate vertical stiffness
k_{eq}	equivalent stiffness of the support
k_p	platform vertical stiffness
k_s	sleeper vertical stiffness
k_{system}	system vertical stiffness
k_{pad}	railpad vertical stiffness
$k_{track\ bed}$	Track bed vertical stiffness
L	length of the beam
l	length of the beam
M	bending moment
m	amplitude ratio
P	Load
P(ω)	load function in the frequency spectrum
p	first harmonic frequency in the frequency spectrum

p(x,t)	distributed load on a beam
p*	stress per area
Q	load
q	second harmonic frequency in the frequency spectrum
q(x,t)	distributed load on a beam
R	radius
r	vertical reaction
S(ω)	shape function in frequency spectrum
s	shape function
T	shear stress
t	time coordinate
v	velocity
W(ω)	vertical displacement in frequency spectrum
w(x,t)	vertical displacement
x	length coordinate
y_{max}	maximum rail displacement
z	vertical displacement

Greek symbols

$\delta(x)$	Dirac function
π	Number pi = 3.14…
ω	Angular frequency
ω_{db}	Circular frequency of the damping system

1

1. Introduction

1.1 Background and Motivations

The growth of the Human population, the climate changes and the present Information Age present new challenges that should be faced correctly, to make sure that best decisions are taken and the opportunity windows are seized. It was the worldwide rising demand for passenger and cargo transportation that captured the attention of decision makers and stake holders in the transportation industry, including railway operators and infrastructure managers, and triggered the need for further development within the industry (Mosayebi [et al.], 2016).

Thanks to the technological development, railway transportation is now again an attractive and competitive way of transportation that offers viable and sustainable solutions.

In Figure 1-1 it is displayed the evolution of passenger and freight transportations in the European Union of 28 (EU 28) according to data provided by the European Commission (2016). It is visible the continuous growth of passenger cars, railways, trams and subways and air transportation, except during the years of crisis that started in 2007, when the transport of goods dropped drastically.

Figure 1-2 shows the evolution of CO_2 emissions relatively to 1990 and show that in most cases it followed the growth of the transport use, except in railways. It shall be noticed that the railways values do not include the indirect consumption of electricity, even though it is impressive that its values dropped even though the use of railways increased (EC, 2016), probably due to the increasing number of electrified lines and upgrade/shift from diesel to electrical powered locomotives.

To comprehend the environmental benefits of railway transportation, Figure 1-3 displays the percentage of CO_2 emissions per transportation mode in the EU28 (EC, 2016). Again, it shall be considered that the indirect emissions that result from the electricity production are not included for railways, even though the train in terms of CO_2 emissions is one of the best transport modes.

However, the advantages of railway transportation are not only environmental and related to emission reduction. It is the land transportation mode that requires less land appropriation for its implementation

and it is one of the lowest number of fatalities per billion passenger-kilometres according to the Eurostat (2016).

Other issues like the noise used to be a disadvantage. However, the comprehension that the track vibration is one of the fundamental factors contributing to excessive rail wear and high levels of environmental noise in nearby residential areas. Several other factors including operation speeds, corrugations, track damping, and soil types also influence the vibrations that occur from moving train wheels. Nowadays a common approach to reduce the track vibration is to use viscoelastic railpads or vibration absorbers (Park [et al.], 2017).

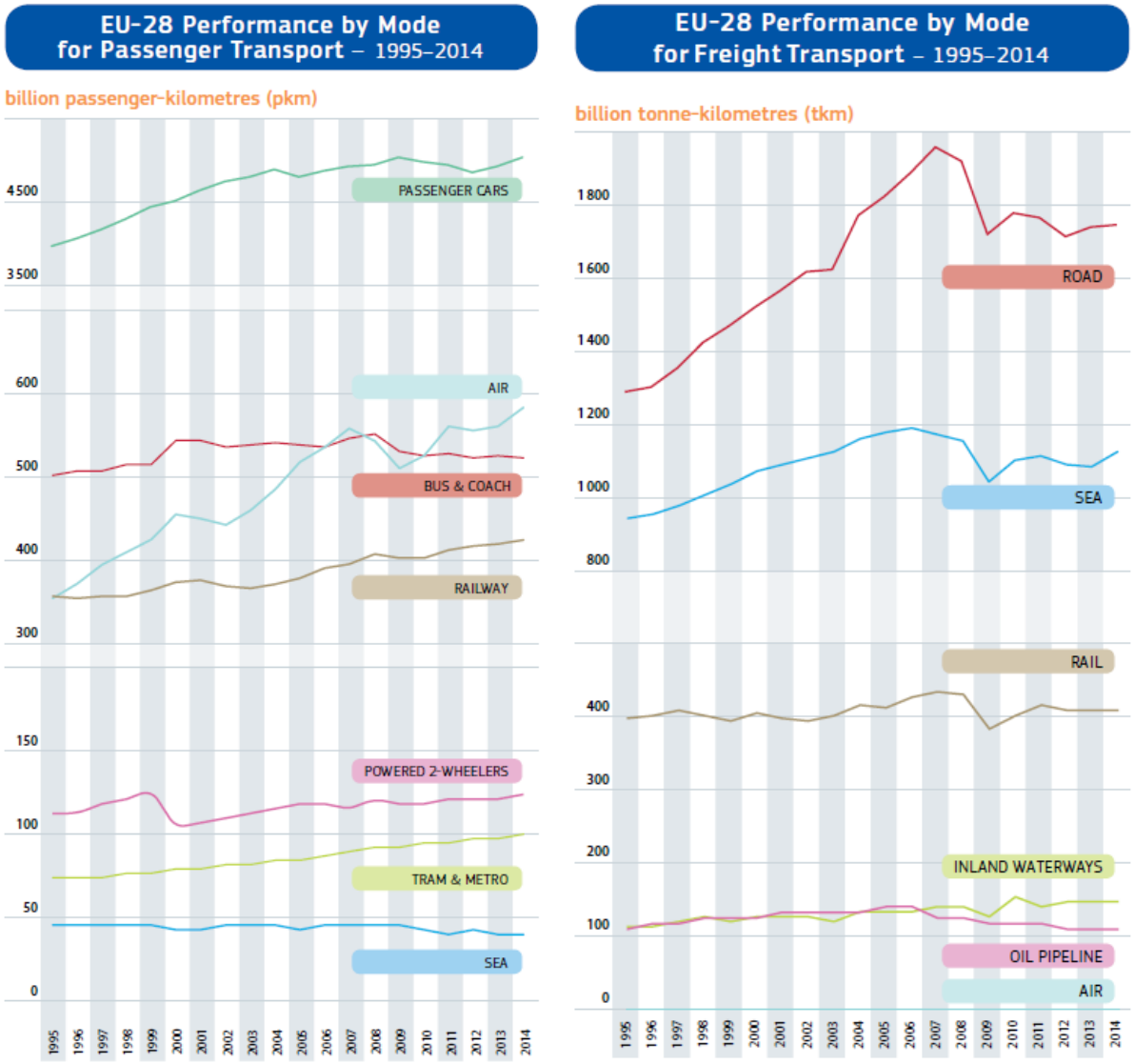

Figure 1-1 – Evolution of the passenger and freight transport in the EU-28 between 1995 and 2014 (EC, 2016)

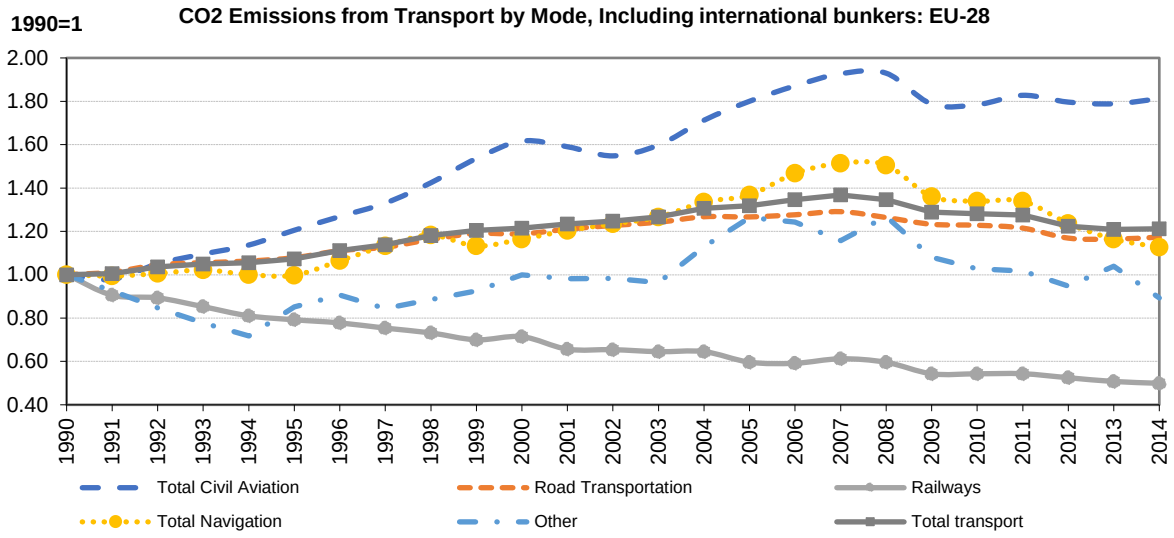

Figure 1-2 - Evolution of the CO2 emission relatively to the year 1990 (EC, 2016)

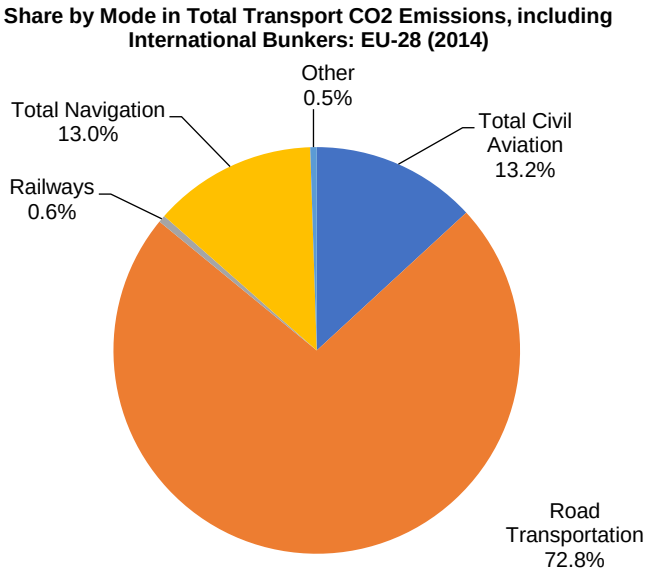

Figure 1-3 - Percentage of CO2 emissions per transportation mode (EC, 2016)

Nowadays 54% of the world population lives in urban areas and according to the United Nations (2014), this value will continue to increase. This creates a lot of challenges in terms of logistics and transportation, not only between cities but also inside the urban areas. The railway, tram and subway networks can be part of the solution to diminish the amount of traffic in the areas and air pollution in the cities. A good urban transportation system is fundamental to improve the life quality in these cities and to reduce traffic jams, a transformation that is already happening in several cities around the world.

The technological advances in this area try to satisfy the new requirements on the rail transport field, regarding to safety, quality of service, environmental efficiency and economic competitiveness are contributing to the optimization of the entire rail transportation system.

A critical component of this transportation system are the railway tracks. Despite the great progresses already achieved, which allowed higher speeds and heavier axle loads, there is still a lot of progress to achieve in several key areas.

The maintenance of the railway track system consumes billions of euros every year worldwide as it can be seen in Figure 1-4 where the amount of money spent in the USA with 2013 data in railways and its different usages is displayed. It can be seen that 66% was spend in the direct bills regarding the activity, such as fuel, staff, between other; 20% was to modernize and expand the capacity of the rail network and 14% of the money was applied in the maintenance of the railroads which is equivalent to 8.9 billion dollars (AAR, 2013).

According to the data in Figure 1-4, the achievement of more efficient maintenance would not only save a lot of resources but also enable higher levels of performance and productivity in the entire railway system (Karttunen, 2012, Khouy [et al.], 2014).

The railway track system has a macro importance. Adequate track support is important not only for the quality and comfort of passengers during the journeys but also to reduce track and vehicle maintenance costs. Poor track support can enable the development of adverse track geometry, this can lead to an increase in the vehicle loading and track damage (Priest and Powrie, 2009). The subgrade also has its role in maintaining satisfactory performance of railway tracks, a role that becomes more important when the axle loads by the trains increase (Selig, 1995).

Figure 1-4 - Share of the total investment and expenditure on the railways in the USA in 2013 (AAR, 2013).

The identification and comprehension why some stretches of railway tracks are not performing properly would results in more cost-effective and preventive maintenance, which may lead to a reduction in the costs in the medium-long term (Le Pen [et al.], 2014).

Both Berggren (2009) and Puzavac et al.(2012) agree that the track stiffness and track deflection measurements are important to understand the cause of track failure and its behaviour. In this scope, it is important to improve our current knowledge towards these topics.

Even though in the last two decades several technologies and methodologies to measure the track support modulus, k, have been appearing around the world, most of them only perform well at low speeds (60 km/h) which may cause disruptions and disturbances of the normal traffic and consequently high costs of such procedures are involved (Berggren [et al.], 2014) and others are difficult to use or of questionable validity (Kerr, 2000).

1.2 Main objectives and contributions to achieve

The main objective of this thesis is to contribute to the comprehension of the structural behaviour of railway tracks and its substructure. To set that goal, it is here proposed the assess the applicability of a recent method to evaluate the track system modulus. Firstly, these studies aim to recreate the work developed by Le Pen, et al.(2016) to evaluate the method and to verify the validity of a MATLAB script designed to be a tool capable of applying the method by itself. It is also a goal of this thesis to increase our knowledge towards this new method by applying it to different situations and to analyse it, identifying its main strengths and limitations. Such studies shall then improve our knowledge towards a recent tool that may help in the future the improvement of insight knowledge regarding the railway track and make the evaluation of the track system modulus easier.

Aiming these goals, this thesis will focus on the following more specific objectives:

- Rewrite the theoretical basis on which the method was developed and to enhance the comprehension towards it;
- Develop a MATLAB script capable to be used to apply the method efficiently and to make easier its application;
- Analyse the results obtained by Le Pen et al.(2016) by applying the developed MATLAB script to try and achieve the same results as the ones obtained by those authors.
- Apply the method to new cases aiming at testing and exploring its limitations. The application of the method to transition zones, while testing different data, like accelerations and displacements, and evaluating the influence of changes in the geometric characteristics of the problem, such as the use of under sleeper pads (USP), meets the needs of this goal;
- Develop and implement improvements to the method that may make its application easier.

Considering the work to be developed, it focusses mainly on the analysis of the method, but using several fields of application and testing environments. The contributions of this work do not start and end with the evaluation of the MATLAB script, but may also help in establishing more appropriate instrumentation techniques that improve the results obtained with the method and which results to expect depending on the way the data is collected. It may also bring improvements to the current way of evaluating the vertical stiffness of railway tracks with all the benefits directly and indirectly related to this issue, regarding the future use of the method.

It is then expected that the research may contribute to the following areas:

- Improve the knowledge, towards the method under test which may provide an alternative to take into consideration to determine accurately and efficiently the track system modulus in different conditions;
- The comprehension and easier determination of the track system modulus through this method may lead to advances regarding the comprehension of the track system of the railways;
- The evaluation and analyses with different data, may help to comprehend the limitations subjacent to some methods of gathering data and limitations and improve its future use as well as the confidence towards the methods;

1.3 Organization of the work

This thesis consists of five chapters. All the chapters start with a brief description of its main goals.

Chapter 2 introduces fundamental theory and basis on which upon the method works. It begins with a description on the railways infrastructure, main characteristics and introduces some concepts like the vibrations of the railway track and its causes. It also introduces several coefficients related to the track stiffness, and the relations between them. It is presented some descriptions of the mechanic behaviour models and theory related to the dynamic behaviour of the track, the basis on which the method under analyse works upon.

Chapter 3 focus on the method under analyse and on the case study already tested by Le Pen et al. (2016), but here, it is presented a different approach since some new assumptions are made and tested. This chapter connects the theoretical basis presented in Chapter 2, and links them to verify the method. It is in this chapter that the case study used by Le Pen et al.(2016) is reanalysed, searching for improvements on the method and validation of a MATLAB script developed here.

Chapter 4 explores new case studies. It starts by presenting a brief description of the sites, the experimental data that was available from earlier studies (Paixão [et al.], 2015), as well as the differences that shall be considered in the method between the new case studies and the previous ones. It tries to evaluate the limitations and the strengths of the method, its applicability on different situations and level of trust we can have upon it.

In the last chapter, Chapter 5, the main conclusions and recommendations achieved are summarized, as well as suggestions for future works.

2

Evaluating Support Stiffness

2.1 Railway Track Structures

Since the beginning of humanity, every organized society has searched for safer, more efficient and quicker way of transportation for goods and people, and it was in this context that railways were developed (Profillidis, 1995). Thus, constant improvement of the rail and track characteristics are crucial to increase the quality of the transportation. Railways are still one of the most important ways of transportation and to keep its development it is imperative to push its boundaries and requirements forward.

To do so, it is crucial that a constant optimisation of its structure and improve the comprehension of what is today a complex system of components and layers (De Man, 2002). The behaviour of the railways is, in fact, dependent on the complex interactions that occur in the track, on which each component must accomplish its function efficiently (Fortunato, 2005). Every part of this whole is required to boost the life cycle of the railway with quality, while reducing the cost of maintenance.

This complex system is composed of a superstructure supported on a substructure. In most cases, the railways track are ballasted track structures (Figure 2-1), but they can also be slab track structures. Since this work is developed on the topic of ballasted tracks, despite the important use of slab track structures, this chapter will focus mainly on the first.

It is, however, necessary to understand the main differences between each other. Slab tracks require more complex design, have high initial costs, the reparations are costly and require hard work when compared to the ballasted track. In a concrete slab track, there is also a problem related to noise which should not be disregarded (Profillidis, 1995). Nevertheless, slab tracks are gaining popularity mainly due to its extremely cheap and easy maintenance with minimal disruption of traffic, long service life cycle, reduced weigh and it produces almost no dust (Indraratna [et al.], 2011).

Ballasted tracks are the most common railway structure worldwide and can be divided in two parts, a superstructure and a substructure, which will be analysed later. It's important to refer that the boundary between substructure and superstructure is not consensual among specialists and the ballast bed is often considered the first layer of the substructure.

In ballasted tracks, the rails normally rest on sleepers that are embedded on a compacted ballast layer. One of the main problems of this type of structure is the progressive deterioration of ballast with traffic,

the breakage of sharp corners, repeated grinding and wearing of aggregates, and also the crushing of the particles that compose the ballast, when heavily loaded. Excessive degradation requires frequent maintenance and routine checks which leads to traffic disruption. The presence of crushed particles and fines can lead to the reduction of hydraulic conductivity. There is also a higher amount of dust and the substructure is relatively thicker than with slab tracks (Indraratna [et al.], 2011).

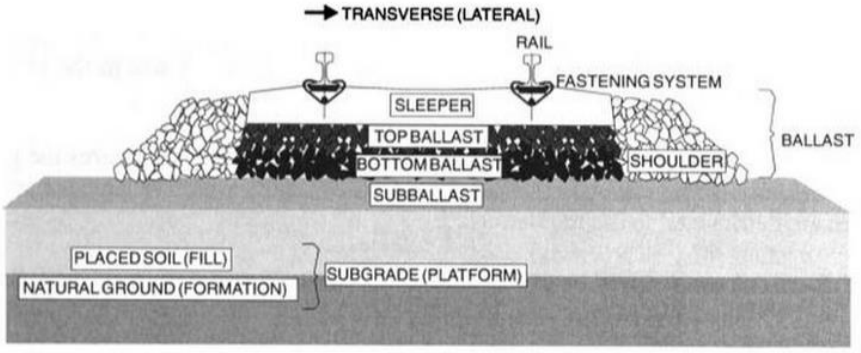

Figure 2-1 - Schematic cross-section of a ballasted track (Selig and Waters, 1994)

However, the lower construction costs, easier maintenance work, simpler design and high hydraulic conductivity turn the ballasted track into a very competitive railway track structure, compared to other solutions. As already stated, this work focuses mainly on ballasted railway tracks, on which rails, fasteners, bearers and ballast bed comprise the superstructure. The main function of the superstructure is to transfer and spread the wheel loads over a bigger area creating a fast reduction of the stresses with depth, so the substructure is not overstressed, as well as to carry the wheel in the right direction and to protect the substructure. Without disregard of the other functions, the distribution of the wheel load is especially relevant when we check that the mean stress at the wheel-rail interface is around 100 kN/cm^2; in the transition between sleeper and ballast stresses are about 30 N/cm^2 can be expected and a few meters below, in the subgrade, the stresses are normally neglectable as we can see in Figure 2-2. The ordinary substructure is composed of the sub-ballast and the subgrade (or platform), if not on a civil engineering structure such as a bridge or tunnel, where is introduced alterations of the vertical stiffness which are related with the alteration of the configurations of the track (Paixão, 2014).

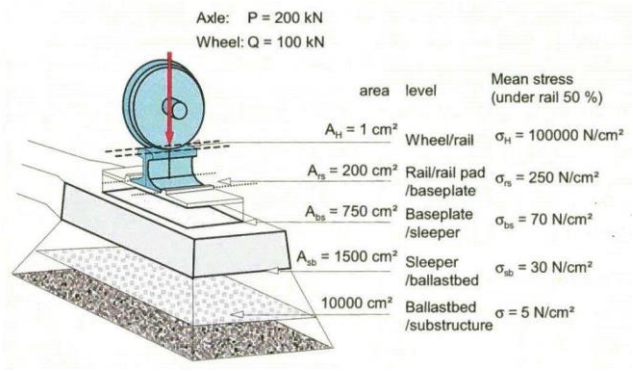

Figure 2-2 - Representation of the stress transfer system (Esveld, 2001)

2.1.1 THE TRACK SUPERSTRUCTURE

As already alleged, the superstructure (Figure 2-3) is composed of rails which are connected by fastenings to the sleepers. These are supported on the ballasted bed.

The rails work as an infinite elastic beam providing a smooth-running surface while guiding the wheel sets in the direction intended and have a flat bottom that enables the transmission of the vertical load to the sleepers. The lateral and longitudinal loads are also sustained by the rails which transfer stresses to the underlaying layers. The rails also work as electrical conductors for the signalling system (T., 2003). The most common profiles are the flat-bottom, grooved and block but their typical shape is characterized by a head and a foot connected through a slim "web". The mass is a typical property of the rails, which are made of steel (De Man, 2002). Rails can be connected by bolted joints which is achieved with drilled plates or welding. Inevitable discontinuities are present in the joints between two sections, which create vibrations (Indraratna [et al.], 2011), a phenomenon that will be analysed later. However, nowadays such vibrations due to the joints are somewhat limited due to the increase use of continuous welded rails (Esveld, 2001). Even though the initial costs are higher, there is a return in capital due to the low maintenance needed. This system also provides more stability in the track, enabled higher running speeds and the introduction of high speed services, request less power consumption and offers a much higher comfort level to the passengers. The development of track defects and equipment fatigue is much slower as well.

The fastening system includes all components with a function of connection between structural elements. They can be direct if they link the rail and the baseplate (also railpad) to the sleepers or indirect if they connect the rail to the baseplates and the connection to the sleepers is made by these. Usually made of steel, the fasteners ensure a steady connection between the rail and sleepers that limits any kind of movement. Coach screws, clip bolts, rigid sleeper clips and spring washers and nuts are the most common components (Indraratna [et al.], 2011).

The protection of the sleepers from the impact of passing trains is made with the railpads, which are components that decisively influence the overall track stiffness. A railpad is a small slice of an elastic material and is placed between the rail base and sleeper, block or slab, which characteristics depend upon its material (De Man, 2002). Soft railpads allow the distribution of the stress from the rails over more sleepers. This softness also protects the sleepers from wear and impact damages while providing electrical insulation and supress the transmission of high frequency vibrations. Wooden sleepers may not require railpads since they introduce these characteristics by their own. Moreover, stiffer railpads give a more direct transmission of the loads, including the high frequency vibrations (T., 2003).

All the components mentioned above rest on sleepers, positioned on the horizontal plane right below the rails, which main functions are to transmit the different loads from the rail down to the ballast, sustain the alignment of the track, the gauge and the inclination, while providing electrical insulation to the rails from one rail to the other (T., 2003). Sleepers are commonly made from wood, concrete or steel and the choice between these materials is often made according to the price.

Ballast is a coarse stone layer that supports the track providing a high compression resistance. It keeps the track levelled and aligned when tamped around the sleepers, which transmit large stresses to the ballast. These stresses are too high to be directly transmitted to the substructure, so one of the ballast main functions is to spread and reduce the stresses. Finally, the ballast has also some important functions as drainage and capacity to add elasticity to the railways (T., 2003). It should also guarantee the damping of most of the train vibrations (Profillidis, 1995).

To ensure the lateral stability of the track, ballast stones are commonly angular with rough edges and uniformly graded, which makes it a granular structure easily rearranged and facilitates its maintenance. To control the desired mechanical behaviour, both laboratory and on-site tests are carried out on the material before placing it on the track. Fatigue behaviour, hardness, attrition resistance and dimensions are the main parameters controlled (Profillidis, 1995).

2.1.2 THE TRACK SUBSTRUCTURE

In Figure 2-4 the aspect and the identification of the several layers of the substructure, such as the sub-ballast, capping layer and other soils that compose the subgrade are presented, and in Figure 2-5 it is displayed the final aspect of the track.

The sub-ballast is the transition layer between the ballast composed by large particles and the fine-graded subgrade. Its function is to spread the loads to the lower layers and reduce the stresses caused by the trains. The sub-ballast must prevent the interpenetration between different layers, the migration of fine particles from the sub-ballast to the ballast can contaminate this layer and affect its drainage capacity. In addition, to protect against freezing and thawing cycles, the sub-ballast also serves as a waterproofing and draining layer that prevents the rise of the water and contributes to direct the rainfall-runoff to the drainage systems (Paixão, 2014).

Sometimes it is even used an extra layer, the capping layer, to give the profile wanted of the track bed. The capping layer is used when it is considered that the foundation soil does not have sufficient quality, which can lead to track failure. (Selig, 1995). As a result of being the border between the soil and the above structure, the capping layer must enable the adequate compaction of the sub-ballast layer, while ensuring the correct conditions to accommodate the stresses transmitted by upper layers.

The substructure is usually not involved in maintenance operations. To minimise such events, the subgrade can be stabilized by one or some of the several ground improvement techniques such as vibratory compaction techniques, lime-cement columns, prefabricated vertical drains, between others (Indraratna [et al.], 2011).

Being the border between the soil and the above structure, the placed soil must enable the adequate compaction of the sub-ballast layer, while ensuring the correct conditions to accommodate the stresses transmitted by upper layers. Besides, an adequate drainage is required to ensure the safety even in the eventual rise of water level, so the construction materials must be of superior quality.

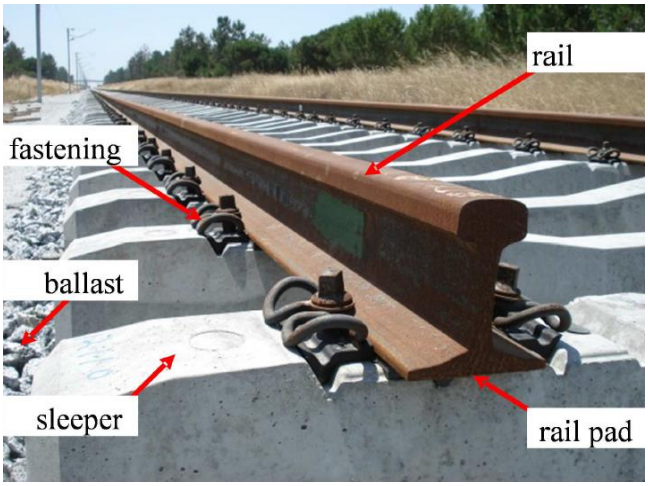

Figure 2-3 - Superstructure of a ballasted track (Paixão, 2014)

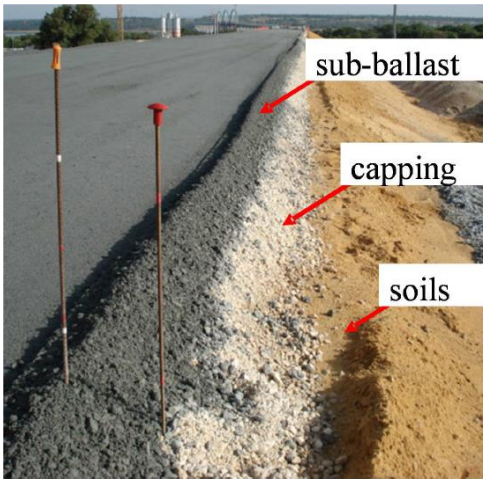

Figure 2-4 - Substructure of a ballasted track (Paixão, 2014)

Figure 2-5 - Aspect of the track completed (Paixão, 2014)

2.2 Mechanical Behaviour

The comprehension of the railway track as a complex structural system started to be imperative with the expansion of the railways all over the world. To do so, it was introduced by Winkler as a support model on which the track consists of two parallel continuous beams representing the rails, supported by sleepers regularly spaced. To represent the structure on which the rail support, Winkler model uses springs so at each point of the support, the compressive stress is proportional to the local compression.

Considering that the Winkler model is a proven method, and to consider\ the stiffness of the ballast and substructure, it will be used the known model "beam on elastic foundation". The importance of these concepts requires a proper introduction.

2.2.1 BEAM ON ELASTIC FOUNDATION

The equation for the original theory of an infinite Euler-Bernoulli beam over an uniform elastic foundations can be shown to be (Frýba, 1979):

$$EI\frac{\partial w^4(x,t)}{\partial x^4}+\mu\frac{\partial w^2(x,t)}{\partial t^2}+2\mu\omega_{db}\frac{\partial w(x,t)}{\partial t}=\delta(x-vt)P \tag{2-1}$$

with the following boundary conditions:

$$w(0,t)=0;w(l,t)=0;\ \left.\frac{\partial w^2(x,t)}{\partial x^2}\right|_{x=0}=0;\ \left.\frac{\partial w^2(x,t)}{\partial x^2}\right|_{x=l}=0 \tag{2-2}$$

and initial conditions:

$$w(x,0)=0\ ;\ \frac{\partial w(x,t)}{\partial t}\Big|_{t=0}=0. \tag{2-3}$$

The symbols used in the above equations and through this research have the following meaning:

- x - length coordinate that runs from the left to the right of the beam;
- t - time coordinate;
- w (x, t) - vertical displacement at point x and time t;
- E - Young's modulus of the beam;
- I - moment of inertia of the beam cross section;
- μ - constant mass per unit length of the beam;
- ω_{db} - circular frequency of the beam damping system;
- P - load over the beam;
- l - length of the beam;
- v – speed of the moving load.

Neglecting inertial and viscous effects, and considering that:

$$\delta(x)=\frac{dH(x)^*}{dx} \tag{2-4}$$

*Heaviside function, more information is available in (Mikusiński and Sikorski, 1961).

is the Dirac function, which expresses the concentrated load as showed in equation (2-5):

$$p(x,t)=\delta(x)P \tag{2-5}$$

It is possible to rewrite equation (2-1) as follows:

$$EI\frac{\partial w^4(x,t)}{\partial x^4}+kw(x,t)=p(x,t) \tag{2-6}$$

Where k is the track system modulus (MN/m^2), EI is the bending stiffness of the rail (MN.m^2) and p(x,t) the distributed loading on the beam.

2.2.2 ZIMMERMANN-TIMOSHENKO EQUATIONS

Regarding the importance of equation (2-6) in the context of this analysis, it will be presented the theoretical basis that leads to the formula.

Assuming that the rails have infinite length and that the foundation upon where they are supported is elastic, according to Winkler:

$$kw=r \tag{2-7}$$

being r the vertical reaction applied by the terrain on the track. In Figure 2-6 it can be seen the displacement curve caused by the wheels loads according to this formulation.

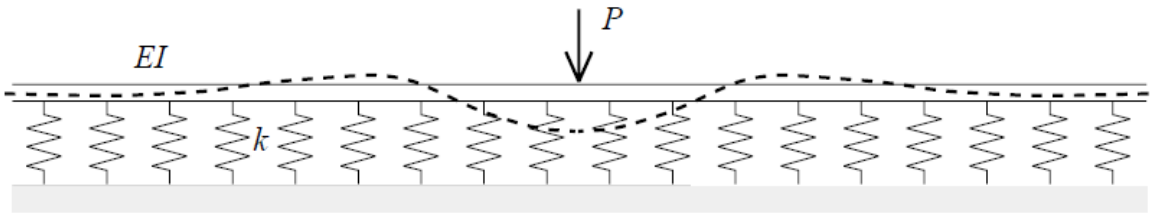

Figure 2-6 - Schematic of the displacement curve on a track over an elastic foundation (T., 2003)

Figure 2-7 is a schematic representation of the actions that actuate in an elementary stretch of the rail. It is the bending moments (M), the shear stress (T) and the ballast vertical reaction (r) which acts like an elastic support that are applied to the section. The variations of the forces dT and dM appear from the equations:

$$dT=r\,dx\;;dM=T\,dx. \tag{2-8}$$

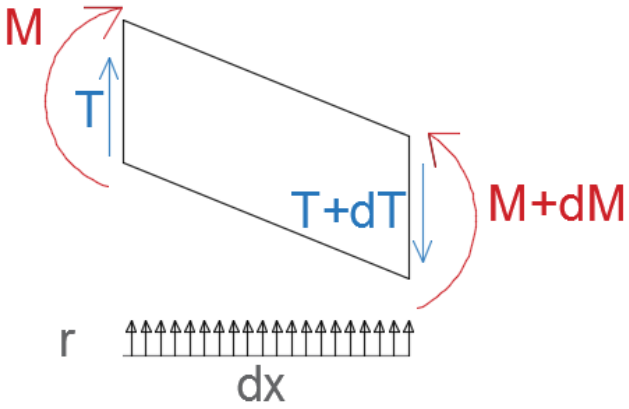

Figure 2-7 - Forces and bending moments over an elementary part of the rail

The expression of the displacement curve radius (R) can be written as (Maynar, 2008):

$$\frac{1}{R}=-\frac{d^2z}{dx^2} \tag{2-9}$$

and one another, relating the bending moment with the radius:

$$M=\frac{EI}{R} \tag{2-10}$$

Assembling the equations (2-8), (2-9) and (2-10)we obtain:

$$\frac{M}{EI}=-\frac{d^2z}{dx^2} \tag{2-11}$$

and knowing that:

$$\frac{dM}{dx}=T;\frac{d^2M}{dx^2}=\frac{dT}{dx}=r=k\,z \tag{2-12}$$

and that the derivation of the equation (2-11) is:

$$\frac{d^2M}{dx^2}=-EI\frac{d^4z}{dx^4} \tag{2-13}$$

we can immediately obtain from the equations (2-12) and (2-13):

$$EI\frac{d^4z}{dx^4}+kz=0 \tag{2-14}$$

To consider loads in the equation, we can add $Q.\delta(x)$ to the right side of the equation, which can lead to:

$$EI\frac{d^4w}{dx^4}+kw(x,t)=q(x,t) \tag{2-15}$$

considering that both z and w represent the displacement of the rails and that $Q.\delta(x)=q(x,t)$.

The solutions to the previous equation are:

$$y(x)=\frac{Q}{2kL}e^{\frac{x}{L}}\left[\cos\left(\frac{x}{L}\right)+\sin\left(\frac{x}{L}\right)\right] \tag{2-16}$$

$$M(x)=\frac{Q}{4}Le^{\frac{x}{L}}\left[\cos\left(\frac{x}{L}\right)-\sin\left(\frac{x}{L}\right)\right] \tag{2-17}$$

With:

$$L=\sqrt[4]{\frac{4EI}{k}} \tag{2-18}$$

2.2.3 RAILWAY TRACK PARAMETERS RELATED TO THE VERTICAL STIFFNESS

The vertical stiffness is one of the key subjects in this analysis and there are several different parameters and criteria to evaluate the railway track stiffness, each of them with their own theory. To introduce a global panorama over this issue, this sub-chapter is going to focus a little on each of them and then try to relate them all, since this is an important theme in the context of the present work.

2.2.3.1 Ballast coefficient

As already stated, the first studies on the mechanical behaviour of railway tracks were developed by Winkler (1867), who stated that the continuous support rail system works as a continuous beam uniformly supported over a compressible layer, a model similar to the one in Figure 2-8. To characterize the vertical opposition of the system to acting loads, it was proposed to consider the proportionality between the displacements and stresses:

$$EI\frac{d^4z}{dx^4}+p(x)=q(x)\ ;\ p^*(x)=C\ z(x) \tag{2-19}$$

where p* is stress per area and C a constant known as the ballast coefficient (N/mm^3).

Considering a base with b as width and substituting:

$$p(x)=b\ C\ z(x) \tag{2-20}$$

in the previous equation, it comes out:

$$EI\frac{d^4z}{dx^4}+b.C.z(x)=q(x) \tag{2-21}$$

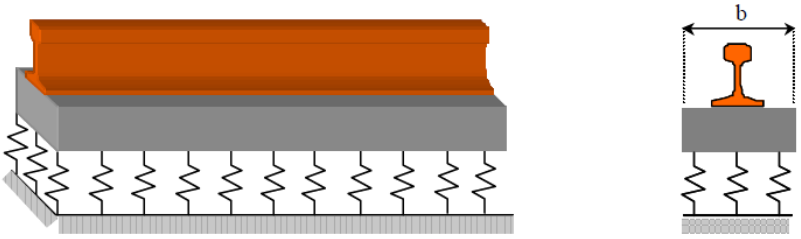

Figure 2-8 - Winkler model for rails on baseplates (Teixeira, 2003)

2.2.3.2 Track modulus

This coefficient appears to characterize the stiffness of the track by length unit, which mathematically results in

$$p(x)=k.z(x) \tag{2-22}$$

where k is the track modulus (N/mm^2).

This coefficient can be easily understood as it is equivalent to a uniform load p(x) applied on the rail which produce a certain displacement. This leads to the model presented in the equation (2-15), which means that the sleeper's area does not influence the result, thus depending only on the vertical stiffness of the track.

2.2.3.3 Equivalent stiffness coefficient

The equivalent stiffness coefficient is one of the most used parameters to characterize the elasticity of the track. The concept behind this parameter is the theory with discrete elastic supports which considers the rail supported by springs. Each spring is supposed to recreate the effect of each sleeper and its stiffness. However, applying the discrete elastic support method requires solving a huge number of algebraic equations (Teixeira, 2003) which is not practical neither easy to do. Considering an equivalent stiffness (k_{eq}) which represents the vertical stiffness of the railway track calculated as shown in the next expression:

$$\frac{1}{k_{eq}} = \frac{1}{k_b} + \frac{1}{k_p} + \frac{1}{k_{bp}} + \frac{1}{k_s} \tag{2-23}$$

Where:

- k_{eq} is the equivalent stiffness of the support (N/mm);
- k_b is the ballast vertical stiffness;
- k_p is the platform vertical stiffness;
- k_{bp} is the base plate (also known as railpads) vertical stiffness;
- k_s is the sleeper vertical stiffness.

2.2.3.4 Vertical stiffness coefficient

Despite the generalized use of the previous coefficients, the development and necessity led to the adoption of a coefficient capable to quantify the stiffness of the track as it is perceived by the vehicles when running on the rails (Teixeira, 2003). That was the beginning of what is established today as the vertical stiffness (K) which is the ratio between the wheel load acting on one rail (Q) and the maximum rail displacement (y_{max}) under that wheel, in a static analysis.

$$K = \frac{Q}{y_{max}} \tag{2-24}$$

The dynamic vertical stiffness characterizes the behaviour of the track when subjected to the vertical dynamic excitations of the wheels over the rail. This study in the frequency domain is easier with the receptance. As stated the receptance is the inverse of the stiffness and can be written as a complex number where the real part is the inverse of the dynamic vertical stiffness while the imaginary part is the phase angle between the load and the response signal (De Man, 2002).

2.2.3.5 Discussion on the stiffness parameters

Mathematically, it is easy to understand the relations between the different parameters and its physical meaning, as shown in Table 2-1.

Table 2-1 - Relations between stiffness-related parameters (Teixeira, 2003)

Parameter	Schematic Representation	Support Reaction	Relation with K
Ballast Coefficient (C) MN/m^3	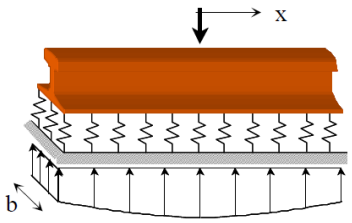	p*(x) (kN/m^2) b=A_t/b	$C = \sqrt[3]{\frac{K^4}{64.EI}\frac{d}{A_t}}$
Track Modulus (k) MN/m^2	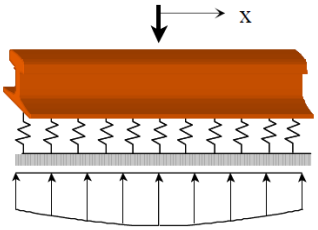	p(x) (kN/m) p(x)=p*(x). b	$k = \sqrt[3]{\frac{K^4}{64.EI}}$
Equivalent stiffness Stiffness (k_{eq}) MN/m	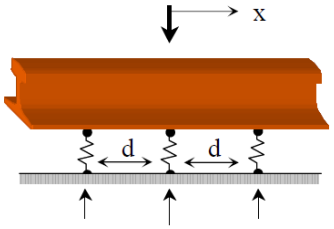	R(x) (kN) R(x)=p(x). d	$k_{eq} = \sqrt[3]{\frac{K^4}{64.EI}}d$

As it can be seen in Table 2-1, the coefficients are related to each other, and they can be related towards each other through the following equations:

$$k = C.\frac{A_t}{d} \quad (2\text{-}25)$$

$$k_{eq} = k.d \quad (2\text{-}26)$$

$$k_{eq} = C.A_t \quad (2\text{-}27)$$

It can be found more information and the deductions of the previous statements in (Teixeira, 2003).

Investigations through the last century proved that the theories where the rails are continually supported, have good results in practical and that they are a good approximation of reality (Teixeira, 2003). However, these models have some limitations when the track presents variations on its geometry or characteristics (Fortunato [et al.], 2013).

Although the track is a complex system composed of different elements, the difficulty in determining the characteristics of each element and linking those characteristics with the stresses suffered by the infrastructure, lead to the use of a single stiffness parameter. The same line of thought was followed in the theories of elastic discrete supports and rail support, leading to global parameters of resistance that are a simplification of the real stresses and behaviour (Teixeira, 2003).

It is also important that the comprehension of the vertical stiffness of the track as a constant is an approximation, since the curves load/deformation (Figure 2-9) of the track are non-linear which proves the existence of a damping factor. This non-elasticity has many sources such as the ballast, under sleeper pads, load amplitude, between others. Teixeira (2003) stated that defects on the sleeper support can have an important role on this non-elasticity.

This is a phenomenon that should be taken into consideration when analysing the vertical stiffness since it creates an inherent inaccuracy subjacent to all the methods if not considered in the models. Even though, the measurement of the vertical stiffness through the vertical deformation introduced by a punctual load on the rail is still one of the simpler and more accurate methods (Teixeira, 2003).

Since most of the experimental measurements to determine the ballast coefficient, track modulus and vertical stiffness coefficient are made on the rail, in fact, the final result is a measurement of the stiffness of the entire system. This means that the calculation of the vertical stiffness parameters are made indirectly thought relations of the elastic foundation theory (Teixeira, 2003).

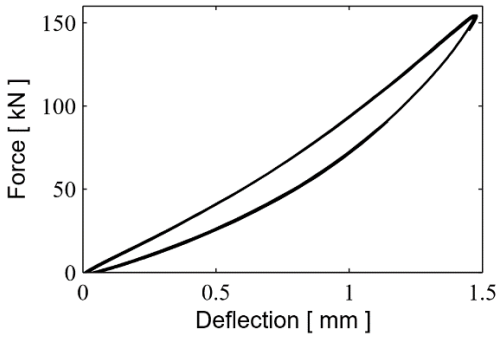

Figure 2-9 – Typical load/displacement diagram for the railway track under a static load (Berggren, 2009)

2.3 Track dynamics

All structures, thus railway track structures as well, will respond to any form of loading they are exposed to (De Man, 2002).

With the aim of understanding the structural behaviour, it is imperative to link the distinct types of loading to the several types of responses obtained. The dynamic behaviour is a key issue in this research since in railways the loads are not constant over space and they change from place to place over time according to a certain velocity and acceleration. This leads to responses from the structures that change over time and can be considered as a sum of vibrations.

The response of the railway track to the wheel loads covers a spectrum that goes from low-range frequencies (0-40 Hz), passing through mid-range frequencies (40-400 Hz) until the beginning of high range frequencies (400-1500 Hz).

In fact, studies tried to link the range of frequencies to the parts of track that plays a main role in the frequency range and the consequences of such vibrations on passengers and structures like showed in Table 2-2.

The dynamic properties of the track can be studied through the evaluation of the structure's response under the application of loads. For example, sinusoidal loads can excite the track on frequencies up to 200 Hz with hydraulic cylinders (T., 2003) or impulse loads can be applied by instrumented hammers (Paixão, 2014). This allows the determination of the receptance which is the ratio between the deflection and load in the frequency domain. This means that, as it can be seen in Figure 2-10, the receptance and

thus track stiffness are dependent on the frequency of the load (T., 2003). To evaluate the dynamic properties and the track response at high frequencies, the excitation of the rail is normally made with instrumented impact hammers (De Man, 2002). The evaluation of the track response in this case can be made with accelerometers (Paixão, 2014).

Figure 2-10 depicts an example of a receptance curve that relates the track receptance with the loading frequency of the excitations. The maximum peaks in the figure represent the resonance frequencies of the structure.

Table 2-2 - Overview of the division in frequency range, adapted from (De Man, 2002)

Frequency Range	**Low**	**Mid**	**High**
Thresholds (Hz)	0-40	40-400	400-1500
Part of the Track	Substructure	Superstructure Excluding Rail	Rail
Human Perception and Discomfort			
Local Resident	Vibrations and Contact Noise (Buildings)	Radiated Sound /Noise	Radiated Sound/Noise
Passenger	Vibrations and Contact Noise (Vehicle)	Radiated Sound /Noise	Radiated Sound /Noise
Structural Damage			
Track	Damage of Substructure and Engineering Structure	Damage of Superstructures	Damage of Rails
Vehicle	Damage of Carriages, Bogies, Axles and Wheels	Damage of Wheels	Damage of Wheels

The first peak appears at frequencies around 50 to 300 Hz and it is the result of the vibration of the track on the ballast bed. The upper part of the superstructure works as a mass and the ballast as a spring resulting in resonance a little above the 100 Hz as it can be seen in the figure (T., 2003).

The second resonance is usually found in frequencies between 200 and 600 Hz and is the result of rail bouncing on the railpads which work as springs between the sleepers and the rails while the ballast works as a damping mechanism (T., 2003).

The highest resonance is often called pinned-pinned resonance and it appears slightly before 1000 Hz. It occurs when the wavelength of the bending waves of the rail is twice the sleeper spacing.

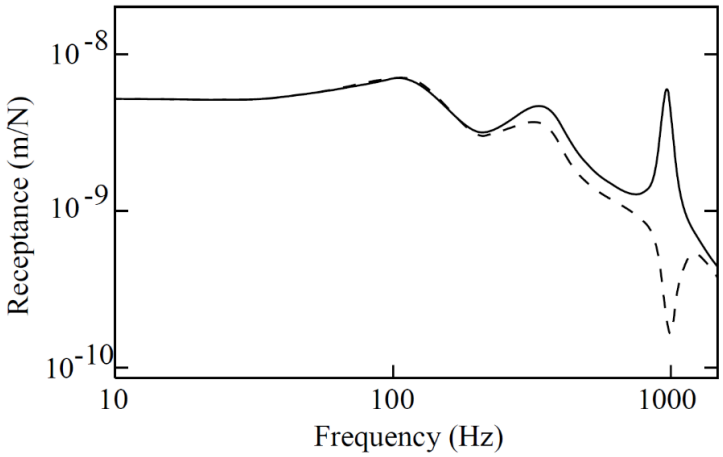

Figure 2-10 - Typical track receptances when the rail is loaded with a sinusoidal force (Load between two sleepers - full line, and above one sleeper - dashed curve) versus loading frequency (De Man, 2002)

There is also a lower resonance that may appear in low frequencies when the track and its substructure vibrates on a ground layer.

The thresholds displayed in Table 2-2 were established by Knothe and Stichel (2016), who made a connection between the frequency range of vibrations and the railways components. It could be concluded then, that the low-frequency behaviour is determined by the substructure while the superstructure components are the ones who induce mid and high frequency vibrations.

2.3.1 EXCITATION SOURCES

There are many sources that induce oscillations, vibrations or even noise in the railway track system, the vehicles and its surroundings. Those sources can be as different as geometric errors or irregularities in the position of the rails, defects in the track geometry quality and the stiffness of the track.

The excitations induced in the track can lead to the deterioration or be a sign of the deterioration. Track settlements induce long wavelength vibrations of the track in both planes: vertical and horizontal. Short wavelength excitations develop due to train passage and generate high frequency vibrations.

Wheel imperfections and out-of-roundness can cause both short and long waves vibrations either on the trains or on tracks. Block-braked wheels are usually linked with short wavelengths (T., 2003).

Probably the most common source is track irregular stiffness, even though the track may have no irregularities. This concept is easy to understand since the track is stiffer at one sleeper and more flexible in between two sleepers, leading to different deflections of the track when subject to the same load and to the excitation of the both the train and the track at a certain frequency which can lead to resonance vibrations.

Some irregularities may be produced during the rail manufacturing process (T., 2003). This can create irregularities in relatively regular intervals of several meters and generate low-frequency vibrations.

It was already stated that track irregular stiffness due to sleepers spacing is one of the most important excitation sources, however, the presence of switches and turnouts may also introduce differences in track stiffness (T., 2003). This is due to the different spacing between sleepers at switches and the absence of symmetry in the track.

Some track embankment settlements may be produced due to non-elastic deformations on the geomaterials. This happen when the ballast and the substructure do not return exactly to its original position when loaded during a train passage and it is usually a sign of a certain non-linearity of the system, unlike what is usually considered (T., 2003). After thousands of trains passages the small deformations added to the system will not be equal and some differential settlements have been occurred and with it a new track alignment. This will increase the track load differences and lead to a faster track settlement. It is a phenomenon often seen in transition areas such as from an embankment to a bridge.

Above are resumed the main phenomenon's that are the cause of structural excitation of railways. However, single impact loadings can create distinct excitations and it is a matter that should be referred. Wheel defects, wheel trend defects or rail joints can create punctual loads that increase the deterioration.

Wheel flats appear when the wheel does not turn around in a spinning movement when the train starts running, but slides on the rail while removing part of the wheel and creating a flat surface. This will create an impact load every time the wheel completes a rotating cycle inducing a high frequency excitation on the track.

It is now clear that the vibrations that occur in the railways are a gather of excitations from different sources and that its frequency is linked to the components excited.

2.3.2 DYNAMIC LOADS

It is important to introduce one more basic concept in this chapter which is the dynamic loads. The dynamic loads referred here are loads that move in space with a certain velocity. This is a case where a beam is subjected to a moving constant force, which is a classical problem already solved.

This problem requires the several assumptions such as (Frýba, 1979):

- The beam behaviour is described by the Euler-Bernoulli beam differential equation (2-1). This suggests that the theory of small deformations, Hook's law, Navier's hypothesis and San-Venant's principle is applied, and that the beam cross section and weight per length is constant;
- Considering also that only gravitational effects are applied to the load, which moves with a constant velocity;
- That the beam damping is proportional to the vibration velocity and considering that the beam has neither deflection nor bending moment at both ends;
- That the beam is without deflection or velocity at the moment of force arrival.

These suppositions will lead us to the equation (2-1) in which its left side represents the load.

$$p(x,t)=P.\delta(x-vt) \tag{2-28}$$

The model represented in Figure 2-11, represents an infinite beam on an elastic foundation, loaded by a schematic train represented as a series of n loads F_n, like P in equation (2-28), spaced by d_n, which is the distance from the point of load application until the front of the train and moving at a constant velocity, v.

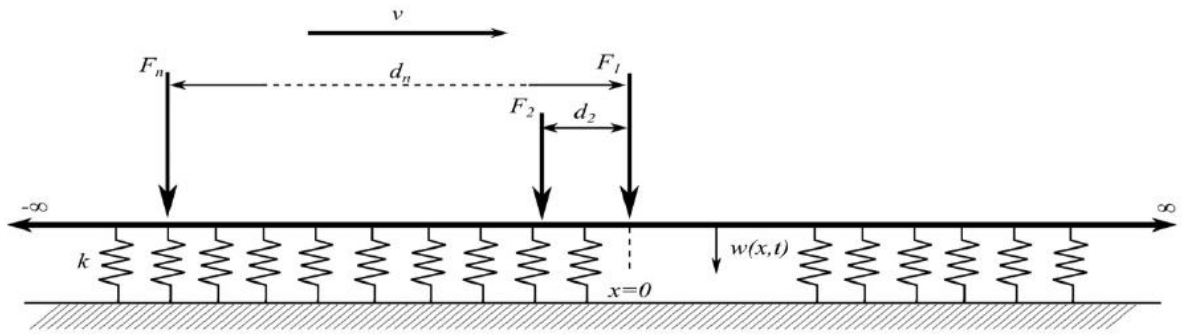

Figure 2-11 - Infinite beam on elastic foundation model considering dynamic loads (Le Pen [et al.], 2016)

This concept will lead to a reformulation of the previous equation (2-28) as

$$p(x,t)=\sum_{n=1}^{N} F_n.\delta(x-d_n-vt) \qquad (2\text{-}29)$$

The previous equations (2-6) and (2-29) describe a beam over an elastic foundation and the consideration of dynamic loads respectively will be the departure point to analyse the method proposed by Le Pen et al.(2016), to determine the track system modulus.

3

Evaluating Support Stiffness

3.1 Introduction

Le Pen et al.(2016), as already stated, developed a new method to determine the track support stiffness. It is based on the use of the Fourier transform of track measured data, interpreted as a beam over an elastic foundation excited by dynamic loads. The main advantage of the purposed method is that it is not required to know the dynamic loads applied by the train on the track, which is a great advance since the measurements of the axle loads can be hard and expensive to get in practice. The other main advantage of this procedure is the fact that, besides the necessity to know several geometry and train parameters, the data can be directly used and it can be either displacements, velocities or accelerations without need of any further information.

To continue the work started by those authors and to develop continue to further analysis it was first decided to recreate the results they obtained. To focus on that goal, this chapter will, firstly, present the theoretical mathematical basis that follows the concepts presented in the previous chapter and that led to the assertion that determining the railway support stiffness in the absence of load data is possible. Then, that proposed method will be implemented independently from that original work, aiming at reproducing the original results presented by those authors.

These steps of implementing the proposed method and of reproducing the same results are fundamental to validate the script that will be developed from scratch in MATLAB environment and then be used in further analysis, which are the main goals of this thesis.

3.2 Mathematical theory behind the method

3.2.1 BEAM ON AN ELASTIC FOUNDATION

As already presented in the previous chapter, the equation (2-15) represents a beam on an elastic foundation, which for a single unit point of load $x = vt$ has the following solution:

$$w(t)=s(t)=\frac{1}{2kL}e^{-\frac{v|t|}{L}}\left[\cos\left(\frac{v|t|}{L}\right)+\sin\left(\frac{v|t|}{L}\right)\right] \tag{3-1}$$

where

$$L=\sqrt[4]{\frac{4EI}{k}} \tag{3-2}$$

is the characteristic length. The shape function s(t) depends on the rail bending stiffness, EI, and the support modulus, k.

Combining the equations (2-29) and (3-1), the solution for the rail displacement according to the assumptions made is:

$$w(t)=\sum_{n=1}^{N}\frac{F_n}{2kL}e^{-\frac{|vt-d_n|}{L}}\left[\cos\left(\frac{|vt-d_n|}{L}\right)+\sin\left(\frac{|vt-d_n|}{L}\right)\right] \tag{3-3}$$

3.2.2 FOURIER TRANSFORM

As known, the Fourier transform is commonly used to convert a signal in the time domain into its frequency domain. In fact, the Fourier transform can be defined as:

$$\dot{f}(s)=\int_{-\infty}^{\infty}e^{-2\pi ist}f(t)\,dt \tag{3-4}$$

Assuming that f(t) is defined by real numbers, integrating f(t) towards $e^{-2\pi ist}$, for any $s \in \mathbb{R}$ produces a complex function of s represented as $\dot{f}$ (s). This suggests that f(t) is a function in the frequency spectrum (Hertz) if considering t on the time domain, since to make s.t dimensionless s must be in 1/time=Hz domain (Brigham, 1988).

In this case study, the equation (3-4) allows to evaluate the frequency content of the track movement.

For the shape function s(t) (3-1), the Fourier transform is:

$$S(\omega)=\frac{1}{2kL}\int_{-\infty}^{\infty}e^{-\frac{v|t|}{L}}\left[\cos\left(\frac{v|t|}{L}\right)+\sin\left(\frac{v|t|}{L}\right)\right]e^{-i\omega t}dt \tag{3-5}$$

and for the load function, the Fourier transform is:

$$P(\omega)=\sum_{n=1}^{N}\int_{-\infty}^{\infty}F_n\delta\left(t-\frac{d_n}{v}\right)e^{-i\omega t}dt \tag{3-6}$$

The angular frequency, $\omega = 2\pi f$, and I, which is the square root of -1, were introduced by the Fourier transform.

It is possible to simplify both the above equations through integration, leading to:

$$S(\omega)=\frac{4v^3}{4kv^4+kL^4\omega^4} \tag{3-7}$$

And:

$$P(\omega)=\sum_{n=1}^{N} F_n e^{-\frac{i\omega d_n}{v}} \tag{3-8}$$

It is also possible to verify that:

$$w(t)=s(t).p(x,t) \tag{3-9}$$

from the equations above we can write:

$$W(\omega)=S(\omega).P(\omega) \tag{3-10}$$

as a product of the Fourier transform of w(t).

Then, it can be written W(ω) as

$$W(\omega)=\frac{4v^3}{4kv^4+kL^4\omega^4}\sum_{n=1}^{N} F_n e^{-\frac{i\omega d_n}{v}} \tag{3-11}$$

It is important to understand that the process shown is formulated for the displacement spectra, and that the velocity and acceleration spectra are easily derived by multiplying the above by iω and $-\omega^2$, respectively (Le Pen [et al.], 2016).

3.2.3 CALCULATION EXAMPLE

A simulation using the beam on elastic foundation (BOEF) model and the frequency analysis was developed for a Pendolino Train by Le Pen et al.(2016), which was recalculated here.

Considering the data from the Table 3-1 and through equation (3-3), it was determined the deflections of the track for different track system modulus, k, as shown in Figure 3-1.

Table 3-1 - Train and track data for Pendolino simulation adapted from (Le Pen [et al.], 2016)

Parameter	Value	Notes
Wheel Load, F_n (MN)	0.063	Average Pendolino Wheel load
Young's modulus of the rail, E (MN/m^2)	2.05e5	Steel
Moment of Inertia of the rail, I (m^4)	3.0383e-5	CEN 60 E1
Axle locations, d_n (m)	0, 2.7, 17.0, 19.7	Axle relative spacing on the first car
Car length, d_c (m)	23.9	Car length when coupled

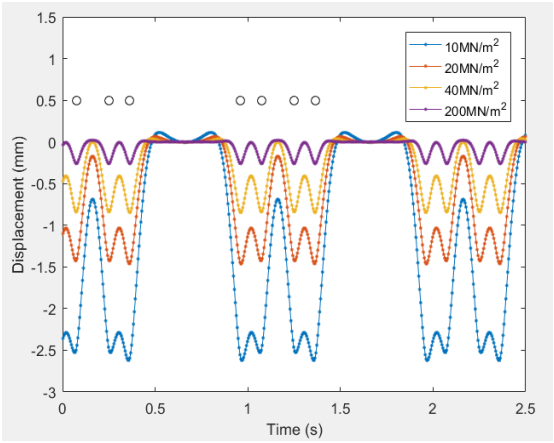

Figure 3-1 - Rail deflections for different system modulus

Figure 3-2 shows that the shape function in the frequency domain changes significantly between 0 and 8 Hz and that the amplitude is highly dependent on the track system modulus.

Notice that the velocity chosen was 23.9 m/s so the car passing frequency was 1 Hz which led, as it can be seen in Figure 3-3, to a loading function with harmonics spaced by 1 Hz. In fact, strong peaks appear at the car passing frequency (1 Hz in this case) and its multiples, in this case the strongest harmonics are the third, seventh and tenth ones. The relative magnitudes of these frequencies are governed by axle spacing of the train.

The result of the multiplication of the shape function (equation (3-7)) represented in Figure 3-2) by the load function in the frequency domain (equation (3-8)), represented in Figure 3-3 is the magnitude of the Fourier transform for displacements which is displayed in Figure 3-4. It also represented the velocity (Figure 3-5) and the absolute values of the acceleration (Figure 3-6), values that can be obtained changing the spectra in the equation (3-11).

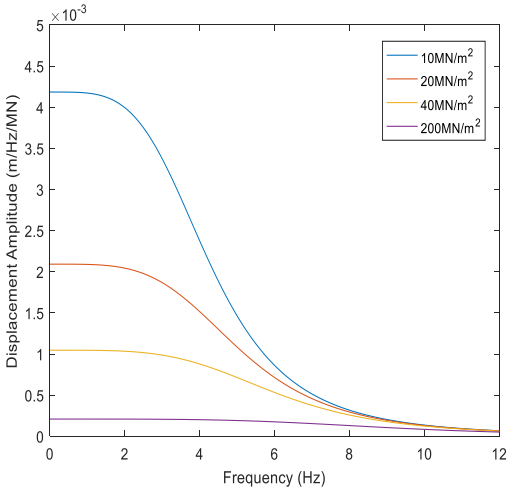

Figure 3-2 - Displacement amplitude in frequency spectrum for different track system modulus

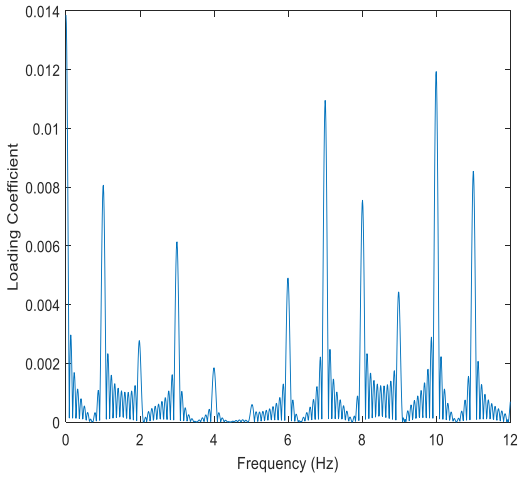

Figure 3-3 - Loading function at a speed of 23.9m/s

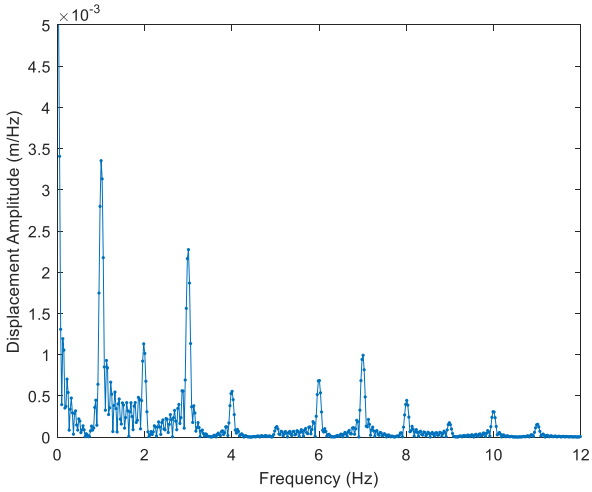

Figure 3-4 - Displacement amplitude in the frequency spectra

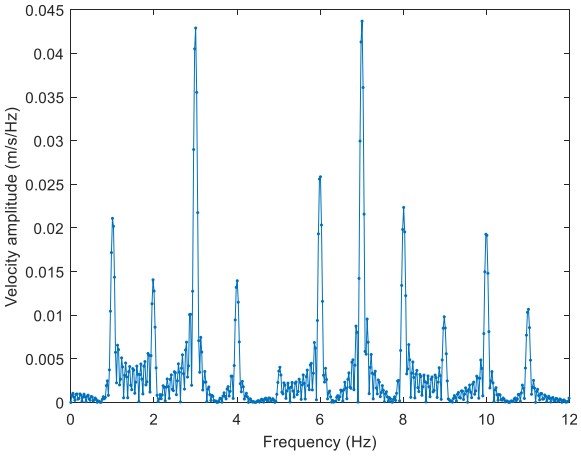

Figure 3-5 - Velocity Amplitude in the frequency spectra

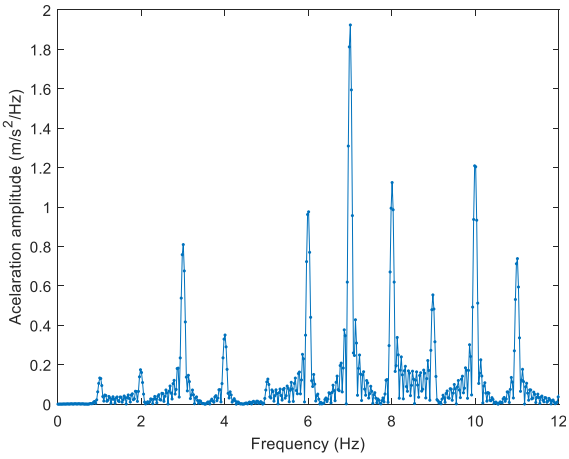

Figure 3-6 - Acceleration amplitude in the frequency spectra

The multiplication of the amplitudes by the shape function has significantly reduced the relative magnitudes at frequencies greater than 12 Hz and kept strong peaks at 1, 2, 3, 7 and 10 Hz. However, in each case, the peaks 3 and 7 stand out as dominant Harmonics of the vehicle passing frequency. In fact, Bian et al.(2015) and Ju et al.(2009) state in their theoretical and fields work that these peaks in the track displacements spectra occur in the car passing frequencies. Both velocity and acceleration have higher frequency components due to the multiplication by ω and ω^2, respectively.

It is important to register that these results are for a specific kind of train, in this case the Pendolino, since it was already stated that these properties are related to the geometric ones. Although, since most trains have similar axle arrangements, it is expected that the third and seventh harmonics will still be the dominants peaks.

Knowing that d_c is the car length and for a train traveling at a velocity v, its passing frequency can be calculated as $f_1 = v/d_c$. This means that the variation of the velocity of the train will lead to a shift in the frequency spectrum, though the frequency should be normalized by f_1 in both cases (displacement amplitude and loading coefficient (Figure 3-2 and Figure 3-3)).

3.2.4 DETERMINATION OF THE TRACK STIFFNESS

Since the magnitude of W(ω) is dependent of the train speed but the relative one is not, Le Pen et al.(2016) suggested the use of the ratio of the amplitudes at two selected harmonic frequencies to determine the track track system modulus.

The periodicity of the train, which came from the similar axle loads, F, coupling distances and equal axe spacings, leads to the approximation between the dominant frequencies, and the car passing frequency and its harmonics as the number of cars increases (Ju [et al.], 2009). The periodicity can be seen in equations (2-29) and (3-8) and the harmonic frequencies are given by $\omega = 2\pi n f_1$ for integer values of n, for a vehicle length d_c and with $f_1 = v/d_c$.

Considering two harmonic frequencies $f_p = pf_1$ and $f_q = qf_1$, where p and q are integers, and through the equation (3-11), we can proceed as shown next:

$$kL^4 = k\left(\sqrt[4]{\frac{4EI}{k}}\right)^4 = 4EI \tag{3-12}$$

$$S(\omega) = \frac{4v^3}{4kv^4 + kL^4\omega^4} = \frac{v^3}{kv^4 + 16EI\pi^4 n^4 {f_1}^4} \tag{3-13}$$

Dividing the two frequencies, one by the other, and replacing for L^4 we get

$$\frac{W(n=p)}{W(n=q)} = \frac{\frac{v^3}{kv^4 + 16EI\pi^4 n^4 p^4 {f_1}^4} \sum_{n=1}^{N} F_n e^{-\frac{i2\pi n f_1 p d_n}{d_c}}}{\frac{v^3}{kv^4 + 16EI\pi^4 n^4 q^4 {f_1}^4} \sum_{n=1}^{N} F_n e^{-\frac{i2\pi n f_1 q d_n}{d_c}}} \tag{3-14}$$

then simplifying the previous equation, we obtain

$$\frac{W(n=p)}{W(n=q)} = \frac{{d_c}^4 k + 16EI\pi^4 q^4}{{d_c}^4 k + 16EI\pi^4 p^4} \frac{\sum_{n=1}^{N} e^{-\frac{i2\pi p d_n}{d_c}}}{\sum_{n=1}^{N} e^{-\frac{i2\pi q d_n}{d_c}}} \tag{3-15}$$

Both the load and the velocity were eliminated, creating a function only dependent on the train geometry, which can be calibrated for each kind of train (Le Pen [et al.], 2016).

Since the first term of the equation is, beside the length of the vehicle, only dependent on the track properties, it is possible to create calibration curves for each type of train for a certain rail bending stiffness and track system modulus.

With the measurements of the displacements, velocities or accelerations during the train passage, it is possible to obtain the ratio between main harmonics and to obtain the track system modulus from the appropriate calibration curve. The harmonics p and q should be dominant peaks in the frequency spectrum so that the harmonics correspond to the car passing frequency. The harmonics used in this chapter were the third and seventh, but each case should be analysed to find its dominant harmonics.

This process can be adapted to create similar relationships for velocity and acceleration through the derivation.

$$\frac{W(n=p)}{W(n=q)} = \frac{V(n=p)q}{V(n=q)p} = \frac{A(n=p)q^2}{A(n=q)p^2} \tag{3-16}$$

3.3 Calculation using field data

3.3.1 General aspects of the case study

In the previous subchapter, it was mathematically proven that the possibility of determination of the track system modulus without knowing the wheel loads. It is now important to verify the applicability of the method in practice.

To do so, first, as already explained, it will be used a MATLAB script developed in the scope of this thesis to implement the proposed method, to determine the track support stiffness of four sites with data kindly provided by Le Pen et al.(2016) and to check if the results obtained with the MATLAB script were the same, in order to validate the script developed. It will also be compared the obtained results with the ones from the traditional method.

For the appropriate interpretation of field measurements, several criteria in the choice of sites were considered by the authors. In first place, they choose a track with a reliable performance, i.e. without voided sleepers, excessive variation in support stiffness from one sleeper to another. Low variations in the axle loads in the same train may help to improve our trust in the obtained data. These conditions are usually fulfilled in well-maintained sites traversed regularly by periodic trains (Le Pen [et al.], 2016).

The general characteristics of each site studied and its traffic are presented in Table 3-2 and Table 3-3. According to Le Pen et al.(2016) the sites were selected because the track is believed to be performing well and because they cover a wide range of situations, including plain lines and curves.

Sites 3a and 3b are contiguous to each other on the same section track but were considered two subsites, since twice as many sleepers were instrumented than on other sites which led to a high volume of data. Site 4a and 4b are also on the same route, however, they are separated by several hundred meters (Le Pen [et al.], 2016).

According to the authors, these studied sites have periodic passages from the trains over them and cover the most common situations, including curved track. The characteristics of the trains types are displayed in Table 3-4.

Table 3-2 - General characteristics of sites (Le Pen [et al.], 2016)

Site	Type of line	Location	Notes	Type of train	Speed (km/h)
1	Classic high speed	England midlands	Stoneblown* 2013	Pendolino (class 390)	200km/h
1	Classic high speed	England midlands	Stoneblown* 2013	Supervoyager (class 221)	200km/h
2	Branch line	SE England	Renewed 2013	Turbostar (class 171)	112km/h
3a,3b	True high speed (HS1)	SE England	Opened 2003	Javelin (class 395)	225km/h
4a,4b	Branch line	SE England	Renewed (2012,2014)	Electrostar (class 377)	120km/h

* Stoneblown – this is a maintenance process to re-level and realign the track by lifting the sleepers and track and blowing smaller size gravel between the ballast and the base of the sleeper (Anderson and Key, 2000)

Table 3-3 - Characteristics of sites (Le Pen [et al.], 2016)

Site	Date of measurements	Radius of track (m)	Cant (mm)	Rail type (BSI 2011)	Railpad	Sleeper	Sleeper spacing (m)
1	14 of August	2777	72	CEN 60 E1	Pandrol 6650	Monoblock (G44)	0.65
2	14 of May	2777	72	CEN 56 E	Vossloh ZW900	Monoblock (EG47)	0.65
3a,3b	14 of May	n.a. (straight)	0	CEN 60 E1	Pandrol 6650	Twin block	0.60
4a,4b	13 of February and 15 of April	n.a. (straight)	0	CEN 56 E	Pandrol 6650	Monoblock (EG47)	0.65

Table 3-4 - Train characteristics (Le Pen [et al.], 2016)

Site	Train Class	Name	Published axle weight (t)	Car length, dc (m)	Axle location per car, dn (m)
1	390	Pendolino	12.9	23.9	0, 2.7, 17, 19.7
1	221	Supervoyager	14.1	22.9	0, 2.6, 15.9, 18.5
2	171	Turbostar	11.0	23.6	0, 2.6, 15.8, 18.4
3	395	Javelin	10.9	20.0	0, 2.6, 14.2, 16.8
4	377	Electrostar	11.0	20.0	0, 2.6, 14.2, 16.8

The authors mentioned that despite the brief time range of measurements, the data collected showed that the track behaviour was considered consistent. Besides, only representative types of trains from each site were considered. One other issue that required some analysis was the possible variations between

axle loads. Measurements for the class 395 show that the variations of axle load were less than 4% in more than 90% of the trains, which reveals a certain consistency as desired.

With the general characteristics, it was possible to redrawn the referred calibration curves (CC) relating the track system modulus to the amplitude ratio of the seventh and the third harmonic peaks of the velocity through equation (3-15), as shown in Figure 3-7. The construction of the CC required the following process: it was considered a certain track system modulus and the characteristics of both, trains and sites, which allowed the MATLAB script to determine the ratio between the amplitude of certain harmonics. Repeating this process a certain a number of times we get both the track system modulus and the ratio between the amplitudes of the harmonics considered, which allow the construction of the CC.

The ratio of third to seventh harmonics converges to within 2%, if at least the train is made of four cars, which happens in this case (Le Pen [et al.], 2016).

The calibration curves (Figure 3-7 (a)) obtained are not equal to the ones obtained by Le Pen et al.(2016) (Figure 3-7 (b)). The differences may be due to the absence of information related to the way the authors solved the equation or to different assumptions made during this case. However, this is a problem that will be later discussed in the analyses of the results in 3.4.4.

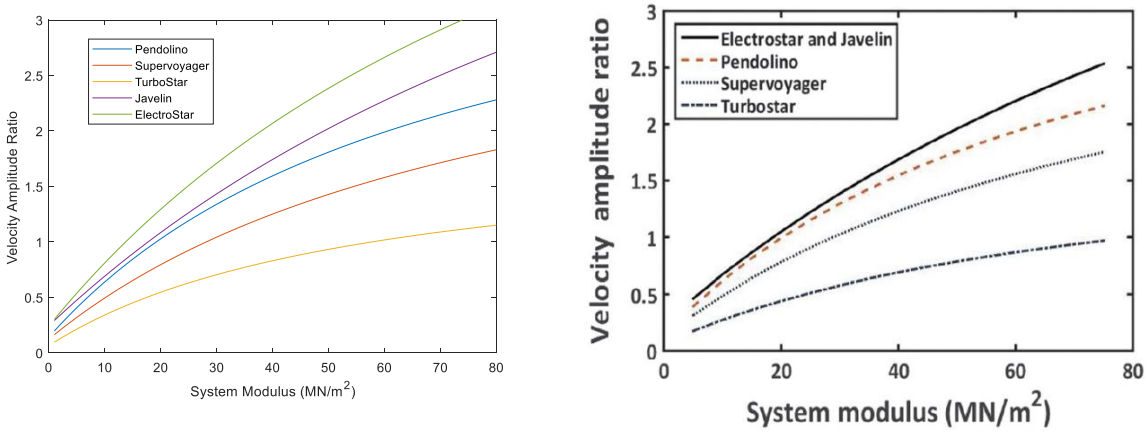

Figure 3-7 – Calibration Curves (CC) obtained with the velocity amplitude (a) using the MATLAB script developed and (b) by Le Pen et al.(2016)

3.3.2 FIELD MEASUREMENTS AND DATA POST-PROCESSING

Le Pen et. Al (2016) used velocity data collected on the sleepers by geophones to test the method. This equipment is of proven reliability to determine the track movements (Bowness [et al.], 2007).

A typical arrangement of geophones was composed of up to 28 sensors, fixed to brackets mounted on sleeper ends of adjacent or alternate sleepers like the ones displayed in Figure 3-8.

In Figure 3-9 it can be seen the set-up of the geophones which enables the measure of both vertical and lateral velocity.

The data logging was trigged automatically as the trains approached and lasted at least 20 seconds, with an acquisition rate of 500 Hz, an acquisition rate that, according to Le Pen et al.(2016), is enough to provide good results on the method in analyse.

Figure 3-8 - - Geophones at the end of the sleepers, (Le Pen [et al.], 2016)

Figure 3-9 - Geophones orientation to measure vertical and lateral velocities, (Le Pen [et al.], 2016)

Deflections were determined by integrating velocity values obtained in the field with geophones. Once more, it shall be referred that the same method can be applied to calculate accelerations. Then, it was used a Butterworth band-pass filter with a lower cut-off frequency of 1Hz and the upper cut-off of 30Hz. This would ensure the filtration of low frequency data below the threshold of linearity for the geophone used and high frequency data that is not relevant to calculate the main displacements in this kind of application (Le Pen [et al.], 2014).

In Figure 3-10 it is shown the deflections due to eight axles belonging to four bogies, data calculated with geophones data. It is important to state that the data provided by Le Pen, et al. (2016) was displacements integrated from velocity data. The use of displacement data converted into velocity was done in this case to approach the methods so the comparison between results was easier and between CC possible.

To change from the time spectra to a frequency spectra, it was applied the numerical discrete Fourier transform (DFT) to the unfiltered data obtained by Le Pen et al.(2016). The DFT transform implemented in the developed MATLAB script and applied to the filtered data was the fast Fourier transform (FFT) function available in MATLAB, which is a very efficient way to compute the DFT.

As it can be seen in the following figures (Figure 3-11 to Figure 3-15), the third and seven harmonics, which appear highlighted by a downward arrow above, are always among the highest peaks. The previous conclusion supports the theory that those harmonics can be dominant and used in the method (Le Pen [et al.], 2016).

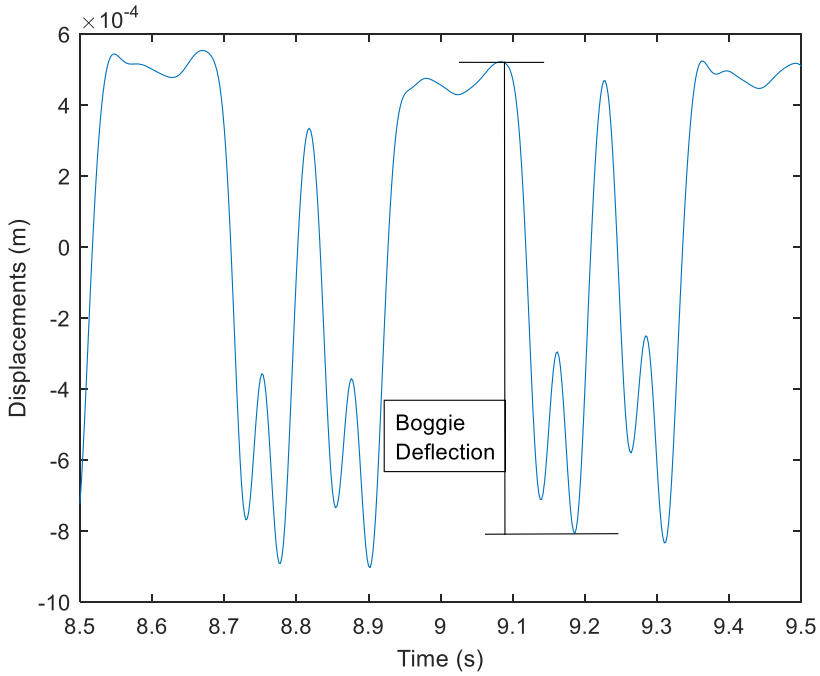

Figure 3-10 - Measured deflection data from the Supervoyager at site 1 representing the bogie deflection

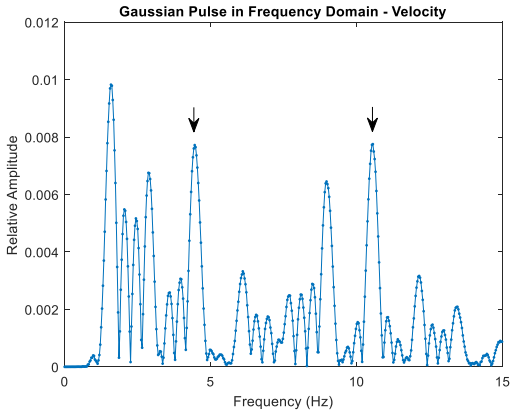

Figure 3-11 - Numerical FFT obtained for velocity data from a Electrostar at site 4a

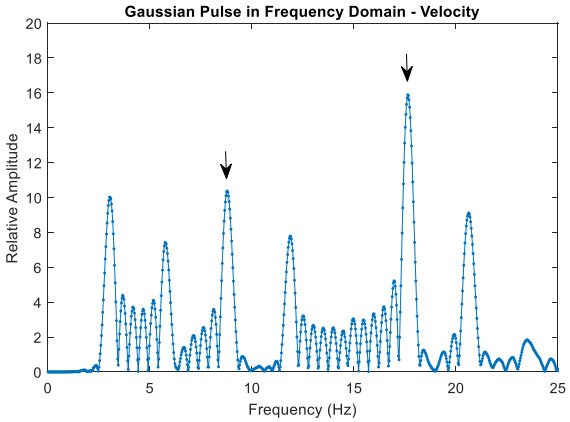

Figure 3-12 - Numerical FFT obtained for velocity data from a Javelin at site 3a

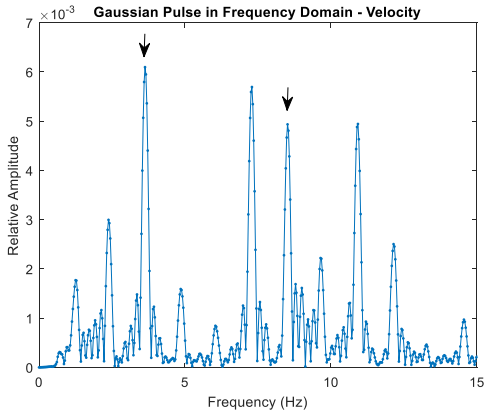

Figure 3-13 - Numerical FFT obtained for velocity data from a Turbostar at site 2

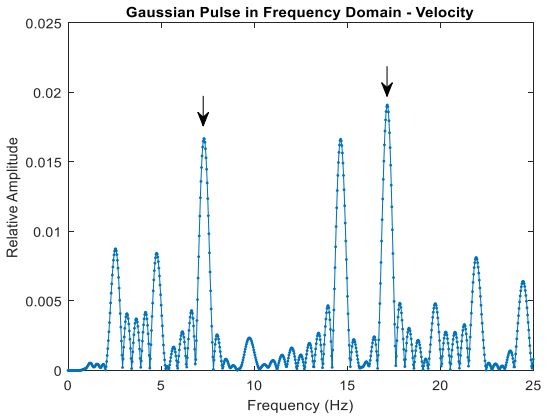

Figure 3-14 - Numerical FFT obtained for velocity data from a Pendolino at site 1

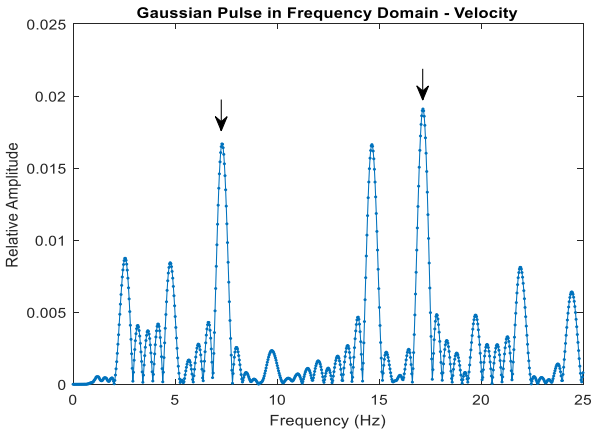

Figure 3-15 - Numerical FFT obtained for velocity data from a Supervoyager at site 1

As explained, there is a link between the harmonic's frequency and the axle arrangement of the trains. The figures above show that the first and sixth harmonics can also be considered dominant, depending on the train characteristics, and thus also used in the procedure.

3.4 Estimation of track support stiffness

3.4.1 INTERPRETATION USING FREQUENCY EVALUATION

The track system modulus can now be determined from the relative amplitudes using the calibration curves. In the context of this thesis it will be recalculated the stiffness for each sleeper and the site average as already done in (Le Pen [et al.], 2016).

To facilitate this process and as an improvement to the original method proposed by Le Pen et al.(2016), it is, here, proposed to invert the axis from the calibration curves, that is, considering the velocity amplitude as the independent variable, *x*, and the track system modulus as the dependent variable, *y*. With this alteration, it is possible to use directly approximate equations from the inverted calibration curves, a tool extremely easily to use in most programs.

The velocity ratios between the seventh and third harmonics were obtained using a MATLAB script developed for this purpose in the scope of this dissertation. The next step was to approximate a polynomial curve of x^{th} order (the maximum norm of residuals was 0.01) to each of the calibration curves in Figure 3-7 (a) and to use the equations obtained to calculate from the amplitude curves (Table 3-5) the track system modulus (Table 3-6). This is a very simple method that allows a high discretization of the calibration curves and minimize the mathematical errors on the results obtained. It is here suggested its use, since it increases the model definition without the use of additional computer effort in the MATLAB script, for simple curve approximations. However, some curves may be quite complicated, and this method may not be worth the effort in those cases.

Since, in this case, it is easy to approximate a polynomial curve, it was used the referred method for a demonstration. Since the purpose of such method is to guarantee a high definition of the calibration curves for a high number of results it was decided that the maximum norm of residual would be 0.01, a value quite high for this purpose and that may not be worth on regular cases. To achieve such values, it was necessary to use polynomials till the seventh degree. Since the MATLAB can provide the polynomial coefficients directly (Table 3-7), it is very easy to programme the Excel to use the coefficients obtained in order to get the track system modulus for a determined ratio.

The programming of the Excel, to use the polynomial coefficients to replace the Calibration Curves (CC), is done with the use of a polynomial equation like the one represented on equation (3-17). It shall be pointed out that the degree of the polynomial equation used must assure a good representation of the CC.

$$k=am+bm^6+cm^5+dm^4+em^3+fm^2+gm+h \tag{3-17}$$

Table 3-7 shows the coefficients of the polynomial equations that were adjusted to fit the inverse of the calibration curves. As explained, considering the track system modulus equal to k and introducing the velocity amplitude ratio as m, it is possible to obtain the track system modulus directly. Considering a linear behaviour from the railpad and track bed for the range of movements in question, the amplitude ratios are the same for the velocities measured either on the sleeper or on the rail, which means that this method provides the track system modulus directly (Le Pen [et al.], 2016).

Table 3-5 - Amplitude ratios (seventh/third harmonics)

		Amplitude Ratio for Sleepers Numbers:									
Train	Site	1	2	3	4	5	6	7	8	9	10
390	1	1.23	1.23	1.04	0.93	1.04	0.94	0.79	1.08	-	-
221	1	1.15	1.15	0.96	0.75	0.85	0.93	0.79	0.87	-	-
171	2	0.81	0.63	0.63	0.78	0.72	0.69	0.7	0.72	0.66	-
395	3a	0.88	2.07	1.17	1.87	1.96	1.7	1.73	1.32	2.18	2.35
	3b	1.96	1.69	1.96	1.68	1.45	1.83	0.58	1.92	1.38	1.58
377	4a	1	0.88	0.7	1.21	0.9	0.91	1.31	0.56	1.13	0.82
	4b	1.09	0.37	1.35	1.19	0.94	0.64	1.12	1.45	0.58	0.91

Table 3-6 – Track system modulus

Track system modulus (MN/m²) for sleeper's numbers:											
Train	Site	1	2	3	4	5	6	7	8	9	10
390	1	26.3	26.3	20.4	17.3	20.4	17.5	13.6	21.5	-	-
221	1	34.9	34.9	26.5	18.4	22.1	25.2	19.8	22.8	-	-
171	2	38.2	25.0	25.0	35.7	31.1	29.0	29.7	31.1	26.9	-
395	3a	14.6	51.8	22.4	44.4	47.7	38.5	39.6	26.6	56.2	63.2
	3b	47.7	38.2	47.7	37.9	30.5	43.0	7.4	46.2	28.4	34.6
377	4a	13.7	11.3	7.9	18.2	11.7	11.9	20.4	5.4	16.4	10.2
	4b	15.6	2.1	21.3	17.7	12.5	6.8	16.2	23.6	5.7	11.9

Table 3-7 – Coefficients of the calibrated 7th order curves

Coefficients								
Train	a	b	c	d	e	f	g	h
Pendolino	0.000	0.201	-0.948	2.497	-1.705	5.533	16.002	-2.371
SuperVoyager	0.000	0.423	-1.487	3.376	-0.998	7.495	22.174	-2.846
TurboStar	19.547	-62.431	93.583	-66.599	38.421	7.537	29.652	-1.963
Javelin	0.000	0.000	0.033	-0.065	0.614	2.486	19.628	-4.951
ElectroStar	0.000	0.000	0.034	-0.115	0.657	1.690	15.251	-3.784

3.4.2 CALCULATION OF THE TRACK STIFFNESS USING THE "TRADITIONAL METHOD"

Another way to determine the track system modulus is through the track deflections and by estimating the axle loads. Typical bogie deflections can be determined by integration of the velocity values obtained with the geophone values and after applying the abovementioned pass-band filter. Even though the authors considered a good behaviour from the tracks, significant variations in the movement of each sleeper occurred, a situation that is not abnormal in ballasted tracks (Le Pen [et al.], 2016).

The determination of the track system modulus, k, was calculated using the BOEF model and the solution was obtained iteratively since k appears in both equations (3-2) and (3-3).

The estimation of the loads per wheel had to be adjusted to consider the curving speed and cant of the track. Then, it was possible to determine the track system modulus from the deflection data for sleepers during the passage of a bogie in the middle of the train which took in consideration the particular behaviour caused by the trains, rails, sleepers and railpads at each site, and the estimated loads (Le Pen [et al.], 2016).

It is important the comprehension that in this methodology, despite its common use and its reference in (Le Pen [et al.], 2016) as "direct", is, in fact, quite indirect and depends of factors with several inaccuracies like the wheel loads. As already said, the wheel loads are a fundamental parameter to consider when using this methodology, but errors are implicit in its determination which reduce the reliability subjacent to this method.

The common use of integration of the acceleration and velocity values for the determination of the sleeper displacements, means that this methodology is also not so direct. Instead, it seems more reasonable to use of the acceleration and velocities in the frequency method directly without the need of integration.

3.4.3 INFLUENCE OF THE RAILPADS

The measurements for sleepers during the passage of a bogie do not consider the also present rail movement due to railpad compression. When in the presence of stiff railpads (with stiffness of about 500 kN/mm), track bed and sleeper movements tend to be usually several times higher than the movement introduced by the railpad, which means that it is reasonable to neglect the influence of the railpad deformation in such cases. Though, if the track bed stiffness is similar to the railpad it should not be neglect, since significant errors may arise.

To take this influence into account, Le Pen, et al.(2016) considered a system with two linear springs in series, where one is the stiffness of the track bed and the other the railpad stiffness. The track system modulus can then be calculated as

$$\frac{1}{k_{system}} = \frac{1}{k_{pad}} + \frac{1}{k_{track\ bed}} \tag{18}$$

Knowing the k_{system} and the k_{pad} it can be directly determined the $k_{track\ bed}$.

Tests in the sites 1, 2 and 4, which have Pandrol 6650 pads, showed an equivalent spring stiffness of about 60 MN/m per railpad, a value that was also considered for the Vossloh railpads (Table 3-3).

Table 3-8 shows the results of both the track system modulus and the ballast modulus, which considers the railpads influence.

3.4.4 COMPARISON OF RESULTS

Using the approaches previously explained, the track system modulus average results per site and the track bed stiffness are displayed in Table 3-8 as well as the results obtained by Le Pen et al.(2016) through the two methods described above: using calibrated curves and traditional method.

The absolute differences between the frequency amplitude ratios obtained by Le Pen, et al.(2016) and in the context of this thesis are displayed in Table 3-9. It shows small differences that can be a result of the way the transform from time to frequency spectrum is done. In fact, there is no available information of how Le Pen et al.(2016) obtained the results. The track bed stiffness was determined considering the railpads with the methodology already explained.

The Table 3-8 shows average results for each site and the results are very similar to the ones obtained by the original authors, in fact, a maximum difference of 4 MN/m^2 between the results obtained in the scope of this thesis and the ones under comparison was achieved.

Table 3-9 displays the differences between the amplitude ratios obtained and the ones obtained by Le Pen. et al.(2016). Excluding the results at three locations - on sleepers 7, 8 and 9 in site 3a - the differences change between 0 and 0.06, which means that the highest differences are around 6%, which is a value perfectly acceptable. It shall be noticed that for each site, it was measured between 7 to 10 consecutive sleepers.

Table 3-10 and Table 3-11 display the absolute differences between the results obtained and the ones obtained by Le Pen. et al.(2016) and Table 3-12 displays the ratio between the average results for each site.

Some differences can be noticed between the results from the three approaches, differences that will now be analysed to understand not only its causes but also to help with the comprehension of these processes, aiming at reducing in the future the impact of such differences.

Table 3-8 - Average results for system and track bed support modulus

Average track bed support modulus (MN/m²)							
Method		**SDM**		**FM**		**FM-T**	
Site	Train	System	Track bed	System	Track bed	System	Track bed
1	390	17	21	21	27	20	26
	221	19	24	26	35	26	35
2	171	31	47	34	53	30	45
3a	395	33	52	40	70	41	68
3b	395	42	77	35	57	36	57
4a	377	10	11	14	16	13	15
4b	377	18	23	13	16	13	16
Average		24	36	26	40	26	37
SDM		Sleeper Displacement Method results obtained by (Le Pen [et al.], 2016)					
FM		Frequency Method results obtained by (Le Pen [et al.], 2016)					
FM-T		Frequency Method results obtained in the scope of this Thesis					

Table 3-9 - Absolute differences between both frequency methods amplitude ratios

Amplitude Ratio for Sleepers Numbers (Absolute Differences):													
Train	Site	1	2	3	4	5	6	7	8	9	10	Average	Average (%)
390	1	0.03	0.02	0.01	0.02	0.02	0.02	0.02	0.02	-	-	0.02	2.0
221	1	0.01	0.01	0.02	0.01	0.01	0.01	0.01	0.01	-	-	0.01	1.1
171	2	0.04	0.05	0.04	0.05	0.05	0.03	0.04	0.04	0.03	-	0.04	4.1
395	3a	0.03	0.03	0.03	0.06	0.03	0.02	0.11	0.15	0.16	0.02	0.06	6.4
395	3b	0.05	0.03	0.04	0.05	0.01	0	0.07	0.02	0.03	0.03	0.03	3.3
377	4a	0.05	0.04	0.03	0.05	0.03	0.04	0.06	0.02	0.05	0.03	0.04	4.0
377	4b	0.01	0	0.01	0.01	0	0.01	0	0.02	0	0	0.01	0.6

Table 3-10 - Absolute error between the Frequency Method Results obtained by (Le Pen [et al.], 2016) and the Frequency Method Results obtained in this work

Absolute error between FM and FM-T												
Track system modulus (MN/m²) for sleeper's numbers:												
Train	Site	1	2	3	4	5	6	7	8	9	10	Average
390	1	1.75	0.75	0.64	0.74	0.64	0.46	0.39	0.46	-	-	0.73
221	1	0.06	0.06	0.55	0.37	0.07	0.22	0.18	0.16	-	-	0.21
171	2	3.78	4.02	3.02	5.27	3.89	3.03	3.33	3.89	2.07	-	3.59
395	3a	1.36	1.17	0.65	2.58	0.68	0.46	3.55	4.64	6.16	0.76	2.20
	3b	1.68	0.79	0.68	0.87	1.47	0.00	1.62	0.22	0.41	1.39	0.91
377	4a	1.27	0.66	0.48	0.85	0.26	1.07	1.63	0.31	0.57	0.82	0.79
	4b	0.41	0.02	0.27	0.28	0.53	0.17	0.22	0.40	0.05	0.07	0.24

Table 3-11 - Absolute error between the Sleeper Displacement Method obtained by (Le Pen [et al.], 2016) and the Frequency Method Results obtained in this work

Absolute error between FM-T and SDM												
Track system modulus (MN/m²) for sleeper's numbers:												
Train	Site	1	2	3	4	5	6	7	8	9	10	Average
390	1	10.25	6.25	4.36	0.26	1.36	0.46	5.39	10.54	-	-	4.86
221	1	17.94	13.94	7.45	1.63	1.07	6.22	0.18	9.84	-	-	7.28
171	2	0.78	0.98	7.02	8.73	5.11	3.03	4.33	2.11	9.07	-	4.57
395	3a	1.64	38.83	5.35	30.42	2.32	2.54	16.45	27.36	5.16	33.24	16.33
	3b	2.32	2.79	3.68	14.13	7.47	2.00	19.62	0.22	16.59	2.39	7.12
377	4a	1.73	3.14	1.58	6.15	1.26	1.93	14.37	4.61	5.43	0.18	4.04
	4b	6.41	13.88	5.73	10.28	4.47	10.17	5.78	6.60	3.25	2.93	6.95

Table 3-12 - Ratio of Results between the different methods

		Ratio of Results (FM/SDM)		**Ratio of Results (FM-T/SDM)**		**Ratio of Results (FM-T/FM)**	
Site	Train	System	Track bed	System	Track bed	System	Track bed
1	390	1.2	1.3	1.2	1.3	1.0	1.0
1	221	1.4	1.5	1.4	1.5	1.0	1.0
2	171	1.1	1.1	1.0	1.0	0.9	0.8
3a	395	1.2	1.3	1.2	1.3	1.0	1.0
3b	395	0.9	0.8	0.9	0.7	1.0	0.9
4a	377	1.3	1.4	1.3	1.3	0.9	0.9
4b	377	0.7	0.7	0.7	0.7	1.0	1.0
Average		1.1	1.2	1.1	1.1	1.0	0.9

It can be seen some differences in the results obtained for the amplitude ratios (Table 3-9) as already referred. Since the data used in the scope of this thesis through the frequency method (FM-T) was the same as the one used by Le Pen et al.(2016) (FM) to determine the amplitude ratios, it would be expected that these results would be equal. Such variations maybe be due to different ways to apply the Fourier transform. In FM-T it was used the FFT (Fast Fourier Transform) function from the MATLAB script, to calculate the DFT (Discrete Fourier Transform), to change from the time spectre to the frequency one. There are no explanations of how the DFT was calculated in FM results. However, the average differences between the values obtained are low. The average difference is 3.1%, not counting sign mistakes since it was used the modulus value, which could lead to a reduction of this value through several measures.

To calculate the track system modulus, it was necessary to use the calibration curves. The absolute difference between results can be seen in Table 3-10. The errors are, in general, similar in amplitude with the ones obtained for the amplitude ratio. In fact, comparing the calibration curves (Figure 3-7) used in both calculations, they are really similar for the Pendolino, the Supervoyager and the Javelin. The other train model calibration curves, particularly, the ones for the Turbostar and the Electrostar models, have some differences between the curves obtained.

Most of these differences can easily be explained by suppositions made in each approach. Regarding the FM approach, it was concluded that the authors considered the CEN 60 E1 rail type in every site, an affirmation supported by the fact that the calibration curves of both Electrostar and Javelin are equal. In fact, despite the same axle locations between these models, their sites were different and presented different geometric characteristics. It was also concluded that the authors used a sleeper spacing of 0.65 m in all sites, but in site 2, this distance is 0.6 m. Table 3-3 shows that sites 2, 4a and 4b have CEN 56 E rail type. This will lead to different calibration curves and, therefore, different values of track system modulus. To prove that different assumptions were made in the scope of this thesis, when comparing to the case study under analysis, it was programmed the CC using only CEN 60 E1 as rail type and the results are displayed in Figure 3-16. It is clear that the new CC are almost equal to the ones in Figure 3-17, which supports the theory that Le Pen, et al.(2016) consider always the same railway type in all the sites.

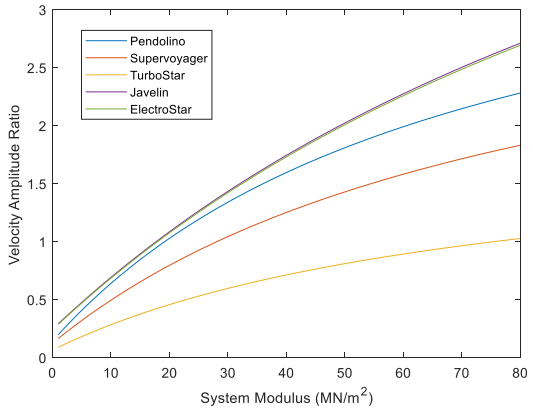

Figure 3-16 - Calibration curves created with the MATLAB script with the same assumptions than the ones made by (Le Pen [et al.], 2016)

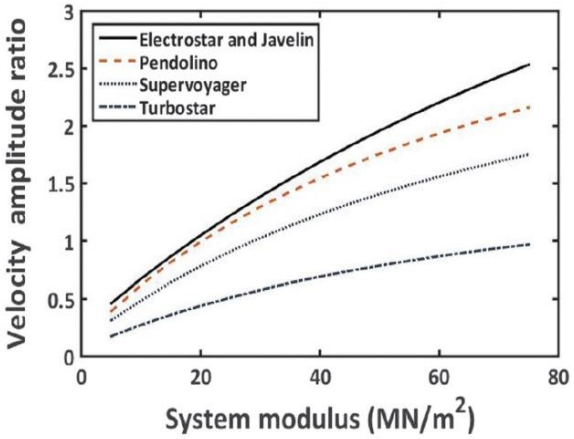

Figure 3-17 - Calibration Curves made by (Le Pen [et al.], 2016)

Small discrepancies may also appear due to the fact that different resolutions were considered in the numerical models. In fact, this is a really important aspect that influences in different ways the influence of diverse trains and site characteristics.

Changing the velocity will not change the amplitudes neither the CC, as already explained. This singularity is proved since the equation (3-15) does not depend on the velocity, in fact, changing the velocity only changes the frequency which the harmonics appear. However, the discretization between values of the results (in time, space and frequency) depends on the velocity, which means that different velocities can lead to different values. Therefore, changing the velocity will only change the frequency on which the harmonics appear.

After the use of the FFT, the developed script displays the numerical DFT that links amplitude values with frequencies in a graphic (as in Figure 3-11 to Figure 3-15). These values are influenced by several factors such as the number of bogies and their spacing, among other geometric characteristics.

These graphics display discrete numerical data and the information appears as an association of points, each one representing the amplitude for a certain frequency. If a small number of data points is considered, the exact frequency of the harmonics may fall between two data points and the maximum amplitude values may be underestimated, thus introduces an error in the method.

These numerical errors can be very small, but in this case, the presence of high variations in the amplitudes calculated can introduce significant errors, even in the small intervals between data. To solve this issue, the intervals between two consecutive data points should be reduced, which can be achieved by introducing zeros in the Fourier Transform – this is normally called “zero padding”.

It is also necessary to consider the dependence between the results obtained and the velocity. Such correlation appears with the increment, dx, between values of the model and will be now explained.

The frequency of data recorded (sample rate of measurements in this case) ($f = v/dx$) depends on the velocity (v) and on the distance increment between measurements (dx is the distance travelled by the train until the next recorded value). For a certain velocity, our data will be spread over a finite range on the frequency spectrum. This is, for a certain number of output values or bins, the dx will define the reach of these bins in the frequency spectrum, which defines the discretization of the frequencies (df) in the frequency domain. However, since the Fourier Transform is more efficient if the size of the input data has a base 2 exponential number of bins, the number of bins is only changed when a new base 2 exponential number of bins is reached.

Until then, the same number of bins is being spread over an increasing frequency range which results in increasing gaps between two consecutive data points and abrupt changes in the discretization when the next base 2 exponential number is achieved. Therefore, the reduction of the time interval (dt) in our physical model that will define dx will decrease the discretization until a new base 2 exponential number of outputs is achieved, which will increase the number of bins drastically and lead to a much higher discretization, after this point, the process repeats itself. As explained, the dx is the distance travelled by the train in a certain time at a certain constant velocity, dividing the velocity by 200 means that dx will be the distance run by the train at a certain velocity during 1/200 s, which is the interval considered in our physical model (dt).

Figure 3-18 displays, the influence that the velocity has on the harmonics, and it is easily comprehended that the velocity only affects the frequency on which the harmonics appear but not the amplitude of the harmonics, as previewed. However, the change of velocity for lower discretization introduces changes in the CC because the points of data will not probably match the exact frequency of the peak, and will have significant changes depending on the velocity and dx.

It was considered as standard the division of the velocity by 200, which creates data spaced in time by 0.005 s, however for this value, alterations in the velocity create changes on the CC due to the low

number of bins, which is not recommended to happen since it may introduce divergent results. To consider a smaller interval between data points it is necessary the introduction of zeros in the Fourier Transform.

It was considered that the division of the velocity per 500 and the improvement of the discretization by introducing zeros in the FFT by multiplying the length of the standard vector by four would be enough in this case. The achievement of a good discretization should be analysed case by case, to make sure the df considered is enough. It is here stated also that all the CC plots in this thesis were made with these definitions.

Figure 3-19a shows the velocity amplitudes for the first four harmonics achieved with the base FFT and it is clear the low discretization this approach produces, compared to the plot obtained with a higher discretization in Figure 3-19b. Thereby, it is important to make sure that the discretization is accurate enough to provide trustworthy results and that the data collected enables reliable results.

a) b)

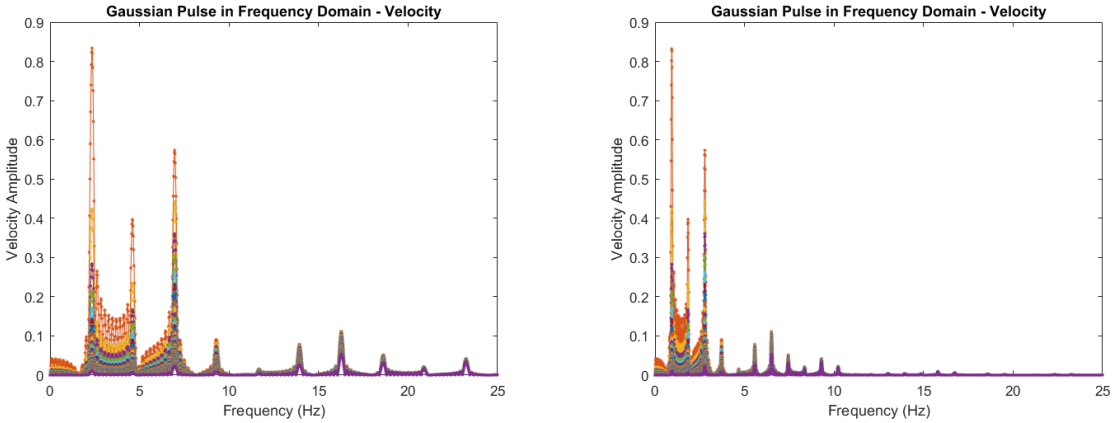

Figure 3-18 – Velocity amplitude in the frequency domain for the Pendolino train at: a) 200km/h and b) 80km/h

a) b)

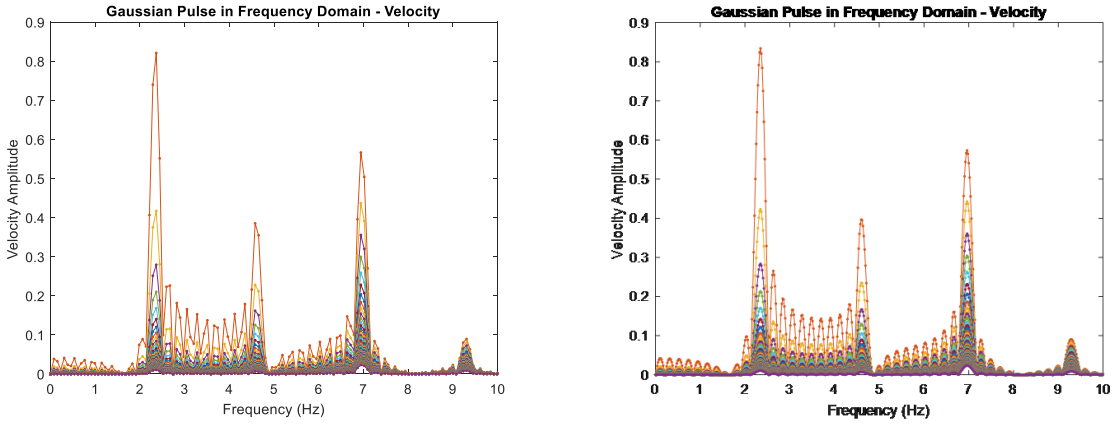

Figure 3-19 – Velocity amplitudes for the first four harmonics of the Pendolino train a) with the base FFT and b) with a high discretization achieved with the introduction of zeros

A further analysis over the importance of the discretization will be made in the next chapter.

3.4.5 COMPARISON BETWEEN METHODS

Figure 3-20 shows the comparison between the two methods: the frequency method as calculated in this thesis (FM-T) and the sleeper displacement method (SDM): 81.5% of the results agree well in a range within $\pm 10 MN/m^2$, a state that covers all the data. Though, some considerable differences appear between two methods that can be explained when considering the characteristics of two sites. A better result than the one obtained by the original authors that may be due to the suppositions made by them.

Sites 1, 2, 4a and 4b present the closest agreement between the two methods, which may indicate that the beam on an elastic foundation is a good representation of the railway track behaviour on the studied sites. These sites cover a high range of stiffness values, which may suggest the capacity of this method to be used in different ranges of track stiffness.

Site 3 shows the highest differences between the two methods. At site 3, according to Le Pen et al.(2016), despite the fact of being a truly high speed site, some voided or partly voided sleepers were observed forming a dip in the track which could have caused changes in the dynamic load and the validity of the model. This creates uncertainty in the actual load, introducing doubt in both methods, which might have affected the agreement. In fact, the railway track behaviour under cyclic load is non-linear and the support conditions vary along the track, which is a reflection of the complex mechanical behaviour of these structures as well as its variability along the line. Nevertheless, some good results were obtained.

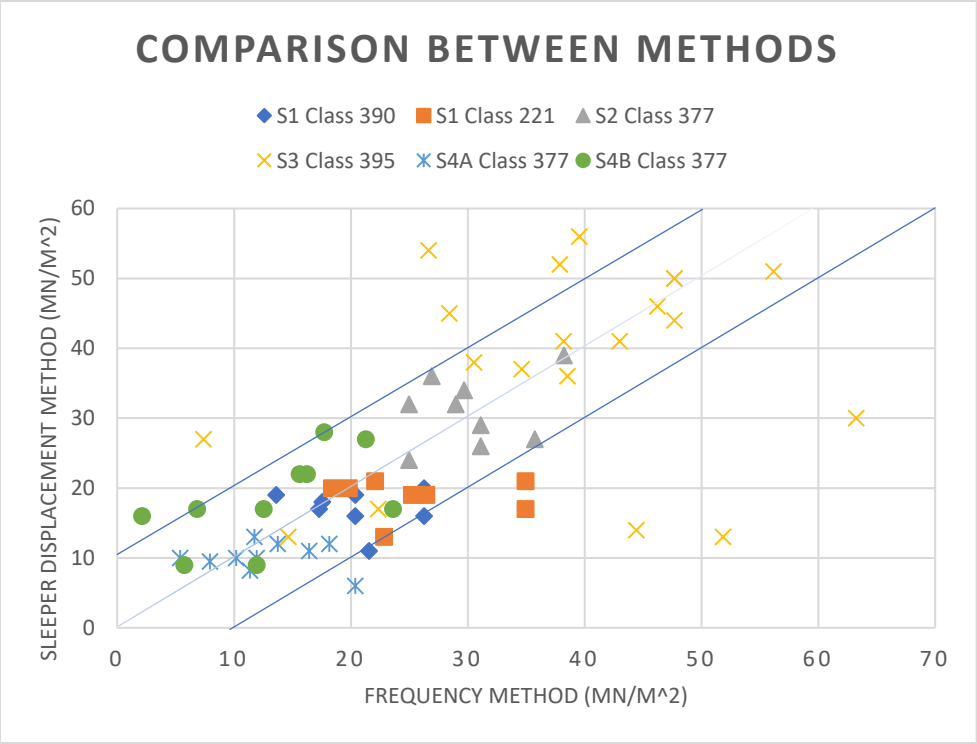

Figure 3-20 – Comparison between frequency and traditional methods

The somewhat less consistency of the results obtained at site 4b can be due to the higher variation between support conditions along the track. The variations at site 1, regarding results of two types of trains, suggest that the support stiffness of the system increases for the Supervoyager. This behaviour is

most certainly due to the non-linear response of the track, in which, the heavier train induce a stiffer track system modulus. This observation is in agreement with Kargarnovin et al.(2005) who stated that different results can be observed at low frequencies (<30Hz) between non-linear and equivalent viscoelastic model.

In general, the results are consistent and the frequency method seems a valid method to adopt to determine the track system modulus. Some inconsistencies may be a result of the presence of voids in some sleepers, like in site 3, or some pronounced non-elasticity subjacent. Some methods have been developed in order to prevent the hanging of sleepers and voids, such as (Muramoto [et al.], 2012).

In this chapter, it was compared the results obtained with the ones from the previous work. The analyses between the results FM and SDM may be found in (Le Pen [et al.], 2016).

3.4.6 FINAL CONSIDERATIONS

The results obtained with the MATLAB script through the frequency method were practically the same as those obtained with the method by Le Pen, et al.(2016). The average track system modulus was 26 $\mathrm{MN/m^2}$ in both cases and the average ratio between these results is 1.0 for both the system and 0.9 for track bed stiffness. These results suggest a good agreement between both results. As explained, part of the differences between results may be explained with different suppositions considered in each approach, some of them, related to the CC's, were discovered, however, other suppositions, especially related to the way of doing the FFT are unknown.

Table 3-11 showed that the results obtained with the MATLAB script and the ones obtained by Le Pen et al.(2016) are consistent with an average between 4.4 and 7.3 $\mathrm{MN/m^2}$ in most cases. Only the site 3a shows lower consistency which could be due to the lower performance of the track.

Table 3-12 showed a better agreement between the FM-T and the sleeper displacement method in site 2 than between the FM and SDM methods, which suggests that the different considerations introduced in the context of this thesis are closer to reality.

It is also important to refer that there is no mention on the work by Le Pen et al.(2016) of the number of cars considered per train, which is another characteristic with important influence in the frequency content of the response of the track, and thus on the calibration curves.

It should be noted, that the average track system modulus for sites 4a and 4b, using the traditional method, seem to be incorrect and do not correspond to the average of the values present in table 7 in (Le Pen [et al.], 2016). In table 5 of the same article, the track system modulus for the fifth sleeper probably should have been 32 $\mathrm{MN/m^2}$ and not 22 $\mathrm{MN/m^2}$. These are minor mistakes that were corrected in the course of this analysis aiming at assessing and minimizing the differences between the approaches under comparison.

The approximation between results from the sites 4a and 4b may be due to the annulation of errors, that is, the several assumptions made and errors through the process may cancel each other or the site/train is not so sensitive to the alteration of such characteristics.

The analysis made above, upon the recalculation of the results from the frequency method, allows the validation of the MATLAB script developed and its capacity to deal with different problems. In fact, several of the assumptions were made to narrow the distance between the model and the reality as shown in the course of that sub chapter, which should lead to more representative results and closer to reality.

However, it seems clear that with the use of the same assumptions, the results would be more similar.

4

Case study: application to two transition zones

4.1 Introduction

After some good results with the use of this method, as displayed in the previous chapter, it will be tested now its capacity when dealing with transition zones.

To do so, the method will be tested for a section of the Portuguese South Main Line, using the results analysed in (Paixão [et al.], 2015) during the study of the transition zones. The data available in the context of this study refers to accelerations and displacements measured as different kinds of trains crossed the transition zones, such as the *Alfa Pendular* (AP), which are the Portuguese high-speed trains, the *Intercidades* service trains (Intercity Express (IE)) and the Coal Freight trains (CF). This creates a wide range of challenges while testing the method in various situations.

Firstly, this chapter will present a brief description of the Alcácer bypass, more concretely, the two sites studied and the train types under analysis. Secondly, the way the data was collected and the differences that were introduced in the developed script to adapt it to this new situation will be explained. Finally, it will be presented the results obtained as a consequence of the implementation of the method to the sites in study, the respective analysis towards these results and in comparison with results obtained using the conventional methods considered in (Paixão [et al.], 2015). The study of the two sites selected was only possible due to the data kindly provided by the authors.

4.2 The railway tracks

Both transition zones under study are part of a recent section of the Portuguese South Main Line - the Alcácer Bypass - that is approximately 28.98 km long and was designed for mixed traffic that allow the trains to pass by with velocities up to 220 km/h (Paixão, 2014).

The track allows loads up to 25 tonnes per axle, with broad (Iberian) gauge of 1.668 m, made of continuously welded UIC60E1 rails. The sleepers used were 2.6 m long monoblock concrete sleepers (SATEPOR TBMP 02) spaced 0.6 m and have the particularity of being compatible with the standard gauge (1.435m). The fastening system in the local is Vossloh W14 with elastomer railpads Zw700/148/165 which static stiffness is around 50 to 70 kN/mm (Paixão, 2014).

A scheme of the track cross section is displayed in Figure 4-1.

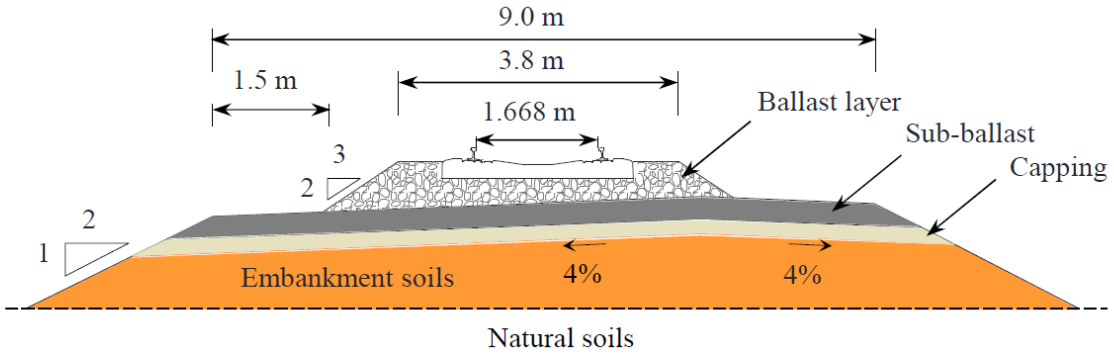

Figure 4-1 - Schematic representation of the standard track cross section on embankment (Paixão, 2014)

A detailed analysis on the Alcácer bypass can be found in (Paixão, 2014). For the purposes of this work, the focus will be on two transition zones, located at km 62.940 and km 81.187 of the bypass, called UP1 and UP2 respectively.

4.3 The Traffic

As already stated, the line allows mixed traffic which includes high speed trains to freight traffic. This will expose the new method under test to different train categories, which will allow an analysis on the influence of different trains in the results obtained. To do so, this subchapter describes the main services on the track and introduces main geometric and load characteristics for each kind of train.

The *Alfa Pendular* (Figure 4-2) train is the fastest passenger train in Portugal. It consists of a 6-coach tilting passenger train that travels at a maximum speed of 220 km/h. Under normal conditions, there are two daily trains per direction connecting Lisbon to Algarve. This model is similar to the ETR 401 Pendolino from the family of the Pendolino trains used in the previous chapter.

It is important to notice that the distribution of loads per axle in the model is not regular and has slight changes that derive from the fact that all the cars are different. However, besides these differences, the average loads are similar with the biggest differences, between loads, being around 6% of the axle load.

The *Intercidades* (Intercity Express (IE)), represented in Figure 4-3, consists of an electric locomotive and 3 to 7 coach cars, depending on the expected number of passengers. At present, the locomotives are usually the CP 5600 model by Siemens but used to be the CP 1900 model. This service uses the Alcácer bypass since 2011 when the travel maximum speed of this trains was 160 km/h. An update on the coaches' bogies allowed the IE to a new maximum service speed of 200 km/h. Nowadays, there are usually 3 daily trains linking Lisbon to the Algarve in each direction.

The average loads per axle are extremely consistent in the Intercity Express Trains, a detail that agrees well with the good use of the method in experiment. However, the previous statement is valid only for the passenger cars and not when considering the locomotive. So, to improve the efficiency of the method, only the passenger cars shall be considered, thus excluding the locomotive. It must also be noticed that the high differences present between the locomotive and passenger car loads (213.4 kN and 123.1 kN respectively) may influence the method, a topic that will be analysed later in this chapter.

a)

b)

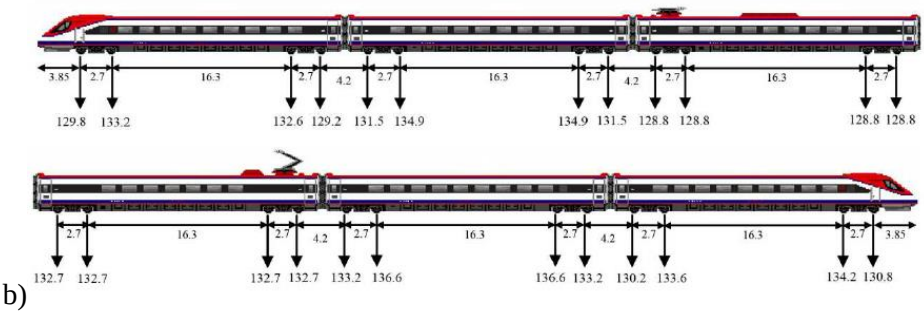

Figure 4-2 - The Alfa Pendular train: a) general aspect and b) schematic representation of the axle spacing and respective axle load estimation (Paixão, 2014)

a)

b)

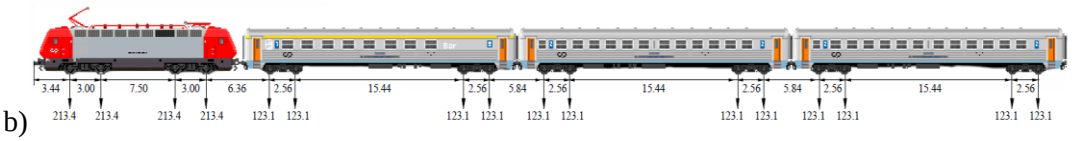

Figure 4-3 - Intercity Express (IE) - a) General aspect and b) schematic representation of the IE and respective axle position and loads estimation (Paixão, 2014)

The freight traffic in the bypass is a way of transportation of a wide variety of goods such as coal, liquids fuels or even containers. Normally, there are about 15 to 20 freight trains per day, running at speeds

about 60 km/h to 100 km/h. The longest and heaviest ones are usually those carrying coal from the Sines Port to the Pego power plant.

The data provided by Paixão (2014) comprehend several Coal Freight Trains (CFT), displayed in Figure 4-4 and containers trains. However, significant differences between axle loads of the container freight trains were found due to the fact that containers come in different shapes that require different wagons (with different axle arrangements) and the containers are usually filled with different products, thus creating an obstacle to the proper use of the method under testing. Therefore, these trains were not considered in this analysis.

The Coal Freight Trains have three advantages for their consideration in this analysis: i) they have regular weight/axle load; ii) the wagons are mostly identical, thus have regular geometry and iii) normally they consist of a high number of cars (up to 25 cars). For an efficient use of the method, the locomotives should not be considered so the tested axle load is as regular as possible, since there are high differences between the loads and geometry between the locomotives and the wagons.

a)

b)

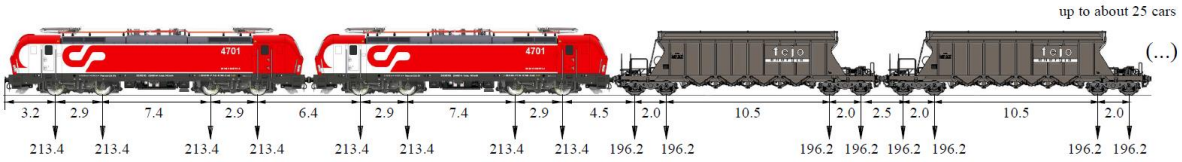

Figure 4-4 – Coal Freight Train (CFT) - a) General aspect and b) schematic representation of the CFT and respective axle position and loads estimation (Paixão, 2014)

4.4 The transition zones to underpasses UP1 and UP2

As already explained, the goal of this chapter is to test the method using data obtained in two transition zones to underpasses UP1 and UP2 (Figure 4-5).

Their design is in accordance with the requirements established in the design by the Portuguese Infrastructure Manager as explained by (Paixão, 2014). Different track support conditions can be found along these transition zones. A scheme of the track with the main characteristics and identification of key locations from S1 to S6 can be found in Figure 4-6. An important aspect of the transition zone at

UP1 is that under sleeper pads were added to several sleepers, identified in Figure 4-6. The USP increases the track flexibility significantly, a phenomenon that should lead to a decrease of the track system modulus, as will be addressed later. Moreover, it is possible to observe that there are differences in the composition of the infrastructure along the transition zone (Figure 4-7 and Figure 4-8), which is intended to smooth the transition from the plain track on embankment to the track on the box culvert. The geometry (Figure 4-8) and material applied in the substructure of the transition zone were established with the aim to control long-term deformations that are normal in this kind of structures, as well as to achieve a smooth transition of the vertical stiffness of the track.

a) b)

Figure 4-5 - UP1 (a) and UP2 (b) view (Paixão, 2014, Paixão [et al.], 2015)

For the purpose of this thesis, a small description of the sites is presented below.

The layers of the backfills (Figure 4-7) were made with Cement Bound Mixture (CBM), Unbound Granular Material (UGM). An average degree of compaction of 100% and 99% was respectively achieved, regarding the Modified Proctor compaction reference test (OPM).

The presence of a superficial layer of sandy and silty clays at UP1 required the replacement of those soils with well-graded crushed unbound granular material down to a depth of about 3.5m. The natural foundation on both sites was usually made of comprised monogranular fine grained sands which provided good foundation conditions (Paixão, 2014).

The track superstructure has the same characteristics as those explained, previously, in this chapter.

In Figure 4-7 it can be seen the main track cross section present in the transitions represented by the key locations S1 to S4. Only the layer of the ballast was kept on the box culverts locations, with the same minimum thickness of 30 cm under the sleepers (Paixão [et al.], 2015).

The presence of USP in 44 sleepers of the UP1 site will require information towards the USP characteristics to take them into account to use the method efficiently. To do so, it is important to know the main characteristics of the USP, displayed in Table 4-1.

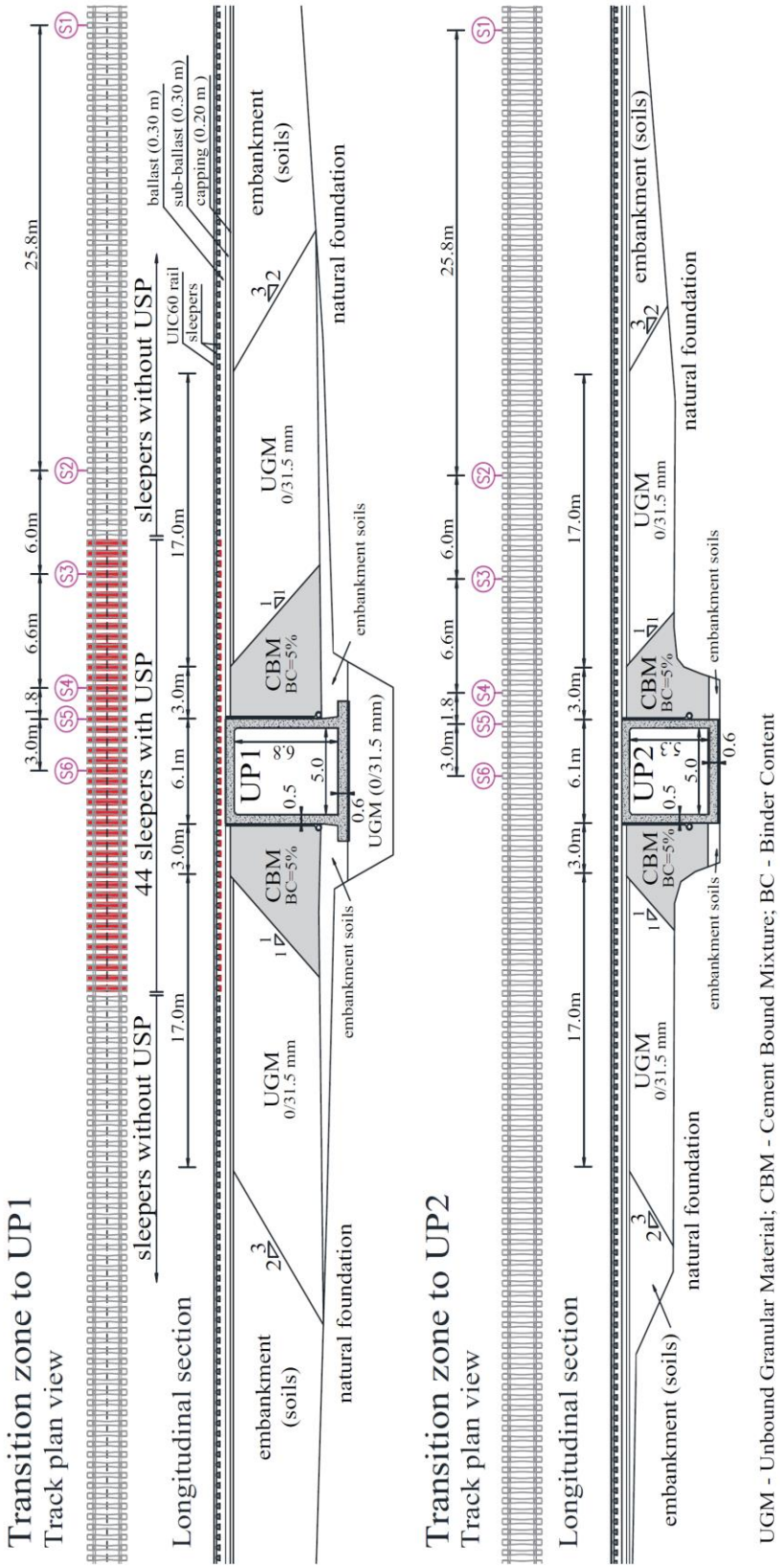

Figure 4-6 - Schematic representation of the sites UP1 and UP2 and its main characteristics

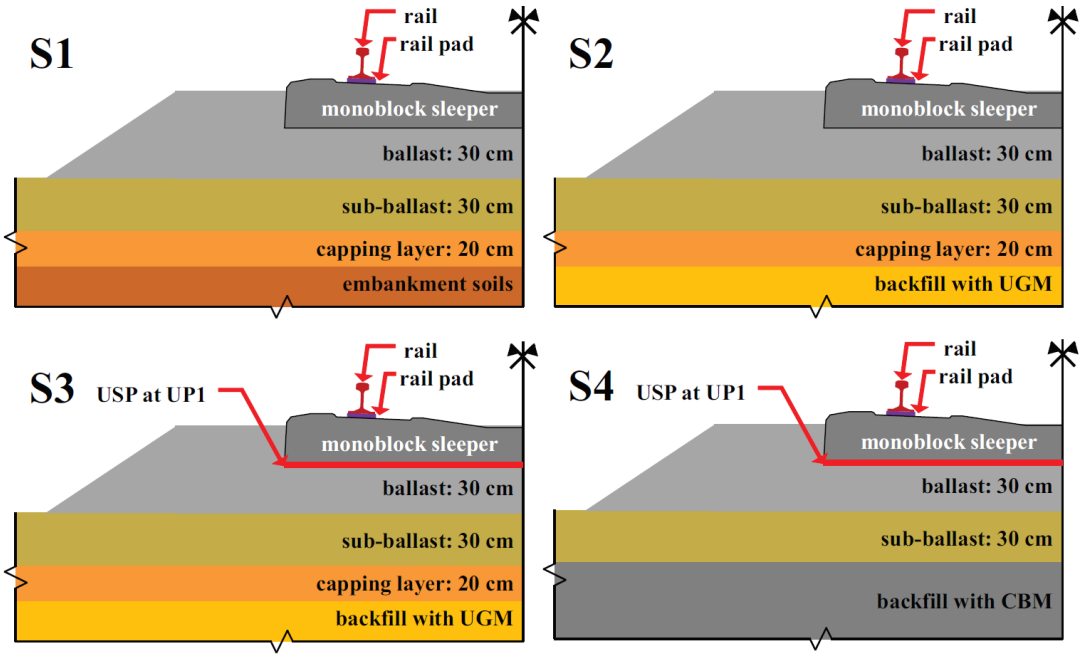

Figure 4-7 - Track cross-section scheme of sites S1 to S4 (Paixão, 2014, Paixão [et al.], 2015)

Table 4-1 - Characteristics of the under sleeper pads, provided by manufacturer, CDM (Paixão [et al.], 2015)

Parameter	Value
Thickness	10 mm
Length	2.6 m
Maximum width	0.3 m
Static bedding modulus, C_{stat} (CEN, 2016)	0.155 N/mm^3
Dynamic bedding modulus, C_{dyn} (CEN, 2016)	0.200 N/mm^3

In the context of our problem, measurements of displacements, velocities or accelerations should allow the use of the script and obtain good results. Shear deformations of the rail were also available to assess the wheel loads, as well as receptance tests (Paixão [et al.], 2015), however, that data was not used in the context of this work.

The data provided included measurements of vertical displacements of the rail, rail-sleeper relative displacements and vertical accelerations of the sleepers. The importance of this chapter is also to analyse the availability of the current technology to get data and how well it can be used with this new method. To do so it is essential to understand how the monitoring of the track behaviour during the train passage was done. With that purpose, it is presented a description of the methods used to collect the data that was analysed.

Identical monitoring set-ups were considered in both sites, as it can be seen in Figure 4-8. Not displayed in the figure was an additional rail displacement transducer placed 40 m away from each box culvert, in open track (Paixão [et al.], 2015).

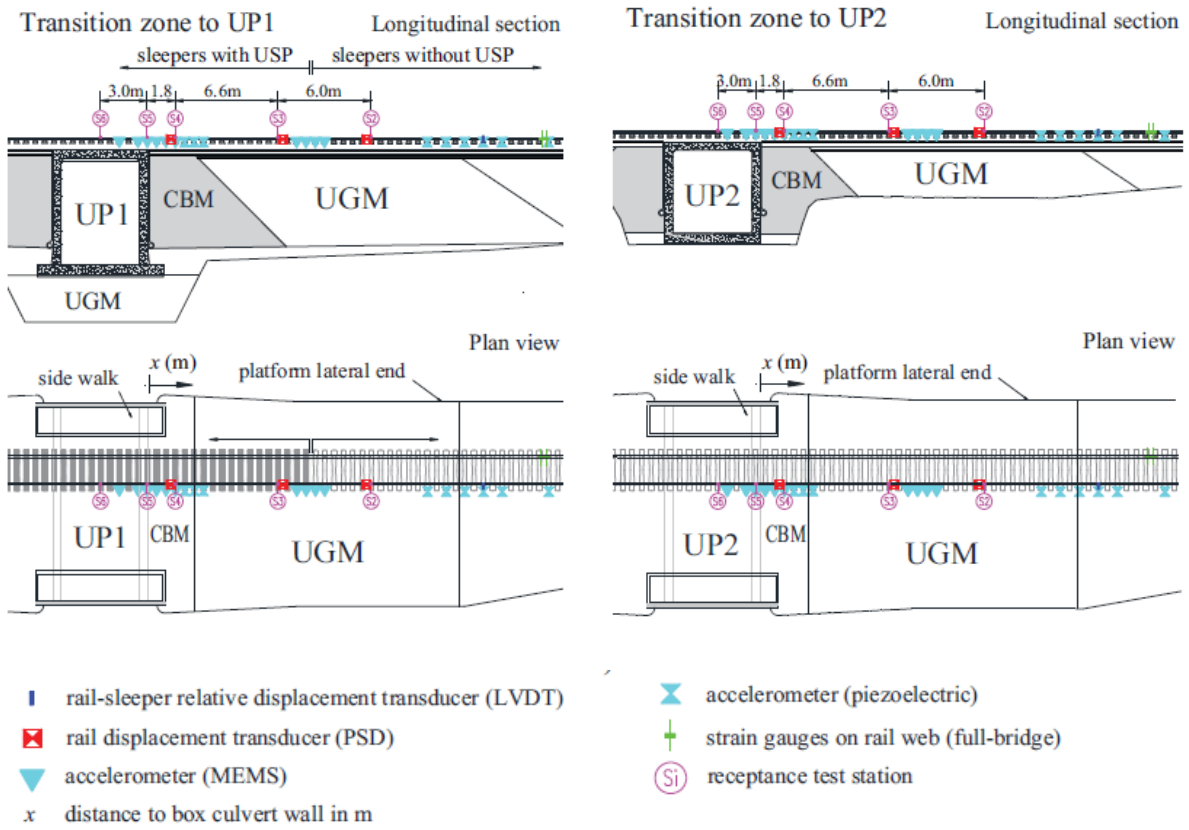

Figure 4-8 - Location of the measurements at sites UP1 and UP2 (Paixão [et al.], 2015)

Absolute rail vertical displacements were measure using optical systems developed to assess the track deflection at a given section (Figure 4-9a and b). Each system is composed by a diode Laser module (wavelength 635 nm; power: 6 mW) that is mounted away from the track and a Position Sensitive Detector (PSD) module (range: ±6 mm) attached to a support fixed to the rail web (Pinto [et al.], 2015). It is possible to calculate rail displacements during train passages thanks to the PSD transducer that allows to measure the variations of the Laser beam position.

The LVDT transducer had a range of ±2.5 mm and a sensitivity of 2 V/mm. Its body was fixed to the sleeper, close to the rail, so that the tip of the armature touched the rail foot.

The vertical accelerations were measured using 9 piezoelectric accelerometers (Figure 4-9d) and 10 Micro Electro-Mechanical System accelerometers (MEMS) and were placed at the sleeper's end (Figure 4-9c). The piezoelectric accelerometers have ±50g of range and a sensitivity of 100mV/g, and the MEMS have ±18g and the same sensitivity.

The acquisition system used in (Paixão [et al.], 2015) comprised a laptop computer, a National Instruments (NI) acquisition unit (compact DAQ 9178 with seven specific modules) and three support units for PSD, MEMS and LVDT transducers. The acquisition frequency rate was of 2000 Hz.

a)

b)

c)

d)

Figure 4-9 – View of the track instrumentation: a) displacements transducers along the studied zone; b) detail of the PSD on the rail web; c) MEMS accelerometers placed on the track and d) Piezoelectric accelerometer.

4.5 Track support stiffness in UP1 and UP2

4.5.1 MATLAB SCRIPT INPUT DATA

The application of the new method to the case studies requires some changes on the developed MATLAB script. To start, it was necessary to add the trains and track main properties. The track main properties will be the same in the course of the entire chapter, since the track sections in study are on a railway stretch that keeps its superstructure characteristics constant throughout its length. The properties of the track superstructure were already described earlier in this chapter.

The train properties vary according to the train category that can be either the *Alfa Pendular*, the Intercity Express or the Coal Freight trains. Data about container freight trains were also available, however, the load per axle on these services showed high variations, as it can be understood from the displacement records in Figure 4-10. Such characteristic could influence the obtained results severely and are against one of the suppositions made to get this method, as stated by Le Pen et al.(2016) and therefore these trains were discarded from the analysis, as mentioned earlier.

The Table 4-2 summarizes the main track characteristics that were taken into consideration on the MATLAB script.

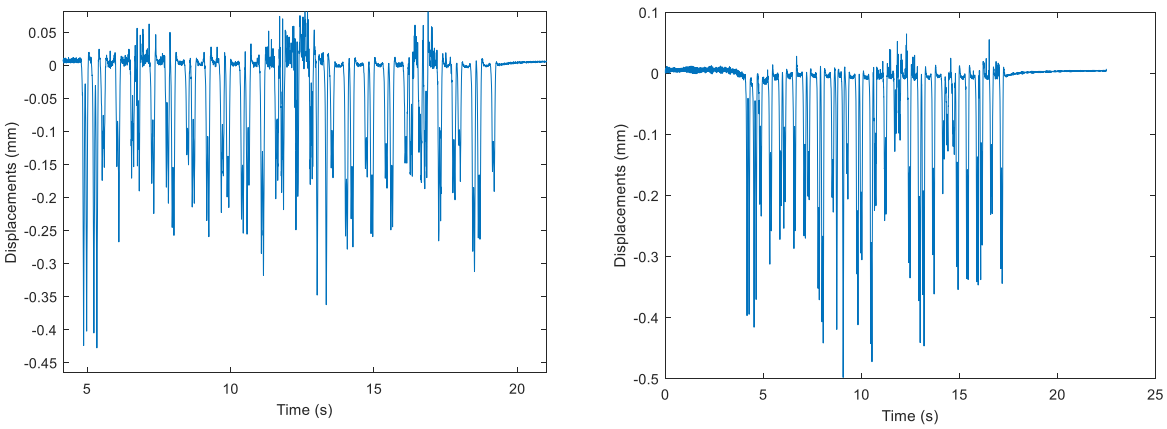

Figure 4-10 - Container freight trains displacements measured with PSD

Table 4-2 - Main track characteristics

Alcácer bypass	
Rail Type	UIC60E1
Sleepers	Monoblock concrete sleepers (SATEPOR TBMP)
Sleeper spacing	0.6 m
Fastening system	Vossloh W14
Railpads	Zw700/148/165

Table 4-3 displays the train data required to run the script to create the Calibration Curves (CC). Although the number of cars of the *Alfa Pendular* service kept the same, the other services are made with trains with different number of cars/wagons.

Table 4-3 – Main train characteristics (excluding locomotives)

	Alfa Pendular **(AP)**	**Intercity Express (IE)**	**Coal Freight Trains (CFT)**
Average weight per axle (ton)	13.25	12.55	20.01
Car length, d_c (m)	25.9	26.4	17
Axle relative position per car, d_n (m)	0, 2.7, 19, 21.7	0, 2.56, 18, 20.56	0, 2, 12.5, 14.5
Average Velocity (km/h)	220	160	80
Number of cars	6	Variable (3-7)	Variable (7-25)

4.5.2 DISCRETIZATION OF THE PROBLEM

A good discretization shall guarantee that differences in the sampling of some variables will produce the same results. For example, in this context, it is interesting to evaluate the importance that the number of cars/wagons has on the final results. As already stated, the Intercity Express has a variable number of cars from 3 to 7, a good sample to evaluate the differences that this variation creates in the CC.

The number of cars/wagons only influences the infinite beam on elastic foundation model due to the number of dynamic loads applied, as can be seen in equations (2-29) and (3-3). To understand its influence, it is displayed in Figure 4-11 the calibration curves of the Intercity Express for different number of cars and for scripts with different characteristics. The differences in the CC in the figures result from the different level of discretization considered in the frequency domain - df. The higher discretization in this analysis was achieved with the FFT with the introduction of more zeros in the vectors of the input data – "zero padding".

In Figure 4-11a it was used a script that divides the velocity during the calculation of dx per 5000 (dt=1/5000), but the discretization achieved is very low. The improvement of discretization can be done by increasing the number of outputs/bins requested, which can be directly achieved in the script by changing the N variable in the algorithm of the script to twice, four times or higher when compared to the base value. This was possible because the algorithm of the Fast Fourier Transform (FFT) is based on decomposing an N point sequence into an N/2 point sequences and obtaining an N point DFT. To do so, $N=2^n$ and "n" is an integer (Rao [et al.], 2011).

The algorithm of the FFT is based on the following equation:

$$X^F(k) = \sum_{n=0}^{N-1} x(n) W_N^{nk} \tag{4-1}$$

with k=0, 1, 2, …, N-1.

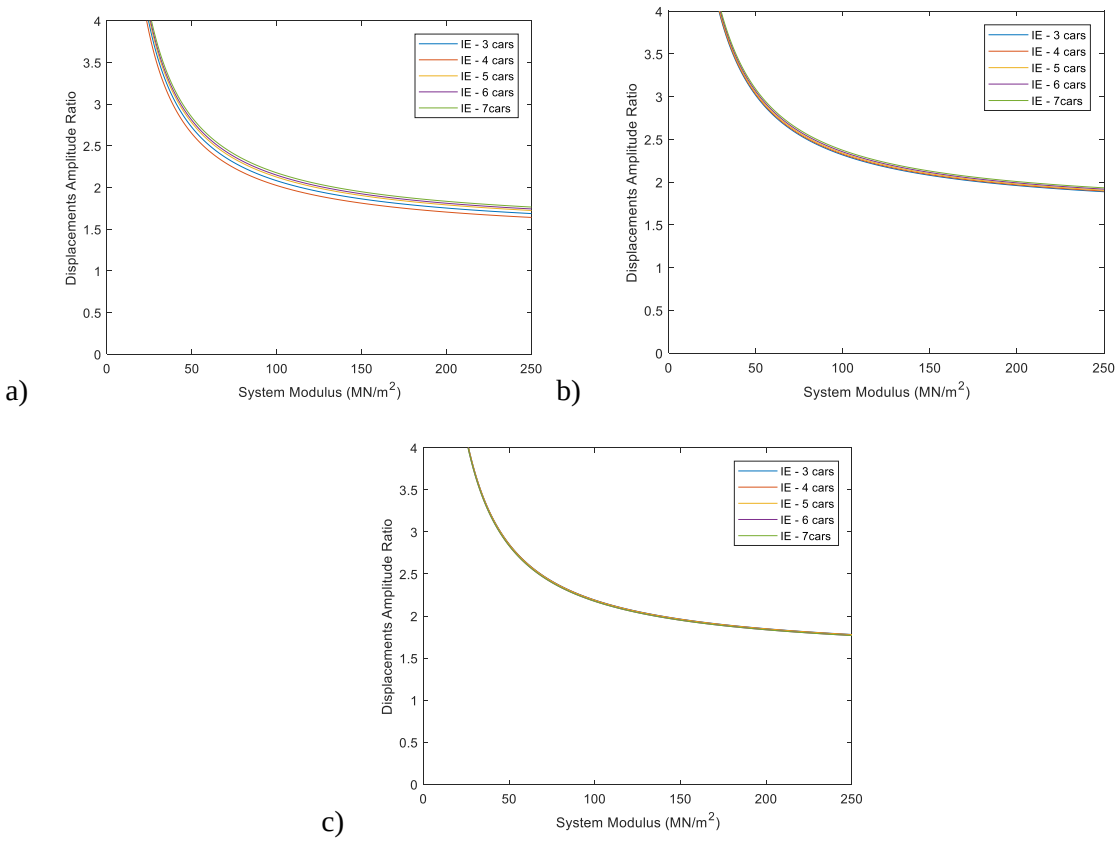

Figure 4-11 - Calibration curves for IE and standard velocity of 160 km/h: a) dx velocity divided by 5000 (df=0.0954); b) dx velocity divided by 500 (df=0.0763); c) dx velocity divided by 500 and introduction of zeros to improve discretization (df=0.0191)

The achievement of a higher discretization by dividing the velocity by a smaller amount of time is very hard to control and happens within a cycle, which means that the values of df go up or down depending on the number of bins per interval, as explained in the previous chapter. This means that it is not possible to reach very high levels of frequency discretization, since geometric characteristics and the Fourier Transform influence the results. Therefore, different trains may have different df according to velocity, or other characteristics that may change the location or introduce more numerical data points. Even a change in the number of cars can lead to different results as it can be seen in Table 4-4.

Figure 4-11b displays the CC obtained when dividing the velocity used to calculate dx, as seen in the previous chapter, per 500 (df = 0.0763 for 7 cars per train), which leads to a higher discretization. It is important to understand that it is considered higher discretization the presence of a higher number of data points on a certain interval. Figure 4-11c displays the CC with a script identical to the previous one but with a higher discretization achieved with the introduction of zeros in the Fourier Transform, as previously explained. A careful analysis over the CC's obtained in c) shows that the differences between the curves are smaller, which suggest that the higher the discretization, the smaller the importance of the number of cars, a phenomenon that happens with other characteristics.

Even though the results in Table 4-4 suggest that having more cars increases the discretization and results accuracy, since the differences in the CC's are dependent on several geometric characteristics and dx, as explained, it shall be defined a minimum df for a certain problem, to make sure the results are trustworthy. Moreover, the achievement of a high discretization is related to several aspects already stated, the introduction of zeros in the Fourier Transform to increase the number of bins is here

recommended as a trustworthy method that does not require much computation effort to achieve reliable results.

Table 4-4 – df according to the number of cars per train for the IE service at 160 km/h

Number of cars in the train	Df
3	0.1907
4	0.1907
5	0.0954
6	0.0954
7	0.0954

Figure 4-12 displays the seventh harmonic for the AP service for several discretization performances. In a) and c) plots, the velocity was divided by 5000 and 500 (dt=1/5000 and dt=1/500) respectively which created quite different peaks that influence the CC's. Even though the peak was quite well recorded in c), it was a matter of some "luck", since a shape like the one displayed in a) could happen changing the geometric characteristics. In plots b) and d), using the respective previous characteristics related to the division of the velocity, it was added zeros through the Fourier Transform to increase the number of bins and the results are very similar between each other, as it can be seen. The df in

Figure 4-12b and d are, respectively, 0.0477 and 0.0381, intervals that enable a good trust in the results obtained. Therefore, it is recommended the use of df less than 0.05 for high velocities and its reduction to 0.03 for lower velocities due to the approximation of the values of the peaks in the frequency spectrum. These values are references based on the results and trains considered (AP for high speed and CFT for lower ones), it is therefore suggested to make an investigation over the train under test, before its application to find an interval df that fulfils the requirements to achieve reliable results.

It was also verified that the application of the method considering a dt=1/500 and the increase by 4 the number of bins led to smaller df (df=0.0191) when applied to coal freight trains with 7 cars due to the lowest velocity (80 km/h) of this service (Figure 4-13), which means that the method adapts to the challenges that appear.

In the rest of the chapter, and to follow the recommendations proposed here, the CC used were obtained with the division of the velocity by 500 (an interval between measurements of 1/500 s) and 4 times the base number of bins to improve the discretization.

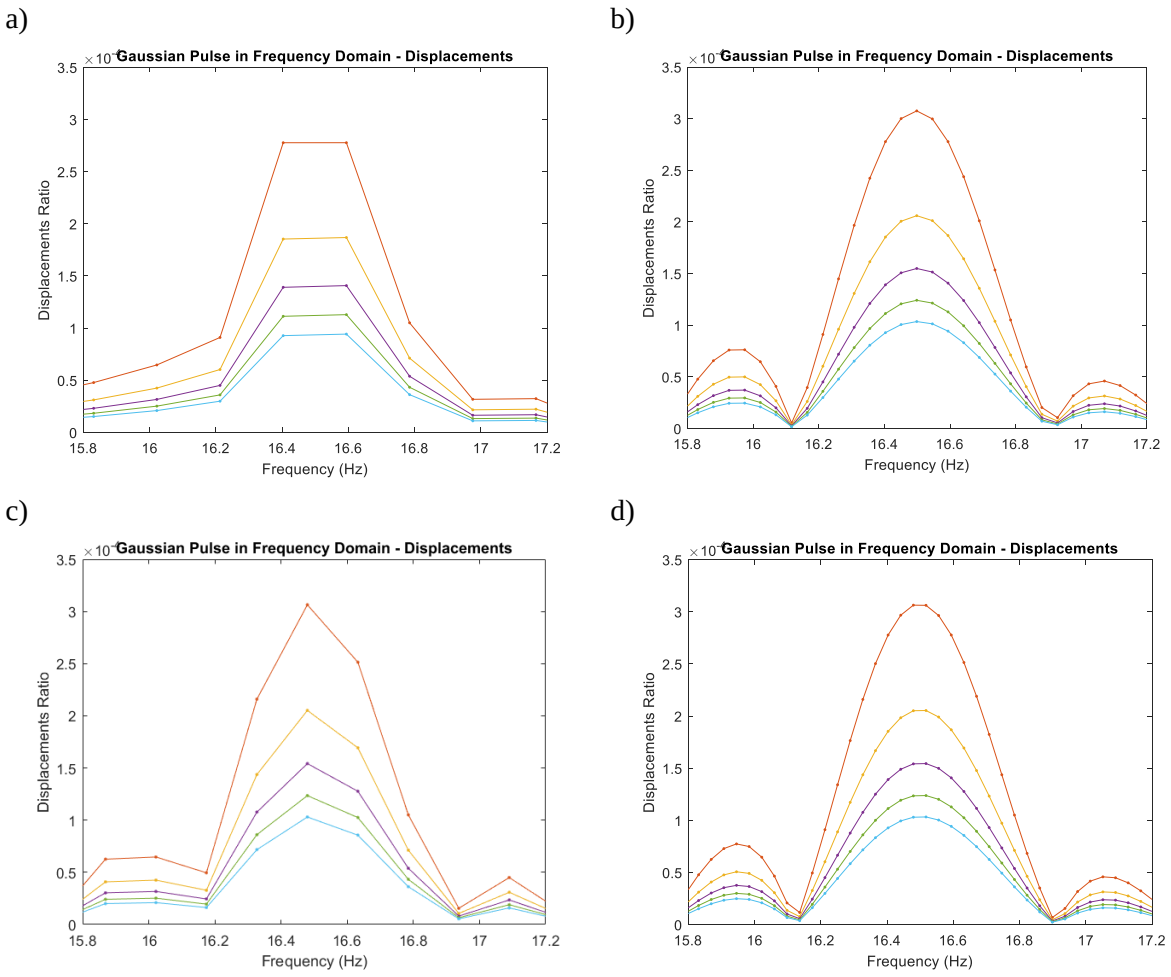

Figure 4-12 – Discretization of the 7th harmonic for the AF: a) dt =1/ 5000; b) zeros were added to the previous plot introduced through the Fourier Transform to increase the discretization; c) dt =1/500; d)) zeros were added to the previous plot introduced through the Fourier Transform to increase the discretization.

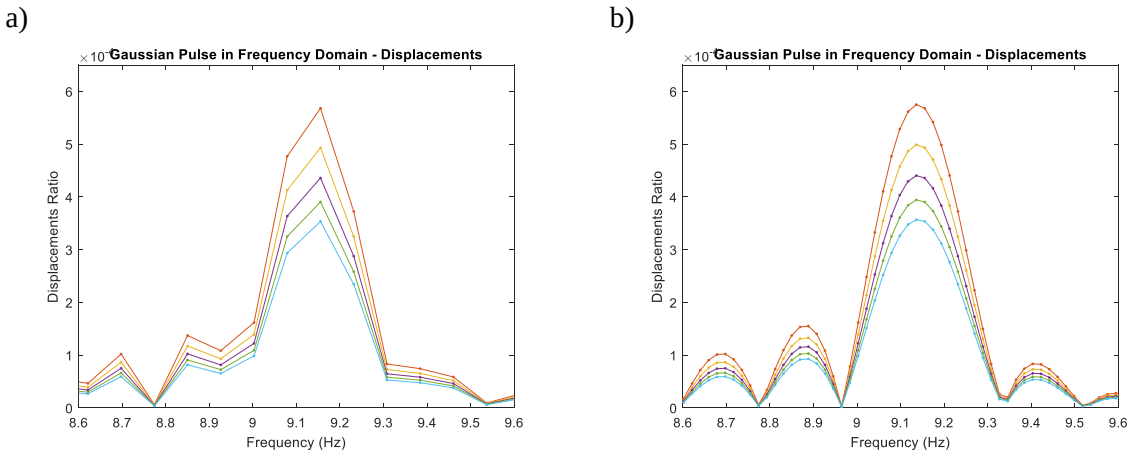

Figure 4-13 – Discretization of the 7th harmonic for the CFT: a) (df = 0.0763) in the dx, the velocity was divided by 500; b) (df=0.0191) to the discretization achieved in a) it was introduced zeros through the Fourier Transform.

4.5.3 DETERMINATION OF THE TRACK SUPPORT STIFFNESS WITH DISPLACEMENT DATA

Firstly, CC were created for this case study and are displayed in Figure 4-14. The displayed CC are for a different number of cars per train for the Intercity Express (IE) service and for the Coal Freight Trains (CFT) service, as a reference to the previous analyse. As expected, the variations in the number of cars are not relevant neither for the CFT neither for the IE service due to the discretization used. The variations on the position of the data points considering different number of cars are not important after the increment of bins of the FFT in the Displacement amplitudes in the frequency domain.

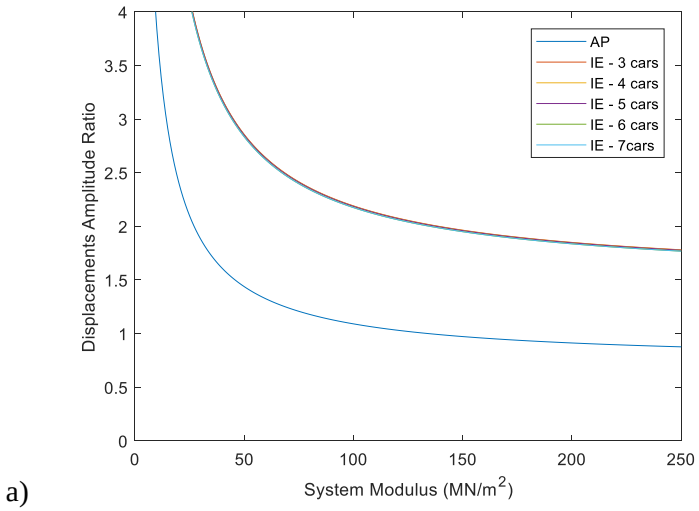

a)

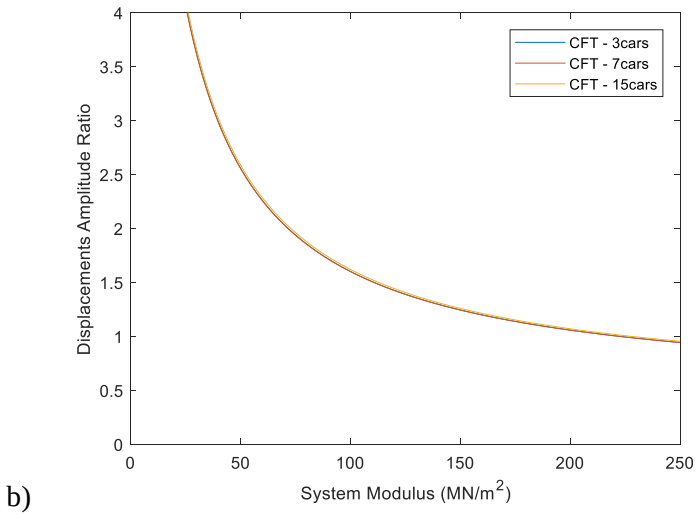

b)

Figure 4-14 - Calibration curves: a) Alfa Pendular (AP) and Intercity Express (IE) for different number of cars and b) for Coal Freight Trains (CFT)

A type II Chebyshev filter with cut off frequency of 80 Hz was applied to the data time history records obtained on site before the application of the developed MATLAB script. This filter was applied to all the data, displacements and acceleration recorded in the bypass. There was no necessity on application of such filter to the model, since values above 80 Hz do not influence the first harmonics.

The use of the MATLAB script previously developed, enabled the quick determination of the displacement amplitude ratios for the available data. To convert these ratios in track system modulus values, the CC was used directly, due to the impossibility to approximate the curves to curves with known equations with the tools available. Therefore, the CC were used as an abacus like the ones displayed in Figure 4-14.

It was verified that the shape of the CC curves that appear bellow, makes it impractical to use the common tools available in MATLAB and Microsoft's Excel to find equations that describe its shape. It is the presence of high alterations in the inclination of the curves with almost two asymptotes, a vertical near k=0 and a horizontal one for variable displacements amplitudes, that prevent the use of the method in practice in the previous chapter. In the previous chapter, the range of the site's track system modulus was lower and the horizontal asymptote did not appear, furthermore, it was used CC related to velocity and not to displacements, which influenced sharply the shape of the CC.

The procedure to determine the track system modulus and track bed modulus were already explained in the previous chapter. For the trains analysed it was also considered the 3rd and 7th harmonics for the determinations of the displacement amplitude ratio.

Table 4-5 and Table 4-6 show the values of the vertical stiffness coefficient (K) as calculated in (Paixão [et al.], 2015) with the conventional method using the PSD displacements data (K_{PSD}), as the *Alfa Pendular* trains passed by, and also using a method based on the receptance curves (K_R). To allow the comparison between the previous values and the ones calculated using the frequency method, the track system modulus (k) values were calculated in the scope of this thesis from the vertical stiffness values thanks to the relations already presented. These methods provide additional information towards the case study to compare with the results obtained. More information towards the receptance method can be found in (Paixão [et al.], 2015).

Table 4-5 - Results obtained via Traditional method with PSD data (PSD) and Receptance method (R) for UP1

Distance (m)	Site	K_{PSD} (kN/mm)	k_{PSD} (MN/m²)	K_R (kN/mm)	k_R (MN/m²)
40.5	S1	83.6	49.7	107.3	69.3
14.1	S2	126.7	86.5	120.8	81.1
8.7	S3	58.1	30.6	58.5	30.9
1.5	S4	47.1	23.1	63.7	34.6

Table 4-6 - Results obtained via Traditional method with PSD data (PSD) and Receptance method (R) for UP2

Distance (m)	Site	K_{PSD} (kN/mm)	k_{PSD} (MN/m²)	K_R (kN/mm)	k_R (MN/m²)
40.5	S1	87.6	52.9	121.1	81.4
14.1	S2	155.2	113.3	147.5	105.9
8.7	S3	133.2	92.4	145.9	104.4
1.5	S4	167.3	125.3	150.7	109.0

It is possible to understand the change of the vertical stiffness, characterized by those two coefficients in the tables above (Table 4-5 and Table 4-6). In UP1, with the approximation to the box culvert and the

improvements made on the substructure to have a smooth stiffness transition, it can be seen that there is an augment in the vertical stiffness from position 40.5 m to position 14.1 m (from section S1 to S2). This is in accordance with the purpose of the transition zone to provide a smooth variation in the track vertical stiffness. However, at UP1, between section S2 to S3, there is a drop in the vertical stiffness with the approximation to the box culvert, a phenomenon that can be explained due to the presence of the USP. On the other hand, at UP2 (Table 4-6), with the absence of USP in sections S3 and S4, the vertical stiffness of the track somewhat increases continuously as approaching the box culvert, despite a small drop between sections S2 to S3. Paixão, A. et al.(2015) stated that this aspect may result from some simplifications made such as the assumption of constant loads of 66 kN. Possible nonlinear behaviour of the track and the influences that the adjacent wheel set in the same bogie might have also influenced the results.

Table 4-7 to Table 4-9 display the track system modulus and track bed system modulus obtained for the different train types analysed and per train and per sections S1 to S4 at UP1, as well as the average results obtained. In general the results are in accordance with the values obtained by Paixão, A. et al.(2015). It can also be concluded that some good results were obtained and that the method has sensitivity to changes in the stiffness along the track, which may indicate applicability in locations like transition zones and not only zones with regular stiffness, though caution is advised due to the limitations of the Winkler model.

Table 4-7 - Track system modulus (k) and track bed system modulus (k_{tb}) obtained with Intercity Express data at UP1 (corresponding to trains 1 to 7)

Distance to box culvert wall (m)			**40.5**	**14.1**	**8.7**	**1.5**	**-0.3**
		Section	**S1**	**S2**	**S3**	**S4**	**S5**
Intercity Express Trains Track System Modulus (MN/m^2)	1	k	65	*	-	-	42
		k_{tb}	85	*	-	-	50
	2	k	48	101	44	47	40
		k_{tb}	58	159	52	77	47
	3	k	56	224	60	44	44
		k_{tb}	70	-	77	52	52
	4	k	84	225	50	50	44
		k_{tb}	121	-	61	61	52
	5	k	92	*	56	51	37
		k_{tb}	138	*	70	63	43
	6	k	54	105	45	49	38
		k_{tb}	67	170	54	60	44
	7	k	58	176	-	47	47
		k_{tb}	74	-	-	57	51
	Average	k	67	166	51	48	41
		k_{tb}	88	165	63	58	48

(*)Values that got out of the range 0 – 250 MN/m^2 and therefore were discarded from the study

(-) Values that were not possible to calculate due to big interferences on the data

Table 4-8 - Track system modulus (k) and track bed system modulus (k_{tb}) obtained with Alfa Pendular data at UP1 (corresponding to trains 1 to 5)

	Distance			**40.5**	**14.1**	**8.7**	**1.5**	**-0.3**
	Site			S1	S2	S3	S4	S5
Alfa Pendular Service Track System Modulus (MN/m^2)	Trains	1	k	-	55	24	-	23
			ktb	-	69	26	-	25
		2	k	-	45	25	-	23
			ktb	-	54	28	-	25
		3	k	27	55	28	27	20
			ktb	30	69	31	30	22
		4	k	31	39	-	25	23
			ktb	35	45	-	28	25
		5	k	29	43	-	22	21
			ktb	32	51	-	24	23
		Average	k	29	47	26	25	22
			ktb	32	58	28	27	24

(-) Values that were not possible to calculate due to big interferences on the data

Table 4-9 - Track system modulus (k) and track bed system modulus (k_{tb}) obtained with Coal Freight Trains data at UP1

	Distance			**40.5**	**14.1**	**8.7**	**1.5**	**-0.3**
	Site			**S1**	**S2**	**S3**	**S4**	**S5**
Coal Freight Trains Track System Modulus (MN/m^2)	Trains	1	k	55	65	34	28	35
			ktb	69	85	39	31	40
		2	k	67	92	36	30	37
			ktb	89	140	41	34	43
		3	k	52	88	30	28	34
			ktb	64	130	34	31	39
		Average	k	58	82	33	29	35
			ktb	74	118	38	32	41

(-) Values that were not possible to calculate due to big interferences on the data

The absence of certain values in the tables, which are represented by a hyphen, is due to the lack of quality on those results, or even sometimes, the impossibility on applying the method due to the quality, corruption or presence of big interferences in the data. It is also important to refer that the tables present the values of the track system modulus and track bed modulus calculated per train passage. That is, for example for the IE service in the UP1, data from 7 trains was available and the respective results are displayed. Each number correspond to a train recorded, a situation that is repeated in every table showing results.

It is also presented values of the track bed modulus (k_{tb}) for low values of track system modulus (k) to evidence the vertical stiffness in the section including the influence of the railpad stiffness. The variations obtained with this coefficient are according to those obtained with the track system modulus, as was expected.

The track bed modulus only seems to be a reasonable approximation to the vertical stiffness modulus for low values of stiffness because the railpad stiffness (k_{rp}) only has influence for these values.

Table 4-10 to Table 4-12 display the results for the IE, *Alfa Pendular* and CFT per section and per train data recorded regarding UP2. Since these values correspond to the UP2 location, it can be noticed the practically constant increase in the track system modulus, a result explained due to the absence of USP. Both tables show an increase in the stiffness with the approach to the UP2, however, the values of the track system modulus obtained in both tables show some variability.

In UP2, the evolution of the track system modulus is similar in the different cases and similar to the ones obtained with both the conventional method and receptance methods (Paixão [et al.], 2015). Which means that by using the frequency method, an increase in the vertical stiffness along the track towards the box culvert was verified.

The differences that exist between the results from both train types may be because the method is better suitable in some situations than in others, due to the specific characteristics of the different situations. This argument will be analysed further below.

Table 4-10 - Track system modulus (k) obtained with Intercity Express data at UP2

Distance to the culver box (m)	**Site**	**Intercity Express Trains Track System Modulus (k) – (MN/m²)**							
		1	2	3	4	5	6	7	Average
40.5	S1	83	41	61	53	100	67	88	70
14.1	S2	-	112	84	-	-	-	-	98
8.7	S3	143	102	*	228	*	*	142	154
1.5	S4	-	*	207	*	195	*	*	201
-0.3	S5	159	159	243	*	175	159	143	173

(*) Values that got out of the range (0 – 250 MN/m²) and therefore were discarded from the study

(-) Values that were not possible to calculate due to big interferences on the data

Table 4-11 - Track system modulus (k) obtained with Alfa Pendular data at UP2

Distance to the culver box (m)	**Site**	***Alfa Pendular* Trains Track System Modulus (k) - (MN/m²)**					
		1	2	3	4	5	Average
40.5	S1	34	38	36	44	35	37
14.1	S2	60	51	52	-	-	54
8.7	S3	55	58	64	49	45	54
1.5	S4	61	80	107	98	64	82
-0.3	S5	50	93	80	70	-	73

(-) Values that were not possible to calculate due to big interferences on the data

Table 4-12 – Track System modulus (k) obtained with CFT data at UP2

Distance to the culver box (m)	Site	CFT Track System Modulus (k) – (MN/m²)
		1
40.5	S1	88
14.1	S2	-
8.7	S3	136
1.5	S4	98
-0.3	S5	123

(-) Values that were not possible to calculate due to big interferences on the data

To help the procedure of making a valid analysis of the results obtained, Figure 4-15 and Figure 4-16 display the average track system modulus per site and per train, as well as the values obtained in (Paixão [et al.], 2015) for both methods: the conventional one obtained with the PSD displacements and with the receptance method.

The values obtained in Figure 4-15 show less dispersion than those in Figure 4-16, except at section S2 in UP1 regarding the IE and at section S1 in UP2. This phenomenon seems to occur and increase with the growth of the track system modulus. The shape of the CC may explain such a phenomenon, since the CC for displacements have almost two asymptotes, as mentioned earlier: one vertical near the zero and one horizontal with the increase of the track system modulus (Figure 4-14). This shape has contrary effects when the track system modulus is high or low: low track system modulus values only change slightly for considerable changes of the displacements amplitude ratio; however, at higher track system modulus ranges, significant changes are verified even for very small changes of the displacements amplitude ratio.

This is a key issue for the application of the method since it shows different levels of accuracy of the method when determining the track system modulus: low values of track system modulus determined with displacement data are more accurate than high track system modulus.

One hypothesis to overcome this difficulty to determine the track system modulus for high values is to use different CC (velocity or acceleration) and/or use other type of trains. It is, therefore recommended an analysis of the train CC, before the collection of the data, and choose the train type according to the analyse made.

At UP1, the values obtained with the 3 types of trains tested are similar, probably due to the lower track system modulus values that enables a high accuracy from the CC, especially at sections 3, 4 and 5, a better agreement were achieved. The IE presents the higher results for track system modulus, especially at section 2, where a small change in the displacement ratio is a huge variation in the track system modulus due to the shape of the CC as explained. The differences that can be observed between the results for low track system modulus may be caused by some non-linearity present in the sections under study which would explain why the track system modulus at both UP1 and UP2 is higher for the CFT (heavier trains) when comparing to the AP service. Though that does not explain why the IE presented the higher values of the track system modulus. Differences between the trains weight depending on the schedule and occupancy and high differences between the weight of the locomotive and the other cars may introduce influences in the data recorded that were not took into account in the model produced to achieve the CC.

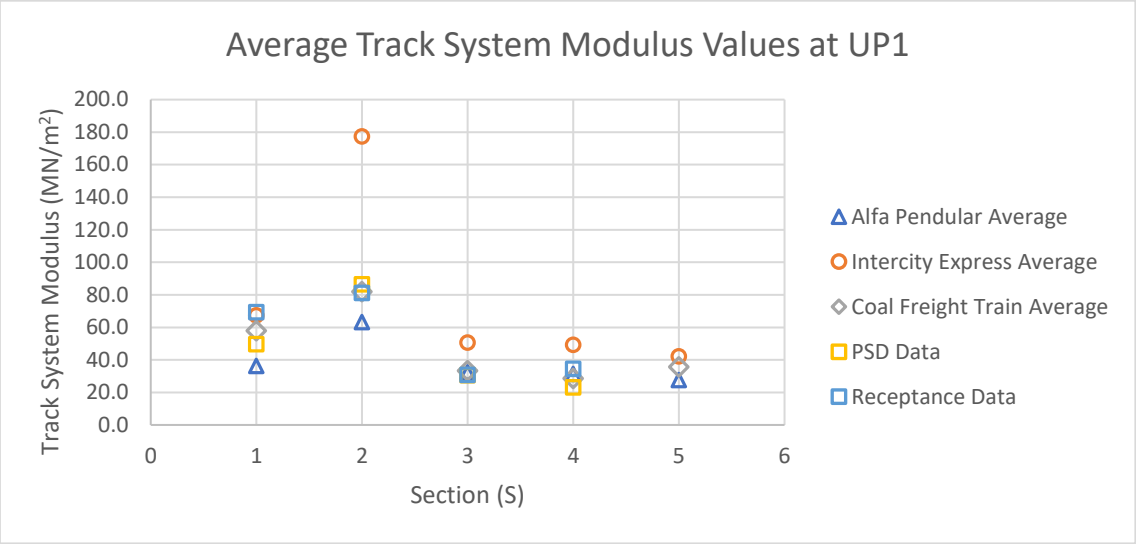

Figure 4-15 - Average values of track system modulus at UP1

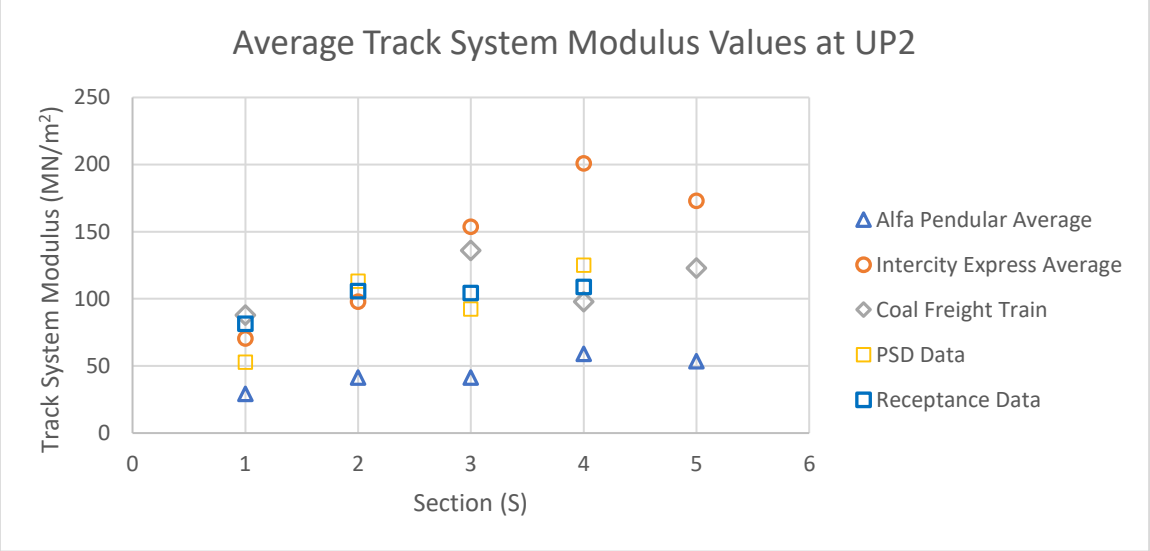

Figure 4-16 - Average values of track system modulus at UP2

Similar issues can be found at UP2, where the IE presented the highest values, and the AP the lowest. It was verified the limitation of using data from the AP to obtain high values of track system modulus on any section studied. The AP trains model present the highest variations between axles along the train when comparing to the other train types used, since all the cars are different. It also possesses the highest variations of dynamic loads due to the highest speed achieved, factors that may explain what happen.

The CFT presented the results more similar to the ones obtained with other methods, a fact that is according to what would be expected. These trains present a high number of cars with similar weight that run at lower velocities, which leads to lower variations on the dynamic loads.

The presence of a high number of cars in each CFT, even though it is according to previous recommendations, may create harmonics with several identical peaks as it can be seen in Figure 4-17a, which is a challenge when the method requires the determination of the peak. To surpass this difficulty,

it was used in these cases, only 7 cars, a number of cars that already achieved good results in the previous chapter, and enough small to create singular peaks for the harmonics as it showed in Figure 4-17b.

a) b)

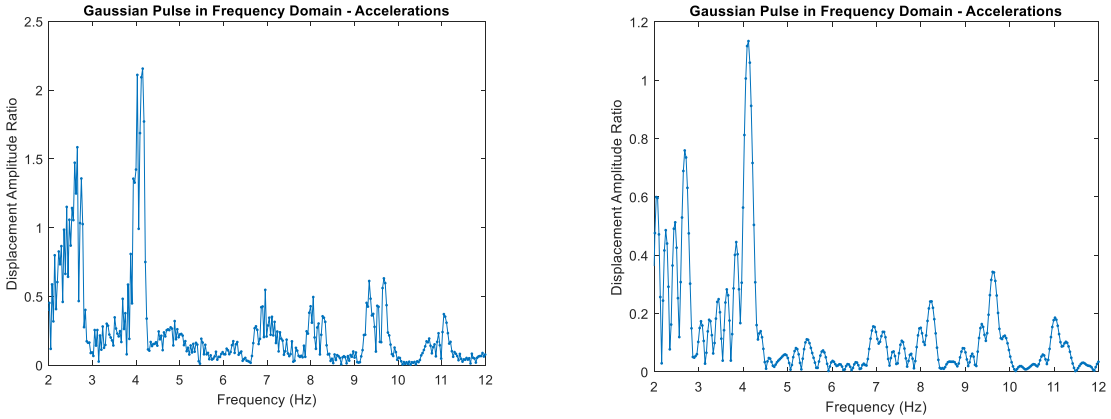

Figure 4-17 – Displacement Amplitude Ratios in the frequency spectrum for a) all cars in the CFT and b) the last 7 cars in the CFT.

It shall be added that the 7 cars considered were the last ones on the train, where there is no influence of the locomotive axle loads. The consideration of fewer cars reduces the window of time under study, which may provide to be safer in the event of the train being increasing or decreasing its speed, probably the reason of appearance of several peaks for the same harmonic. Although it is recommended, in the absence of several peaks for the same harmonics, the use of the higher number of cars possible, which would improve trust in the results achieve, meaning that the reduction of the number of cars considered is a measure to take when there are several peaks for the same harmonic.

The shape of the CC for this kind of trains also benefits its use since the variations in its inclination are not so abrupt and variations of the displacement amplitude ratios will not affect much the track system modulus when comparing to the IE and AP. This phenomenon happens because the inclination of the CC for higher track system modulus is bigger when compared to the other CC.

The high sensitivity of the method at higher track system modulus values is a phenomenon that can be observed through all the data collected and that is explicit in Figure 4-18, where the displacement amplitude ratios obtained and the respective track system modulus for the AP service in UP2 are displayed. It is worth mentioning that even though the dispersion of the displacements amplitudes is quite regular, the track system modulus dispersion is different and increases with the track system modulus. Track system modulus values above 50 MN/m^2 for the AP start to have significant changes due to the slightest variations of the amplitude ratios, which means that high values are a lot more susceptible to the influence of unwanted effects, such as noise in the measurements, than lower values of track system modulus.

It was verified in S1 (see Figure 4-18), for the *Alfa Pendular* train, that variations of about 0.25 in the amplitude ratios correspond to variation of 7 MN/m^2 for low values of track system modulus (values between 20 and 40 MN/m^2), however, that the same variation of 0.25 in S4 leads to variations of about 27 MN/m^2 in the range of track system modulus values between 48 and 75 MN/m^2. Differences that get higher for higher track system modulus.

a)

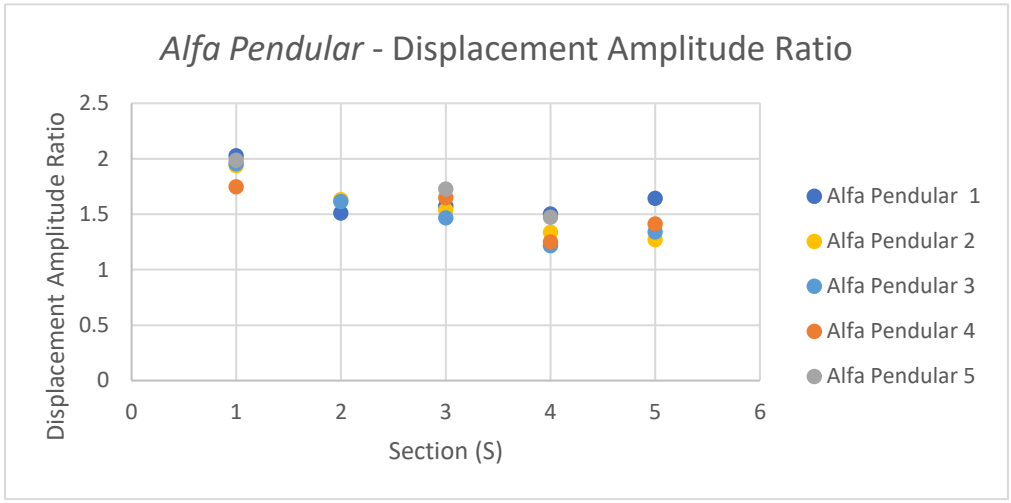

b)

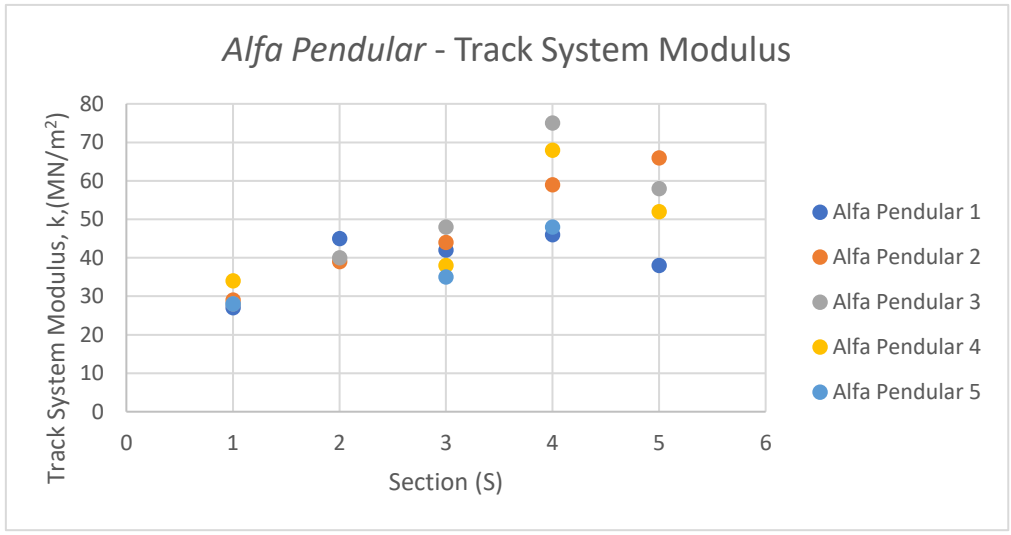

Figure 4-18 – a) Displacements amplitude ratios per section and respective b) Track System Modulus per site for the Alfa Pendular (AP) at UP2

The Table 4-13 and Table 4-14 display the absolute and relative errors between the method in test and the other two under comparison.

Regarding the UP1, the results of the *Alfa Pendular* present differences of 16.5 MN/m^2 towards the traditional method and 22.3 MN/m^2 towards the receptance one. These differences are lower than those obtained in UP2, where the average differences reach 52.2 MN/m^2. Such difference, as already explained, is mainly due to the shape of the CC, a conclusion that may be also applied to the IE results. The high differences between the results obtained according to the sections may be related to higher track system modulus, however, the presence of weight differences and variations in the dynamic loads due to the velocity are probably also responsible for some poorer results, especially with AF and IE services.

Table 4-13 - Errors between the frequency method and the conventional method and the receptance method at UP1

Errors/Differences						
Sections	**Conventional Method**			**Receptance Method**		
	AP	IE	CFT	AP	IE	CFT
	Absolute difference (MN/m^2)					
S1	20.7	15.6	8.3	40.3	4.0	11.3
S2	39.1	79.7	4.8	33.7	85.1	0.5
S3	4.9	20.4	2.8	5.2	20.1	2.5
S4	1.6	24.9	5.6	9.9	13.4	5.9
Average	16.5	35.2	5.4	22.3	30.7	5.0
	Relative difference					
S1	0.42	0.31	0.17	0.58	0.06	0.16
S2	0.79	1.61	0.10	0.49	1.23	0.01
S3	0.10	0.41	0.06	0.07	0.29	0.04
S4	0.03	0.50	0.11	0.14	0.19	0.09
Average	0.33	0.71	0.11	0.32	0.44	0.07

Table 4-14 - Errors between the frequency method and the conventional method and the receptance method at UP2

Errors/Differences						
Sections	**Conventional Method**			**Receptance Method**		
	AP	IE	CFT	AP	IE	CFT
	Absolute difference (MN/m^2)					
S1	23.7	17.6	35.1	52.2	11.0	6.6
S2	72.0	15.3	-	64.6	7.9	-
S3	51.0	61.3	43.4	63.0	49.4	31.6
S4	66.0	75.7	27.3	49.8	92.0	11.0
Average	52.2	42.5	35.2	57.4	40.0	16.4
	Relative difference					
S1	0.45	0.33	0.66	0.64	0.13	0.08
S2	1.36	0.29	-	0.79	0.10	-
S3	0.96	1.16	0.82	0.77	0.61	0.39
S4	1.25	1.43	0.52	0.61	1.13	0.13
Average	1.01	0.80	0.67	0.70	0.49	0.20

The IE yields some of the highest results on both locations with some significant variations when compared to the results obtained with other train types. Part of these variations may be due to the low number of cars present in most of the studied trains and its variability, since more than 50% of the trains

studied had only 3 passenger cars, which may not create the needed harmonics for the use of the method (Le Pen [et al.], 2016). Thereby, it is here also recommended not to use trains with less than 4 cars for study, since the results are not very trustworthy. The big differences between the weight of the passenger cars and the locomotive may also introduce some influence, even though the locomotive data was not considered. Since the locomotive has axle loads significantly higher than the ones from the passenger cars, it will have influence in the results which is not taken into account in the model. This happens because the model is made of a beam that represents the rails. The presence of a high load affects the surrounding areas in the model which means that there will be effects on the rails. This problem could be eliminated in the presence of a higher number of cars and maybe the consideration of only the cars that are further away from the locomotive.

Regarding the UP1 site, it can be easily noted that the CFT has the best results with an average absolute difference of 5.0 MN/m^2 towards the receptance method and 5.4 MN/m^2 towards the conventional method. The results are considered satisfactory and they illustrate that the method can produce good results even in transition zones, where the method was expected to reduce its performance, but it was still possible to assess high variations in stiffness with this approach. The CFT data presents good results when comparing the frequency method to the receptance method, on both cases, which is according to what would be expected. Besides, in UP1 the average error between both methods is 7% and in UP2 20%, which still suggest that the frequency method has some trouble with high track system modulus values that can be related with the already exposed problem of the shape of the CC.

From the previous analyses, it is confirmed the importance of having a high number of cars in the train and the regularity of the weight of the cars in analysis. It is recommended to avoid the presence of trains with big differences in weight, even though those cars/locomotives are not considered in the analyses, since it may have some influence in the results. It is suggested the use a minimum of 7 cars/wagons (like the data used with the CF trains) and never less than 4 cars as recommended in (Le Pen [et al.], 2016). It is also recommended the use of trains with a regular velocity, since that can affect the location of the peaks of the harmonics and produce harmonics with several peaks.

Finally, it can be concluded that some good results were obtained in the course of this chapter with PSD data, especially the ones obtained for low values of stiffness. However, linking the results from this and the previous chapter, it is here recommended to use the data from geophones rather than PSD. It was verified that PSD data is susceptible to noise and interferences which may influence the results, so it is here recommended the use of recording devices that minimize these issues. As already explained, not all disturbances will have influence at low frequencies and most of the interferences can be eliminated with filters. Even though the presence of dust or other elements affects the PSD recording system more, which may create some interferences that are hard to minimize its effect. It is then necessary to make an evaluation of the site to make sure that the recorded signals are as "clean" as possible.

4.5.4 DETERMINATION OF THE TRACK SUPPORT STIFFNESS WITH ACCELERATION DATA

As usual, the application of the script to new data started with the creation of the respective CC (Figure 4-19a). Unlike with the CC obtained for displacement data, the ones for acceleration allow the use of the method introduced in previous chapter to automatize the conversion of the amplitude ratios into track system modulus using MATLAB and Excel tools.

Figure 3-19b and Table 4-15 display the inverted curves and coefficients used to create the inverted CC, respectively, as already explained in the previous chapter. The order of the polynomials was chosen so the norm of residual (error) was less than 1. This means that the curves obtained are already very close approximations to the inverted CC and that the accuracy considered is more than enough so there is no influence over the frequency method and errors that may appear on the final results will not be caused by this process.

a) b)

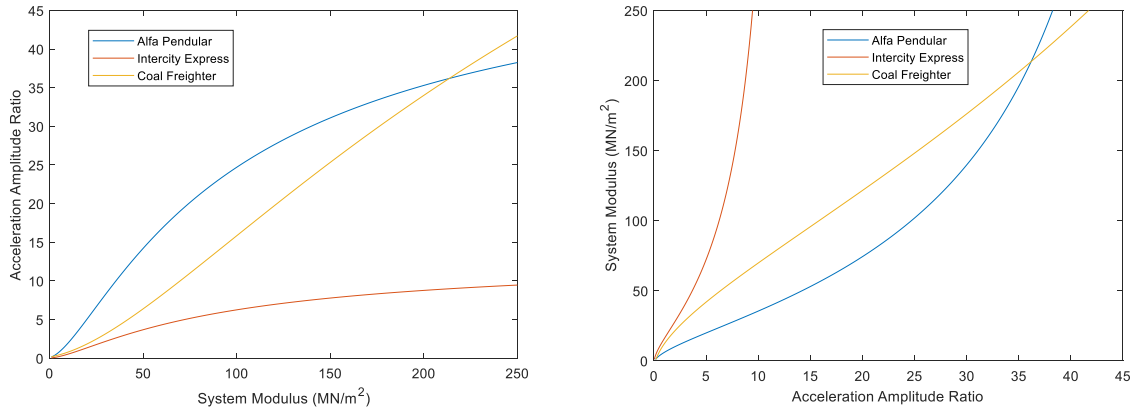

Figure 4-19 – CC for acceleration data for the AP, IE and CFT: a) regular shape, b) with inverted axis

Table 4-15 – Coefficients used to construct the inverted CC

Coefficients	AP	IE	CFT
a	0	-3.58×10^{-6}	-4.80×10^{-12}
b	0	1.87×10^{-4}	1.07×10^{-9}
c	-4.65×10^{-10}	-4.21×10^{-3}	-1.03×10^{7}
d	8.58×10^{-8}	5.36×10^{-2}	5.61×10^{-6}
e	-6.42×10^{-6}	-4.23×10^{-1}	-1.89×10^{-4}
f	2.57×10^{-4}	2.15×10^{0}	4.12×10^{-3}
g	-6.00×10^{-3}	-7.10×10^{0}	-5.82×10^{-2}
h	8.44×10^{-2}	1.50×10^{1}	5.26×10^{-1}
i	-6.67×10^{-1}	-1.93×10^{1}	-2.98×10^{0}
j	5.68×10^{0}	2.52×10^{1}	1.56×10^{1}
k	6.99×10^{-1}	3.74×10^{-1}	-1.15×10^{0}

The accelerations were recorded with 2 types of accelerometers as already explained (piezoelectric accelerometers and MEMS accelerometers). Table 4-16 displays the track system modulus measured with those two types of accelerometers for five AP, three CFT and three IE trains at the UP1 site. It is also displayed the average results per each train type.

The absence of some results on the table is due to the presence of high interferences that occur especially for IE services and for MEMS accelerometers. Figure 4-20 shows acceleration data recorded for AP and IE with piezoelectric accelerometers and MEMS accelerometers. Even though good data was recorded for both AP and IE with the Piezoelectric (PE) accelerometers, the MEMS data shows a lot of disturbances for IE services (Figure 4-20c). While Figure 4-20a-c data allow very good plots, where it is possible to distinguish the passage of the different cars and locomotive, that is not possible with the plot in Figure 4-20c regarding a MEMS recording as an IE train passed by. And since it is required the elimination of the locomotive data because of the huge differences that exist between the weight of the locomotive and the other cars, this data was not considered in the analysis.

Table 4-16 – Track System Modulus values for AP, CFT and IE services at UP1

Track System Modulus (MN/m²)																							
Dist. (m)	11.4	10.8	10.2	9.6	1.8	1.2	0.6	0	-0.6	-1.8	25.8	21.6	20.4	19.2	18	3.6	3	2.4					
Alfa Pendular	MEMS	MEMS	MEMS	MEMS	MEMS	MEMS	MEMS	MEMS	MEMS	MEMS	PE	PE	PE	PE	PE	PE	PE	PE					
AP 1	48.8	40.0	36.4	28.9	25.2	26.3	26.6	21.8	20.0	27.0	24.5	23.4	30.8	41.6	35.0	24.0	23.6	22.8					
AP 2	33.5	40.6	27.2	23.1	24.4	31.0	23.3	21.4	25.2	28.3	25.6	23.9	30.8	36.8	35.1	23.3	23.5	24.4					
AP 3	38.1	49.3	26.1	24.8	23.3	25.3	22.6	21.1	22.2	24.6	26.0	24.3	29.7	38.0	37.0	22.9	22.9	23.8					
AP 4	40.9	42.1	27.1	26.4	24.1	25.1	24.3	22.8	23.7	23.1	25.1	23.8	30.1	38.7	30.7	24.3	22.8	23.2					
AP 5	34.8	28.8	27.0	25.5	23.5	24.9	22.6	20.7	23.1	22.0	26.3	24.9	28.6	40.5	36.9	23.2	23.0	24.2					
Average	39.2	40.2	28.8	25.7	24.1	26.5	23.9	21.6	22.9	25.0	25.5	24.0	30.0	39.1	34.9	23.5	23.2	23.7					
Coal Freight Trains																							
CFT 1	-	-	34.3	29.6	21.2	21.1	22.0	23.2	26.9	16.8	19.4	19.4	23.6	38.1	33.4	22.9	24.7	25.4					
CFT 2	31.1	11.6	37.0	37.1	20.9	22.1	29.7	26.5	27.4	20.3	23.1	20.5	28.0	36.7	44.4	24.5	23.8	24.3					
CFT 3	37.3	-	23.6	23.3	17.7	17.7	22.8	22.8	22.4	28.5	24.3	21.7	38.5	49.6	51.9	19.8	19.0	20.3					
Average	34.2	11.6	31.7	30.0	19.9	20.3	24.8	24.2	25.6	21.9	22.3	20.5	30.0	41.5	43.2	22.4	22.5	23.3					
Intercity Express																							
IE 1	-	-	-	-	-	-	-	-	-	-	47.7	52.9	66.7	90.9	68.0	51.1	45.1	45.1					
IE 2	-	-	-	-	-	-	-	-	-	-	60.9	53.2	57.4	72.2	79.6	42.0	42.5	48.4					
IE 3	-	-	-	-	-	-	-	-	-	-	62.4	50.8	67.1	83.9	90.3	42.6	46.1	49.0					
Average	-	-	-	-	-	-	-	-	-	-	57.0	52.3	63.7	82.3	79.3	45.2	44.6	47.5					

(-) Data with high interferences

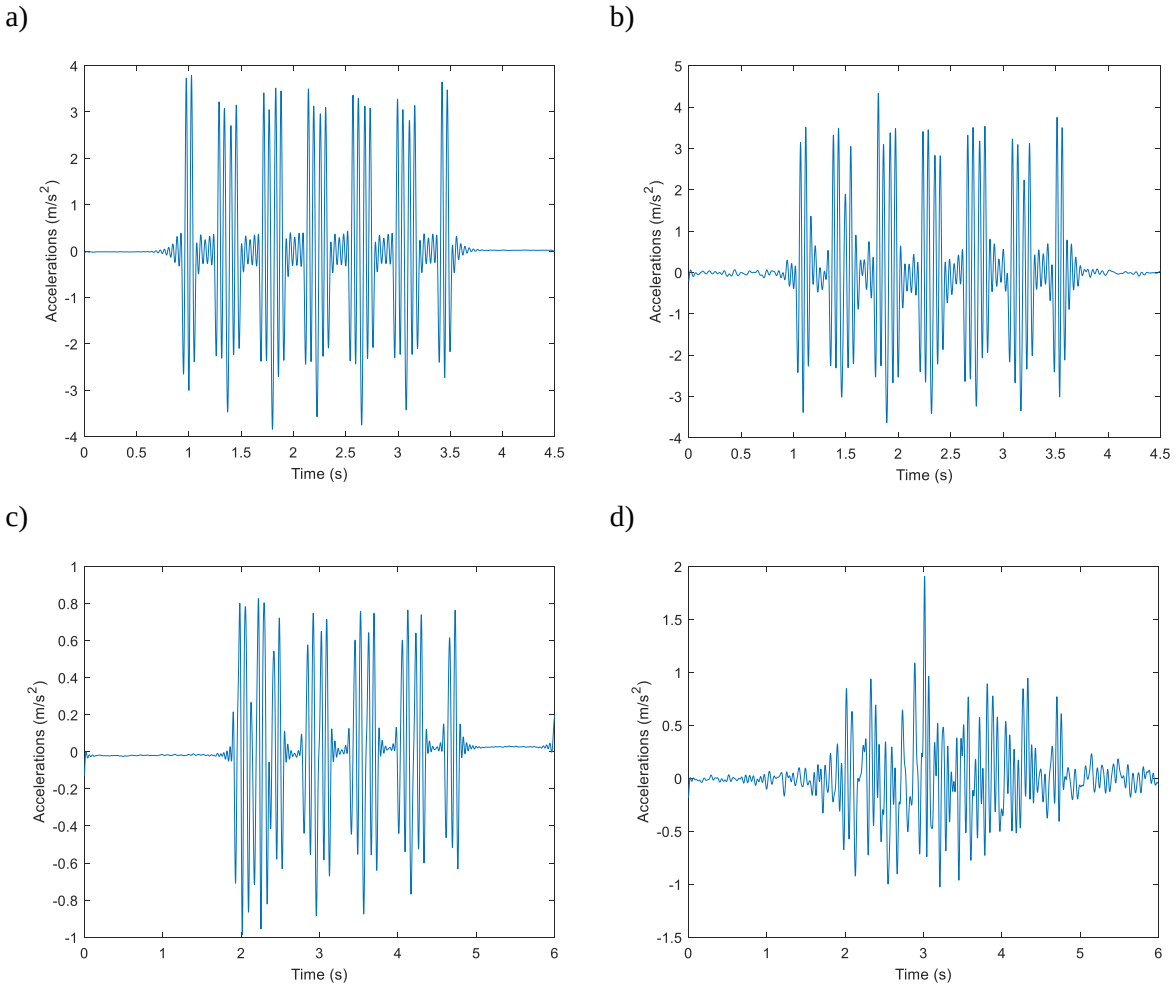

Figure 4-20 – Accelerations data recorded for: a) AP with piezoelectric accelerometers, b) AP with MEMS, c) IE with piezoelectric accelerometers, d) IE with MEMS.

To help the comprehension of all the data displayed in Table 4-16, Figure 4-21 displays the track system modulus for the data recorded according to the distance to the box culvert and the recorded device: piezoelectric (PE) or MEMS accelerometers.

In general, Figure 4-21 and Table 4-16, show the very good connection between the results obtained and the theoretical behaviour of UP1. It is possible to see an increase of the track system modulus from position 25 m until 18 m due to the approximation to the box culvert for all the data collected. The presence of the USP decreases quickly the track system modulus, which can be noticed between 11.4 m and 9.6 m and led to a constant track system modulus along the rest of track recorded. However, although all the values obtained display the same variations of the track along the distance, differences in the track system modulus can be found according to the type of train used.

a)

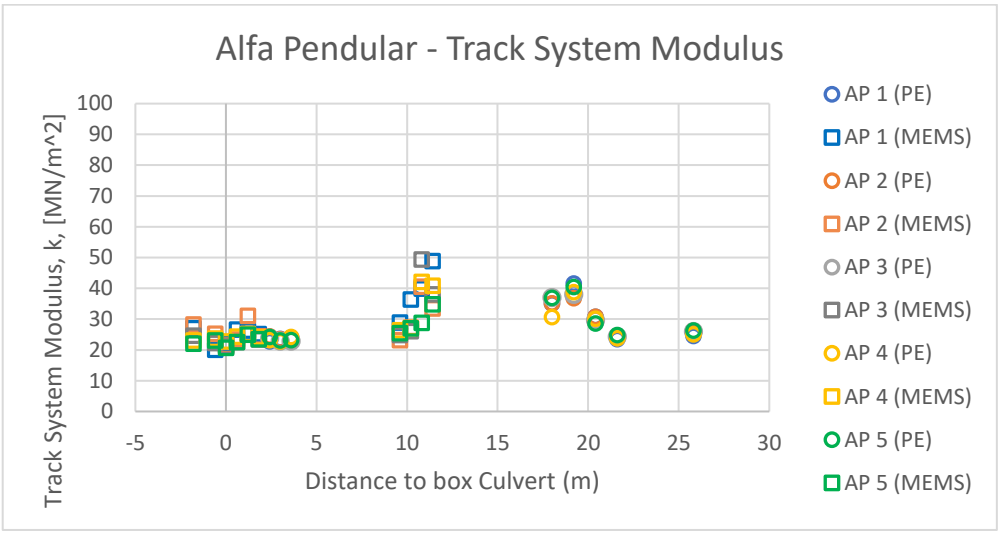

b)

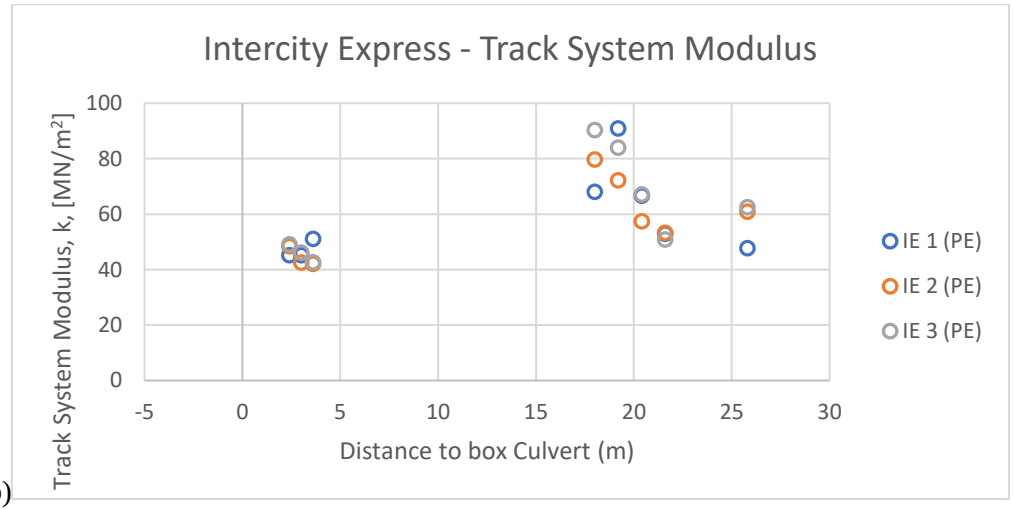

c)

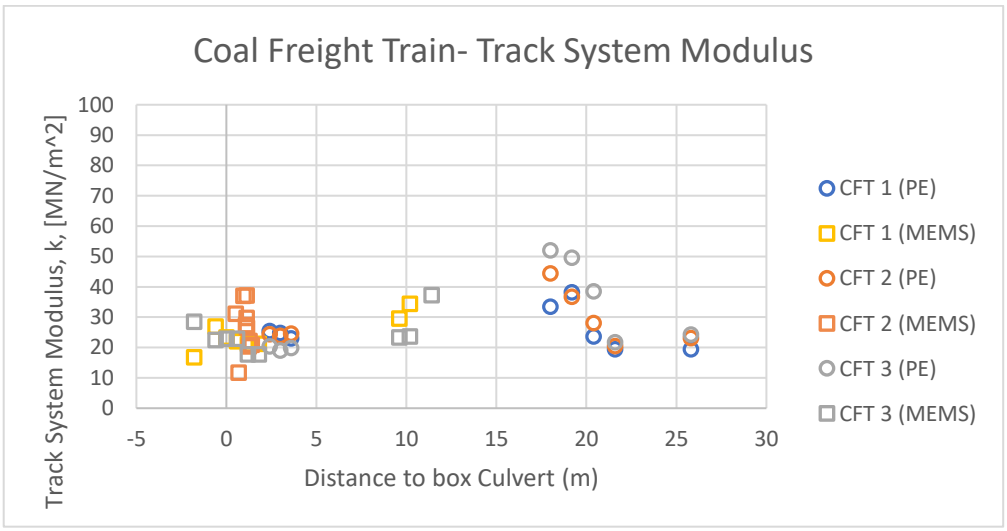

Figure 4-21 – Track system modulus according to the distance to the box culvert for: a) AP, b) IE and c) CFT at UP1

Once again, as already happened with the displacement data, the AP shows the lowest variations of the track system data, that varies from 23 MN/m^2 to 40MN/m^2 in the first stretch analysed, and an average of 23 MN/m^2 near the box culvert area. Even though these values are similar to the ones obtained with CFT, considerable differences exist between the values obtained with IE and the other train types. A similar phenomenon to the one described in the previous chapter and may be explained due to the high difference of weights between the locomotive and the other cars in IE trains, even though the locomotive data was not considerate. Considering that the locomotive is a lot heavier than the rest of the cars, some non-linearity present can be part of the cause to explain these results. The shape of the IE CC, that is approximately plain for higher track system modulus may also be part of the problem, an issue that is very minimized for the AP and CFT calibration curves (Figure 4-19a).

It is also clear that the results obtained, even with the IE and even for higher track system modulus, are a lot more consistent and closer to each other when comparing to the ones obtained with the displacement data, where the results were frequently out of the considered range. Such convergence between the results obtained can be explained by the shape of the CC that do not present horizontal asymptotes for AP and CFT services, moreover, even though the IE calibration curve has the lowest inclination for high track values, this state of the curve appears for values quite high, around 150 MN/m^2. Another factor may be the quality of the data, in fact, the LASER-PSD system is a lot more susceptible to interferences like noise and dust than the accelerometers.

Regarding the accelerometers system, the results obtained with the PE type accelerometers show lower dispersion than the ones obtained with MEMS accelerometers. In the stretch closer to the box culvert, for the CFT, the results obtained with PE data display variations between 20 MN/m^2 and 25 MN/m^2, while the ones obtained with MEMS show variations between 12 MN/m^2 and 37 MN/m^2. The same happens with the AP, where values from the PE accelerometers variate between 22 MN/m^2 and 25 MN/m^2, the ones from MEMS variate between 20 MN/m^2 and 31 MN/m^2. This may indicate that the PE type accelerometers are better suited for this application.

Figure 4-22 displays the track system modulus average per location according to the train type and data record method (PSD or accelerometers), as well as the values obtained in (Paixão [et al.], 2015) through other methods. The data displayed under the legend “accelerometer” correspond to both, MEMS and piezoelectric accelerometers. The presence of higher values of track system modulus for the IE is clear and happens for both displacement and acceleration data, which may indicate, that the model may be not well adjusted, which support the thesis that the locomotive’s higher weight influences the results.

The very good agreement between the values from both accelerometers and PSD per train type also points to the reliability of the method and its robustness, when dealing with different data and recorded devices. This also allows the use of several measurement approaches in order to complement each other.

It shall be noticed that the low track system modulus is a recommendation for the good use of displacement data, which may explain the good agreements between the values obtained for low track system modulus. The values obtained with the PSD and Receptance methods, also agree well with the AP and CFT results for low track system modulus. For higher values of track system modulus (distances greater than 14.1 m from the box culvert), only the CFT presents a good agreement, which supports the argument that this train type is the most suitable from for the application of this method as explained.

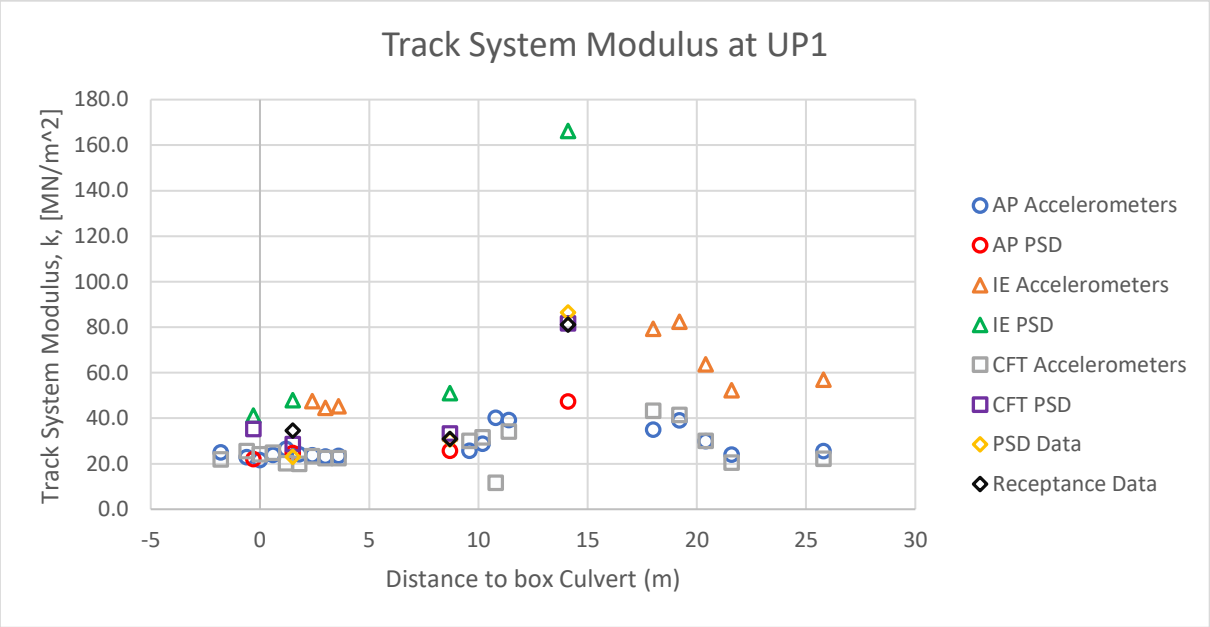

Figure 4-22 - Track system modulus according to train type and data provenience at UP1

The possibility of using several different recording systems may be important to find some issues or disrupted data. One of the accelerometers (the one located 10.8 m from the box culvert) displays very low track system modulus when comparing its results with the ones close to it. This may indicate that there is a dysfunction in the track, or this accelerometer had interferences or was not working very well. Either way, it is important to make sure the data is well recorded and it is here advised the use of several close recorder devices, to mitigate possible errors or malfunctions.

Table 4-17 shows the ratios between the values obtained according to the train type, for PE, results that reveal accordance with the previous analysis. The AP and CFT results ratio average is 1.02, and agrees that the best results are for low track system modulus values, near the box culvert. For higher track system modulus values, recorded 21.6 m before the box culvert and before the USP area, show higher differences that reach 20%.

Table 4-17 - Ratios between the average results according to train type at UP1

Dist. (m)	PE	AP/IE	AP/CFT	CFT/IE
2.4	PE	0.50	1.01	0.49
3.0	PE	0.52	1.03	0.51
3.6	PE	0.52	1.05	0.50
18.0	PE	0.44	0.81	0.55
19.2	PE	0.48	0.94	0.50
20.4	PE	0.47	1.00	0.47
21.6	PE	0.46	1.17	0.39
25.8	PE	0.45	1.15	0.39
Average	PE	0.48	1.02	0.47

The results between the AP and IE also agree upon which the model used to create the CC for the IE service may not be very well adjusted to the reality, since it does not include the heavier influence of the locomotive on the rails, which may explain the higher differences obtained. In fact, the almost constant differences along the sites studied point towards the fact that the model is not very adjusted to reality rather than geometry or the method limitations.

Table 4-18 displays the track system modulus for the UP2 for the several train types at UP2. Like with the results of UP1, several IE and CFT values do not appear in the table, because it was impossible either to find the harmonics due to interferences, either to understand the position of the locomotive and the cars of the trains during the plot of the data, as already explained.

To help the analysis of the Table 4-18, it is displayed in Figure 4-23 the track system modulus according to the train type, accelerometers and distance to the box culvert. Once again, it is clear from the Figure 4-23a that the values obtained with MEMS accelerometers are a lot more dispersed than the ones obtained with PE accelerometers. The highest differences between results for the same section are 12 MN/m^2 for PE accelerometers and almost 50 MN/m^2 with MEMS accelerometers. This may reflect the lower quality of the data recorded with MEMS accelerometers when comparing to the data obtained with the other sensors.

In general, the values obtained with the AP are quite low, a phenomenon already identified with the results obtained with the displacement data. Again, and since the characteristics used to create the CC were the same, it may be due to limitations of this train model when applied to real situations, which may be caused by the differences in the load per axle or even due to the high dynamic loads variations present since we are studying the passage of high speed trains in a transition zone. Another possible reason is the difficulty that this method may have when dealing with high variations of track system modulus.

The IE values are only for PE accelerometers, as explained, even though it is interesting to verify that as with displacement data, the higher the track system modulus, the higher the dispersion of the results. This is directly linked with the shape of the IE CC that tends to a horizontal asymptote for high values, which leads to high variations of track system modulus for small variations of amplitude ratios. The smaller dispersions of the AP and the UP1 results seem to support this argument.

Table 4-18 – Track system modulus for AP, CFT and IE services at UP2

Track System Modulus (MN/m²)																						
11.4	**10.8**	**10.2**	**9.6**	**1.8**	**1.2**	**0.6**	**0.0**	**-0.6**	**-1.8**	**25.8**	**22.8**	**21.6**	**20.4**	**19.2**	**18.0**	**3.6**	**3.0**	**2.4**	**Dist. (m)**	
MEMS	MEMS	MEMS	MEMS	MEMS	MEMS	MEMS	MEMS	MEMS	MEMS	PE	PE	PE	PE	PE	PE	PE	PE	PE		
Alfa Pendular																				
37.8	35.4	49.8	42.2	40.9	42.5	75.1	35.1	39.9	36.4	17.3	22.9	25.0	28.2	34.9	40.6	45.1	39.0	33.3	1	
49.2	49.7	47.0	64.6	44.5	45.0	92.5	43.4	51.6	12.6	23.0	26.6	29.7	23.7	29.7	33.0	52.9	45.7	33.3	2	
30.0	43.2	53.4	36.1	38.3	60.3	61.1	50.4	33.8	29.3	16.6	23.7	26.6	31.7	37.7	45.1	47.8	41.0	29.8	3	
131.4	44.2	30.3	46.8	39.3	91.2	45.8	20.9	36.4	12.5	21.0	22.5	29.1	30.6	31.2	43.4	45.1	46.5	45.0	4	
35.7	36.0	50.2	47.4	39.7	44.4	39.9	56.0	38.4	27.5	17.1	22.9	25.4	27.7	35.1	40.3	44.8	43.4	27.4	5	
56.8	41.7	46.2	47.4	40.5	56.7	62.9	41.2	40.0	23.6	19.0	23.7	27.2	28.4	33.7	40.5	47.1	43.1	33.8	Average	
CFT																				
60.7	-	33.7	-	40.3	60.0	37.4	26.9	33.0	-	26.1	-	34.8	41.7	33.0	38.9	26.0	54.5	60.0	1	
Intercity Express																				
-	-	-	-	-	-	-	-	-	-	32.7	47.0	42.6	65.3	119.6	80.0	102.9	178.8	169.7	1	
-	-	-	-	-	-	-	-	-	-	32.3	-	43.6	56.8	126.7	91.1	130.3	71.3	134.8	2	
-	-	-	-	-	-	-	-	-	-	36.5	-	48.5	50.3	86.1	194.6	173.2	141.4	154.5	3	
-	-	-	-	-	-	-	-	-	-	25.3	53.8	34.0	45.2	-	107.6	138.7	79.5	131.6	4	
-	-	-	-	-	-	-	-	-	-	35.7	62.5	56.5	63.2	106.7	174.5	185.9	84.2	129.3	5	
-	-	-	-	-	-	-	-	-	-	30.6	51.3	52.5	64.5	98.1	86.6	125.9	70.8	104.0	6	
-	-	-	-	-	-	-	-	-	-	32.2	53.7	46.3	57.5	89.5	122.4	142.8	104.3	137.3	Average	

(-) Data with high interferences

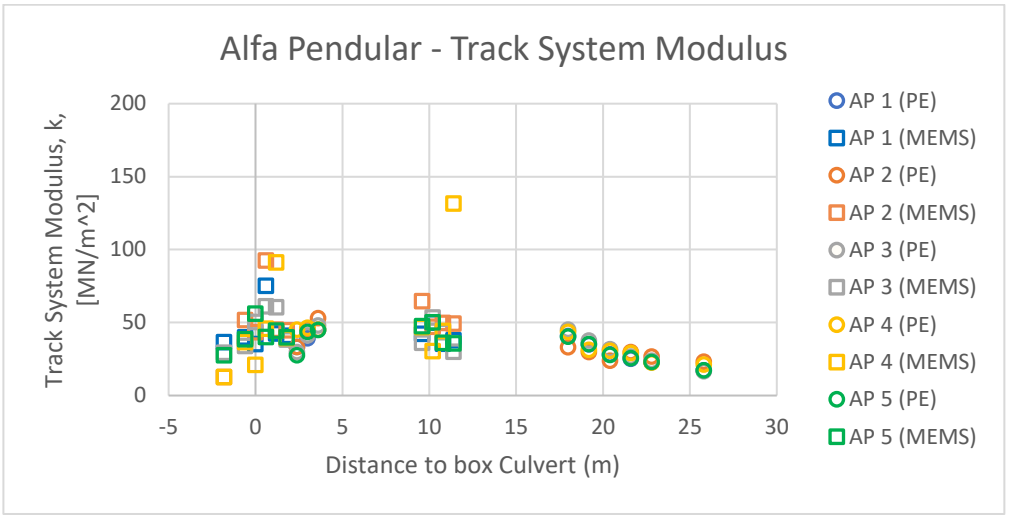

a)

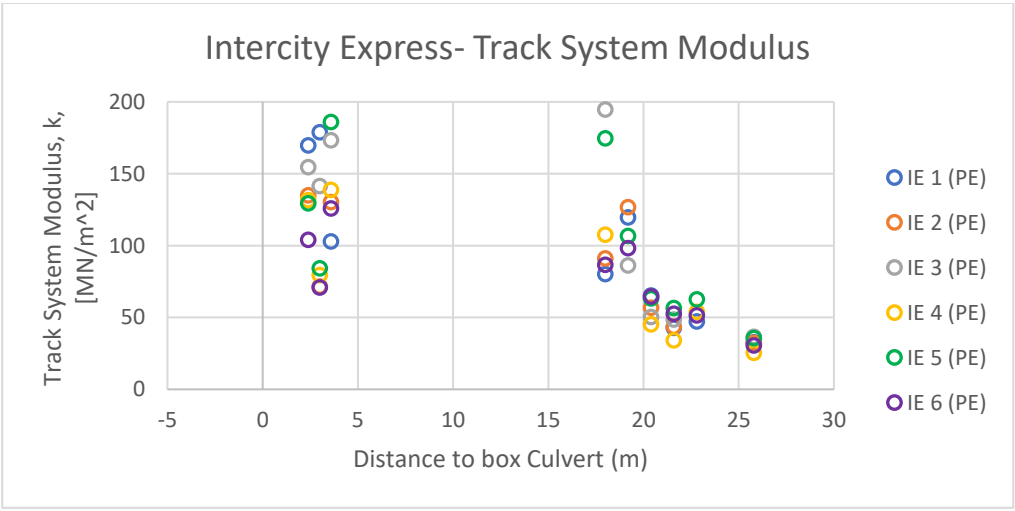

b)

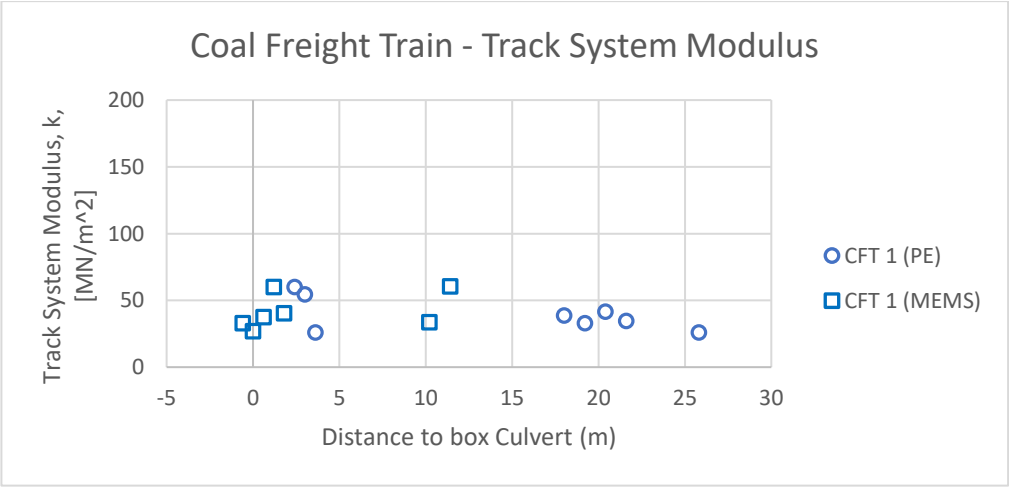

c)

Figure 4-23 – Track system modulus for AP(a), IE(b) and CFT(c) services at UP2

Even thought, it is possible to see an increase of the track system modulus for all the trains, which is according to what would be predicted, since the UP2 is a transition zones.

The presence of only one CFT data limits further conclusions. It can also be seen high variations of the data for higher values of track system modulus, which in case of the PE accelerometers may be due to punctual interferences. In fact, the absence of several values is precisely due to some interference recorded with the accelerometers that did not allow the calculation of the track system modulus.

The results obtained with data from accelerometers for AP are similar to the ones obtained with PSD (Figure 4-24), as it happened with UP1 results, which reveals a good agreement of the method and its capacity to use several and different type of data with the same results. In fact, the data from AP from accelerometers and PSD can complement itself. Though there are differences between the results obtained with CFT, these are only for a train and respective data and it may not represent the general case for the CFT. In fact, the differences between these results may be due to lack of quality of the data recorded, a situation that could be avoided with the recording of more train passages for the CFT.

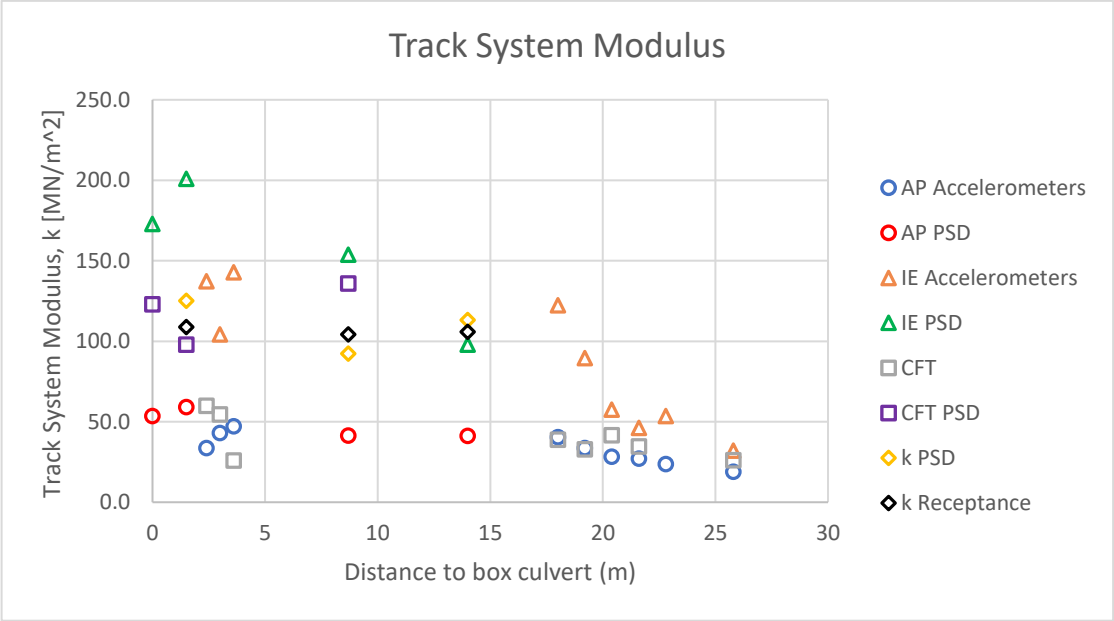

Figure 4-24 - Track system modulus according to train type and data provenience at UP2

It shall also be noticed that the results from IE service, even though they are more dispersed, they also agree between accelerometers and displacement results.

Table 4-19 reveals the accordance between the CFT and AP results for the UP2, a situation already stated for the UP1. These two trains allow the best results from the frequency method, however, with some limitations when dealing with high track system modulus, an issue that did not diminished with the improvement of the CC shape. The ratios between AP and CFT and the IE service are also according to the results already achieved for UP1.

Table 4-19 - Ratios between the average results according to train type at UP2

Dist. (m)	PE	AP/IE	AP/CFT	CFT/IE
2.4	PE	0.25	0.56	0.44
3.0	PE	0.41	0.79	0.52
3.6	PE	0.33	1.82	0.18
18.0	PE	0.33	1.04	0.32
19.2	PE	0.38	1.02	0.37
20.4	PE	0.49	0.68	0.73
21.6	PE	0.59	0.78	0.75
25.8	PE	0.44	-	-
Average	PE	0.40	0.96	0.47

Even though most of the conclusions were made for displacement data and that those conclusions were still valid for the acceleration one, it is interesting the gather of more information through examples. According to these and regarding all the analysis made, one of the main recommendations for the application of this recent method is the use of several data (displacements, velocity and acceleration), collected with several systems, to be possible to cross the information and gather better results.

5

Conclusions and Final Remarks

This chapter gathers the major conclusions and recommendations achieved in the scope of this thesis and presents suggestions for future works and researches, considering the work carried out.

This thesis aimed at deeper analyses on the method developed by Le Pen et al.(2016), the identification of more strengths, limitations and applicability of the method on different environments and situations. The improvement of the present knowledge regarding the data collection and capacity to determine the vertical stiffness of the railway track is also important.

5.1 Main Conclusions and recommendations

Even though in the last decades some new methods to determine the track system modulus and other vertical stiffness coefficients have been proposed, it is still very difficult to determine the vertical stiffness of the track on a regular basis.

For this reason, it is necessary to keep improving our knowledge in this field, trying to discover and validate new methods to determine the track support modulus efficiently and easily, an important coefficient that is directly linked with the behavior of the track and its necessity of maintenance according to several authors.

This thesis focusses on the study of a recent method that appears to ensure an alternative to some of these needs. The biggest advantage of this method, according to Le Pen et al.(2016), is the fact that the method does not need the axle loads to determine the track modulus. An extremely useful tool since the determination of the axle loads is usually quite complicated. It was verified in Chapter 3, as already proposed by Le Pen et al.(2016), that the method in question produces good results and similar to the ones obtained with the conventional method for some situations. It was verified that the method yields good results at sites well maintained and of reliable performance, i.e. sites without voided sleepers neither excessive variation of the track stiffness from one sleeper to the other. These good results achieved in the third chapter were probably influenced by the fact that the variations between axle loads were small and because the data used by the method was collected for periodic trains.

In the scope of this thesis, it is proposed a simplification of the method, as described in the Chapter 3, that requires the inversion of the axis in the CC to allow a quicker analysis of the data. This new approach allows a quicker and automatic conversion of the amplitude values, obtained with the data collected, to track system modulus values through the CC, as already explained.

It was verified with the analysis made in the Chapter 3 that the MATLAB script that was developed here for this purpose can be used to apply the method under study. The main differences that appear between the results obtained with the MATLAB script and by Le Pen et al.(2016) are due to different considerations made in both cases. Such differences can easily be eliminated if the MATLAB script is run with the same considerations as the ones made by Le Pen et al.(2016), as described in the 3rd chapter.

It was also verified that, as expected, the method does not depend on the velocity neither on the axle load, however, the velocity may influence the results obtained through its influence on the discretization achieved. It is however the df the most important parameter to define a suitable discretization on the frequency domain, a parameter that is adaptable to the changes that the velocity may introduce when decreasing the intervals between harmonics. Since there are high variations of the amplitude through frequency, small variations on the data points may cause substantial changes on the results. It is here, thereby recommended the use of a high discretization for the method to make sure that the results obtained are trustworthy.

To summarize, it was concluded in the Chapter 3 that the method under study produces good results in well-maintained environments, without high variations of track stiffness and local problems in the track, like voids under the sleepers, which affect the method. It is then fundamental to introduce a good model with main characteristics that bring it, as close to reality as possible, so the results obtained are reliable.

The analysis of the method in study required other situations to analyse its performance. In Chapter 4, the method was applied to the two transition zones, locations that tend to be critical and hard to apply this kind of method.

Since that in the previous chapter the geophones produced velocity data that yield good results, it was then tested the method applied to displacement and acceleration from LASER-PSD and acceleration systems.

It is recommended the use of high discretization in the model, to make sure that the CC obtained are reliable. In chapter 4 it was recommended the use of df less than 0.05 Hz, for velocities around 220 km/h and 0.03 Hz for velocities of about 80 km/h. These recommendations were for specific velocities on specific situations with a certain type of train. Though it is recommended the analysis of each case in particular to make sure that the df chosen is enough to provide reliable results. It was also verified that for a certain dx and multiplication by four the number of bins, the discretization achieved was good and adaptable to the velocity and the train type.

Moreover, the recommendation made to consider the highest possible number of cars per train when using this method, is still valid and increases the reliability on the results obtained. However, this recommendation is only applicable for trains at a constant velocity; otherwise, variations in the velocity may create several peaks for the same harmonics. It is then recommended the use of at least 7 trains, since good results were achieved with CFT.

The use of signals obtained with the LASER-PSD displacement measurement systems to evaluate the track system modulus through this method was possible and showed good results for the CFT. However, it is here recommended the use of velocity data recorded with geophones when comparing to the data prevenient from LASER-PSD systems, since less disturbances are present in the recorded data. Disturbances that may slightly affect the results obtained through this method. However, it shall be noticed, that this conclusion is based on results recorded on different sites, therefore investigations towards the use of both recording systems on the same sites shall be done.

In the Chapter 4 it was then verified that the accuracy of the method under analysis is dependent on the actual track system modulus. This aspect is due to the shape of the CC that significantly increases the sensitivity of the method with the increase of the track system modulus. The displacements CC are highly accurate for low stiffness and have low accuracy for high stiffness. It was also verified that there are variations of performance according to the train characteristics. It is here recommended, to make an evaluation of the CC accuracy for the track system stiffness previewed and to choose trains that yield reliable results. This point is critical since this issued appeared for high values of track system modulus for both displacement and acceleration data.

The application of the frequency method to acceleration data was also possible and with very good results, especially at UP1, that can be combined with the ones obtained with displacement data. This continuity allows trustworthy on the results obtained, and thereby the complement between both methods. Thereby it is recommended the use of several measuring systems to verify the agreement between data.

However, the acceleration results also showed different results according to the type of train used, which is a problematic issue. This issue happened mainly at the transition zone UP2 results and may be due to the higher track system modulus in that site, but also between the IE and the other train types at UP1. The huge differences between loads of the locomotive and coaching cars for the IE, even though the locomotive was not considered in the data, may explain some of the differences. The presence of interferences on the data, is probably another major cause.

The AP data did not get high track system modulus results even for the UP2 location, which may be due to variations on the axle load, since all the cars are different and also due to the high variations of the dynamic loads due to the high velocity in transition zones. The CFT, as it was expected, led to the best results, which means that the use of train types with a big number of cars at low speeds and constant weights produce better results.

Although, if the acceleration results agree very well for low track system modulus it is also true that the increase of the track system modulus leads to the dispersion of the results, as already stated, which is a limitation of the method.

It was also verified that data from MEMS accelerometers presented a lot more interferences than the PE accelerometers, and therefore the results are more disperse when comparing to piezoelectric accelerometer values. Sometimes, these interferences prevented even the use of that data, consequently it is here recommended the use of PE accelerometers rather than MEMS accelerometers for the frequency method.

According to the results obtained, it is suggested the use for this method of trains at a constant velocity with a high number of cars and regular weights and to make sure that the CC for those trains present

high differences of amplitude ratios for small differences in the track system modulus. Besides, it is recommended the use of geophones and piezoelectric accelerometers at the same time, so these systems may complement each other. It is also recommended a careful selection of the train type, to improve the CC efficiency and above all to avoid high variations of the axle loads.

It is still important to state that nothing on the results obtained point towards the invalidity of the frequency method in transition zones or other areas with high variations in stiffness, it is however a reality that there are differences on the accuracy and especially for high values of track system modulus, differences that may be an issue. It is then necessary to take these differences of accuracy into account, when evaluating these areas.

5.2 Future works

The development of this kind of methods is of great relevance for railway infrastructure managers and shall be taken into consideration in future works. The necessity of new methods, more efficient to determinate the track system modulus and other stiffness coefficients, is a reality and it would help the comprehension of the track behaviour to understand in greater depth and more efficiently its main characteristics. This work focuses on the search that goes on for new/recent methods and its evaluation to determine if they can be applied or not in general.

The method under study, as already explained, presents some simplifications and improvements, however it has also some limitations and disadvantages that may not have been completely mapped. It is therefore necessary to keep testing this method and others that may arise, identifying its boundaries and limits, while make us aware of its strengths. These analyses improve not only our comprehension over the methodologies in test but also, over the track behaviour, instrumentation methods and data recording devices.

Taking into consideration the above paragraphs, it is still necessary:

- To keep searching and analysing not only this method, but also others that may appear, in different situations to check improvements that may allow the determination of track characteristics;
- To create a solid data base, that comprehends a wide range of situations and methodologies of test to create a solid understanding over the method and made conclusions over a large set of scenarios;
- To improve the data recording methodologies, less susceptible to interferences. It would allow the development of new ways and determination methods, and the decrease of limitations in the current methods while improving it’s the reliability.
- A better comprehension of the behaviour this method through the analysis of more data what would lead to a better comprehension of some phenomena like the difficulty on getting high values of track system modulus for certain types of trains and low values of track system modulus for other types.

References

AAR (2013) Total Anual Spending. *Assossiation of American Railroads*

Anderson, W. F.; Key, A. J. - Model testing of two-layer railway track ballast. *Journal of Geotechnical and Geoenvironmental Engineering*. Vol. 126. n.º 4 (2000). p. 317-323. 'doi:' 10.1061/(ASCE)1090-0241(2000)126:4(317).

Berggren, E. G.; Nissen, A.; Paulsson, B. S. - Track deflection and stiffness measurements from a track recording car. *Proceedings of the Institution of Mechanical Engineers, Part F: Journal of Rail and Rapid Transit*. Vol. 228. n.º 6 (2014). p. 570-580. 'doi:' 10.1177/0954409714529267.

Berggren, Eric (2009) Railway Track Stiffness Dynamic - Measurements and Evaluation for Efficient Maintenance. *Doctoral* (in *Royal Institute of Technology (KTH)*

Bian, X.; Jiang, H.; Chang, C.; Hu, J.; Chen, Y. - Track and ground vibrations generated by high-speed train running on ballastless railway with excitation of vertical track irregularities. *Soil Dynamics and Earthquake Engineering*. Vol. 76. (2015). p. 29-43. 'doi:' 10.1016/j.soildyn.2015.02.009

Bowness, D.; Lock, A. C.; Powrie, W.; Priest, J. A.; Richards, D. J. - Monitoring the dynamic displacements of railway track. *Proceedings of the Institution of Mechanical Engineers, Part F: Journal of Rail and Rapid Transit*. Vol. 221. n.º 1 (2007). p. 13-22. 'doi:' 10.1243/0954409JRRT51.

Brigham, E Oran - The fast Fourier transform and its applications. Prentice Hall, 1988. ISBN: 0133075052

Author (2016) European Standart 16730: 2016 Railway applications - Track - Concrete sleepers and bearers with under sleeper pads. CEN

De Man, Amnon Pieter - Dynatrack - A survey of dynamic railway track properties and their quality. Delft University Press: Delft University, 2002.

EC (2016) EU Transport in Figures. *European Union*

Esveld, C. - Modern Railway Track. Second Edition. MRT-Productions, 2001. ISBN: 90-8004-324-3-3

Eurostat - Railway Safety Statistics. 2016.

Fortunato, E. (2005) Renovação de plataformas ferroviárias. Estudos relativos à capacidade de carga. *Ph.D. Thesis* (in *Portuguese) University of Porto, Portugal*

Fortunato, E.; Paixão, A.; Calçada, R. - Railway Track Transition Zones: Design, Construction, Monitoring and Numerical Modelling. *International Journal of Railway Technology*. Vol. 2. n.º 4 (2013). p. 33-58. 'doi:' 10.4203/ijrt.2.4.3.

Frýba, L. - Vibration of Solids and Structures under Moving Loads. Thomas Telford Ltd., Thomas Telford House and Academia, publishing house of the Academy of Sciences of the Czech Republic, 1979. ISBN: 0-7277-2741-9

Indraratna, B.; Salim, W.; Rujikiatkamjorn, C. - Advanced Rail Geotechnology – Ballasted Track. CRC Press, 2011. ISBN: 9780203815779

Ju, Shen-Haw; Lin, Hung-Ta; Huang, Jeng-Yuan - Dominant frequencies of train-induced vibrations. *Journal of Sound and Vibration*. Vol. 319. n.º 1–2 (2009). p. 247-259. 'doi:' 10.1016/j.jsv.2008.05.029

Kargarnovin, M. H.; Younesian, D.; Thompson, D. J.; Jones, C. J. C. - Response of beams on nonlinear viscoelastic foundations to harmonic moving loads. *Computers and Structures*. Vol. 83. n.º 23-24 (2005). p. 1865-1877. 'doi:' 10.1016/j.compstruc.2005.03.003.

Karttunen, K. (2012) Mechanical track deterioration due to lateral geometry irregularities. *Licentiate thesis* (in *English) Chalmers University of Technology*

Kerr, Arnold D. - On the determination of the rail support modulus k. *International Journal of Solids and Structures*. Vol. 37. n.º 32 (2000). p. 4335-4351. 'doi:'

Khouy, Iman Arasteh; Larsson-Kråik, Per-Olof; Nissen, Arne; Juntti, Ulla; Schunnesson, Håkan - Optimisation of track geometry inspection interval. *Proceedings of the Institution of Mechanical Engineers, Part F: Journal of Rail and Rapid Transit*. Vol. 228. n.º 5 (2014). p. 546-556. 'doi:' 10.1177/0954409713484711

Knothe, K.; Stichel, S. - Rail Vehicle Dynamics. Springer International Publishing, 2016. ISBN: 9783319453767

Le Pen, L.; Milne, D.; Thompson, D. J.; Powrie, W. - Evaluating railway track support stiffness from trackside measurements in the absence of wheel load data. *Canadian Geotechnical Journal*. Vol. 53. n.º 7 (2016). p. 1156-1166. Consult. em 2017/02/10. 'doi:' 10.1016/j.jsv.2008.05.029.

Le Pen, L.; Watson, G.; Powrie, W.; Yeo, G.; Weston, P.; Roberts, C. - The behaviour of railway level crossings: Insights through field monitoring. *Transportation Geotechnics*. Vol. 1. n.º 4 (2014). p. 201-213. 'doi:' 10.1016/j.trgeo.2014.05.002.

Maynar, M.M. - Apuntes de introducción a la dinámica vertical de la vía y a las señales digitales en ferrocarriles: con 151 programas en Matlab, Simulink, Visual C++, Visual Basic y Excel. Spain: INGENIERÍA DE FERROCARRILES, METROS Y TÚNELES, S.L., 2008. ISBN: 9788461276868

Mikusiński, J.; Sikorski, R. - The elementary theory of distributions (II). (1961). 'doi:'

Mosayebi, S. A.; Zakeri, J. A.; Esmaeili, M. - Some aspects of support stiffness effects on dynamic ballasted railway tracks. *Periodica Polytechnica: Civil Engineering*. Vol. 60. n.º 3 (2016). p. 427-436. 'doi:' 10.3311/PPci.7933.

Muramoto, K.; Nakamura, T.; Sakurai, T. - A study of the effect of track irregularity prevention methods for the transition zone between different track structures. *Quarterly Report of RTRI (Railway Technical Research Institute)*. Vol. 53. n.º 4 (2012). p. 211-215. 'doi:' 10.2219/rtriqr.53.211.

Author (2017) MATLAB R2017a Natick, MA, USA: The MathWorks, Inc.

Paixão, A. (2014) Transition Zones in Railway Tracks - An experimental and numerical study on the structural behaviour. *Ph.D. Thsesis University of Porto, Portugal*

Paixão, A.; Alves Ribeiro, C.; Pinto, N.; Fortunato, E.; Calçada, R. - On the use of under sleeper pads in transition zones at railway underpasses: experimental field testing. *Structure and Infrastructure Engineering*. Vol. 11. n.º 2 (2015). p. 112-128. 'doi:' 10.1080/15732479.2013.850730.

Park, J.; Ahn, S.; Kim, J.; Koh, H. I.; Park, J. - Direct determination of dynamic properties of railway tracks for flexural vibrations. *European Journal of Mechanics a-Solids*. Vol. 61. (2017). p. 14-21. 'doi:' 10.1016/j.euromechso1.2016.08.010.

Pinto, N.; Ribeiro, C. A.; Gabriel, J.; Calçada, R. - Dynamic monitoring of railway track displacement using an optical system. *Proceedings of the Institution of Mechanical Engineers, Part F: Journal of Rail and Rapid Transit*. Vol. 229. n.º 3 (2015). p. 280-290. 'doi:' 10.1177/0954409713509980.

Priest, J. A.; Powrie, W. - Determination of Dynamic Track Modulus from Measurement of Track Velocity during Train Passage. *Journal of Geotechnical and Geoenvironmental Engineering*. Vol. 135. n.º 11 (2009). p. 1732-1740. 'doi:' 10.1061/(asce)gt.1943-5606.0000130.

Profillidis, V.A. - Railway Engineering. Avebury Technical, 1995. ISBN: 0291398286

Puzavac, L.; Popović, Z.; Lazarević, L. - Influence of Track Stiffness on Track Behaviour Under Vertical Load. *Promet - Traffic - Traffico*. Vol. 24. n.º 5 (2012). p. 405-412. 'doi:' 10.7307/ptt.v24i5.1176.

Rao, K.R.; Kim, D.N.; Hwang, J.J. - Fast Fourier Transform - Algorithms and Applications. Springer Netherlands, 2011. ISBN: 9781402066290

Selig, E. T. - Evaluation of railway subgrade problems. *Transportation Research Record*. Vol. 1489. (1995). p. 17. 'doi:'

Selig, E.T.; Waters, J.M. - Track Geotechnology and Substructure Management. Telford, 1994. ISBN: 9780727720139

T., Dahlberg. - Railway track dynamics - a survey. Linköping University, 2003.

Teixeira, P. F. (2003) Contribución a la reducción de los costes de mantenimiento de vías de alta velocidad mediante la opitimización de su rigidez vertical. *Ph.D. Degree* (in *Spanish) Universitat Politècnica de Catalunya*

UN - World's population increasingly urban with more than half living in urban areas. 2014.

Winkler, C. - Beiträge zur Kenntniss des Indiums. *Journal für Praktische Chemie*. Vol. 102. n.º 1 (1867). p. 273-297. 'doi:' 10.1002/prac.18671020139.

Annex A

Detailed analysis on the values obtained in the first case study present in the Chapter 3

Calibration Curves Construction with velocity ratios – first case study

The ratios between the 3rd and 7th Harmonic produce the curves; Each color line in a chart represents the ratios modelled with the MATLAB script for a certain track system stiffness from 1 untill the value displayed in the CC with intervals of 1.

a)

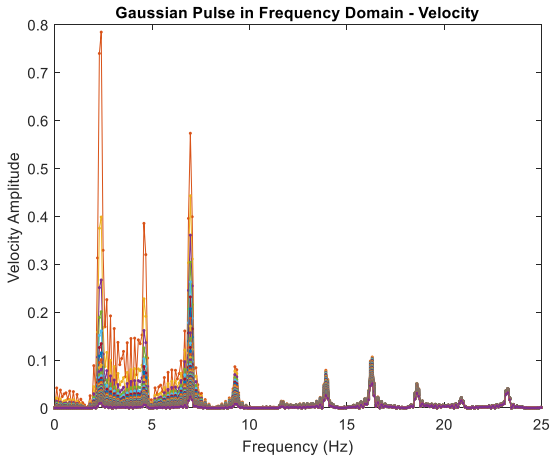

b)

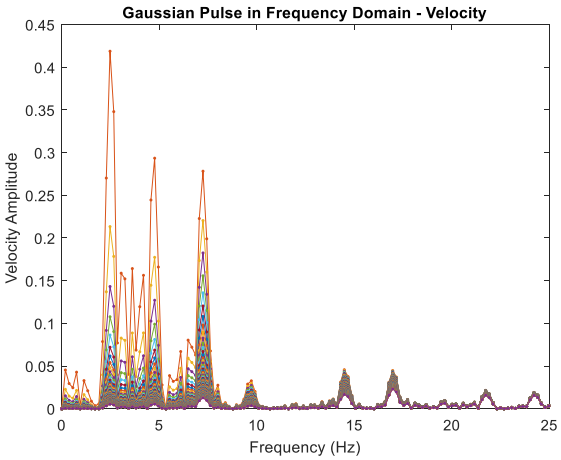

c)

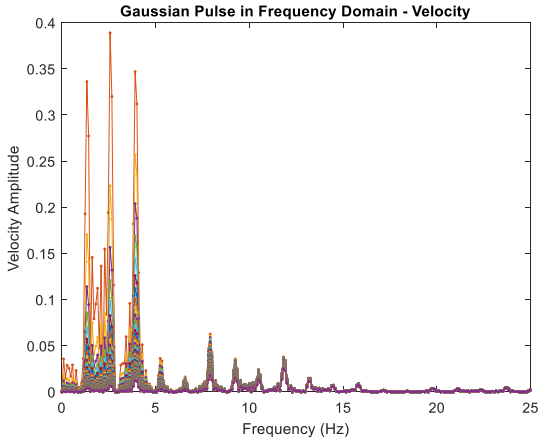

d)

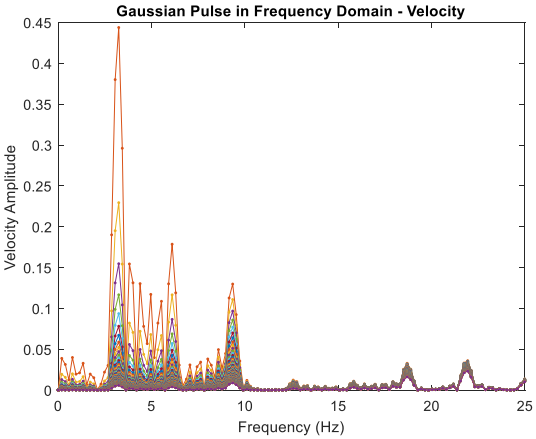

e)

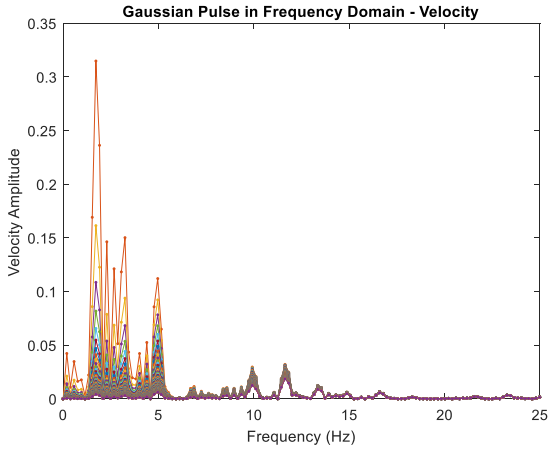

f)

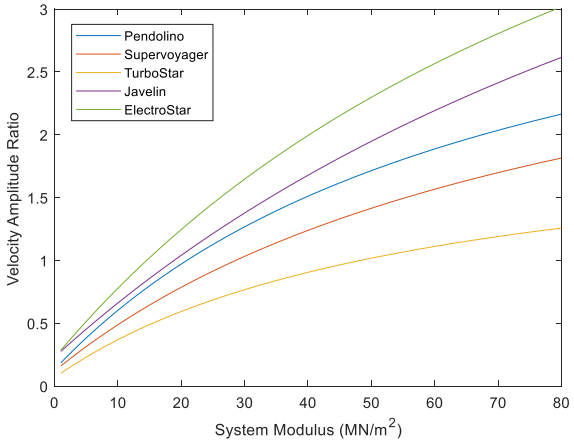

a) Pendolino; b) Supervoyager; c) Turbostar; d) Javelin; e) Electrostar; CC

Calibration Curves Construction with acceleration ratios – first case study

a)

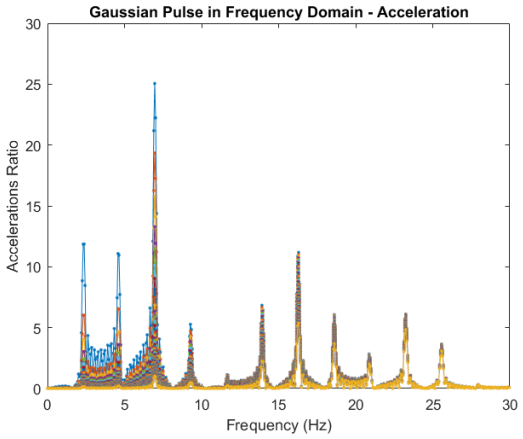

b)

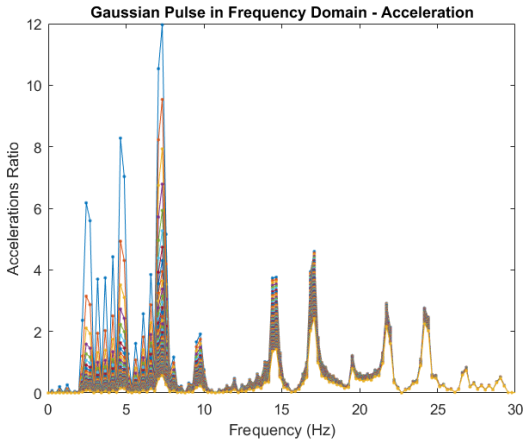

c)

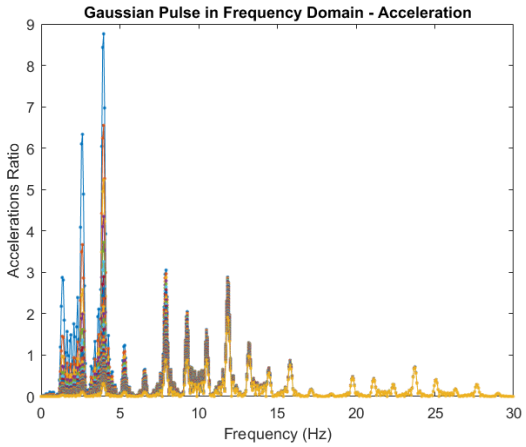

d)

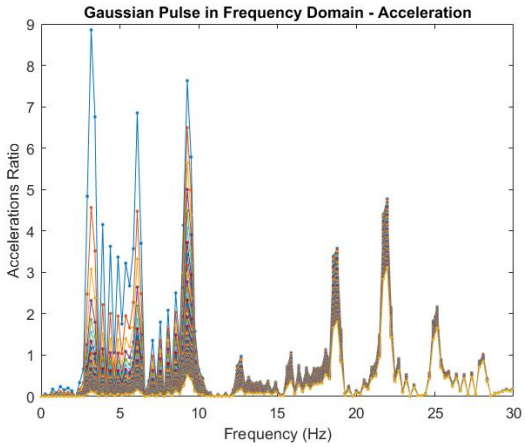

e)

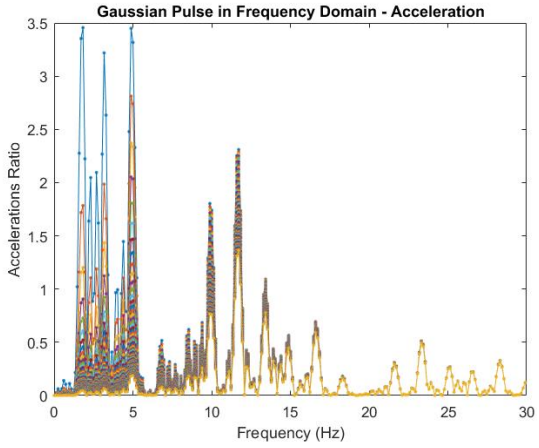

f)

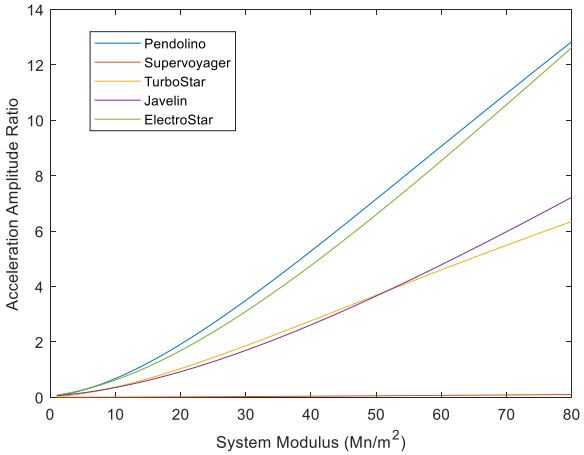

a) Pendolino; b) Supervoyager; c) Turbostar; d) Javelin; e) Electrostar; f) CC

Calibration Curves Construction with displacements ratios – first case study

a)

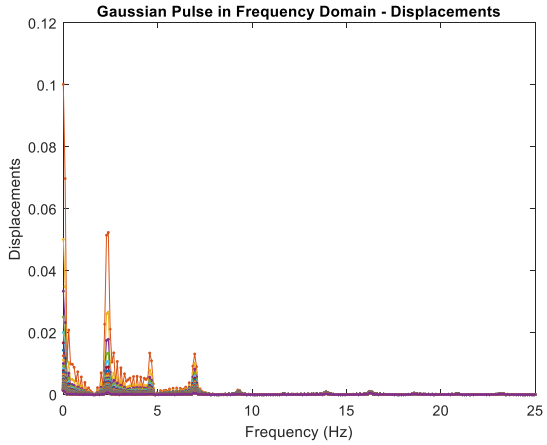

b)

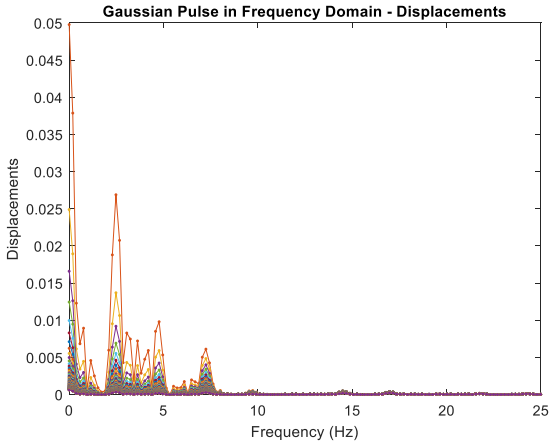

c)

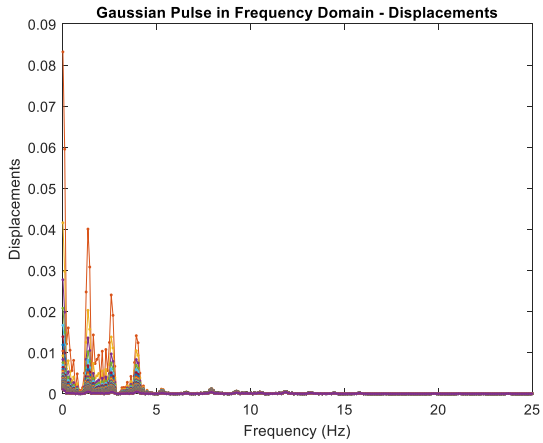

d)

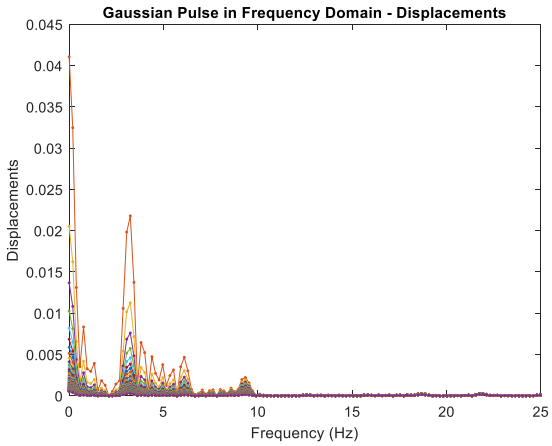

e)

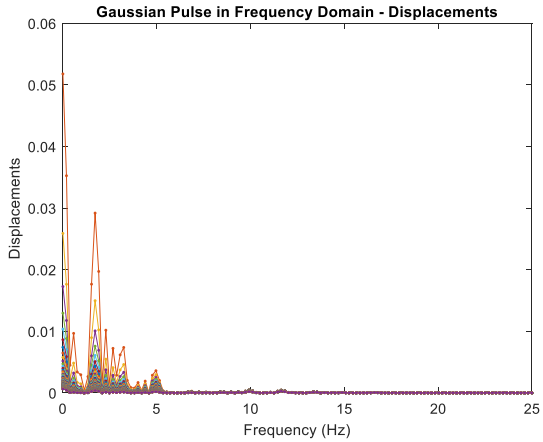

f)

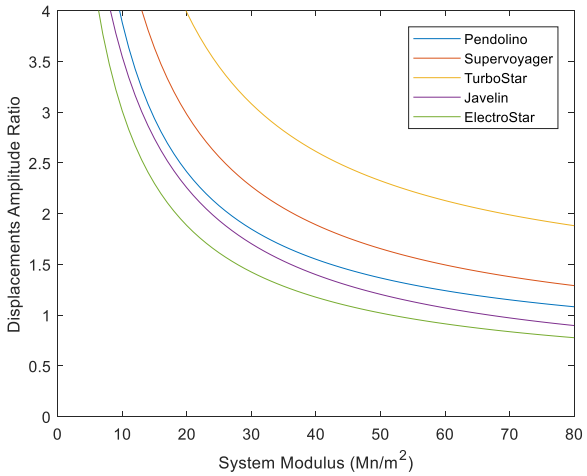

a) Pendolino ; b) Supervoyager; c) Turbostar; d) Javelint; e) Electrostar; f) CC

Calibration Curves Construction with displacements ratios and high discretization (used to obtain the results) – first case study

a)

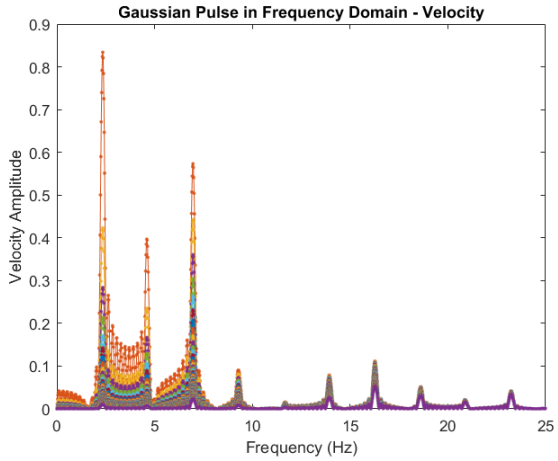

b)

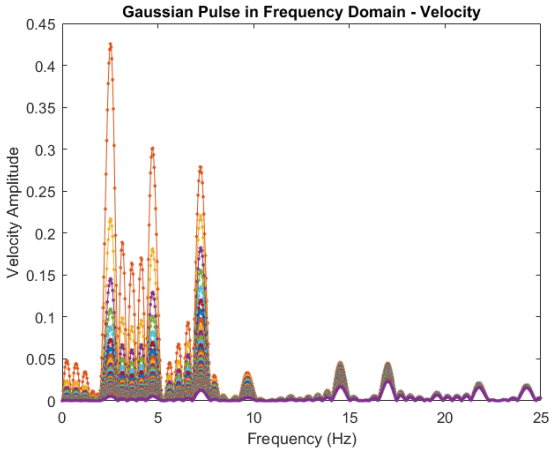

c)

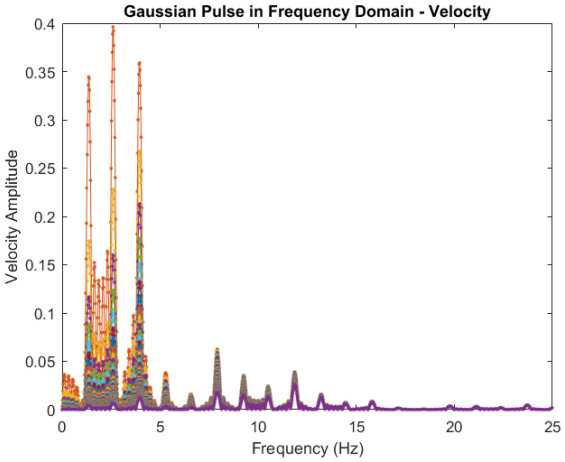

d)

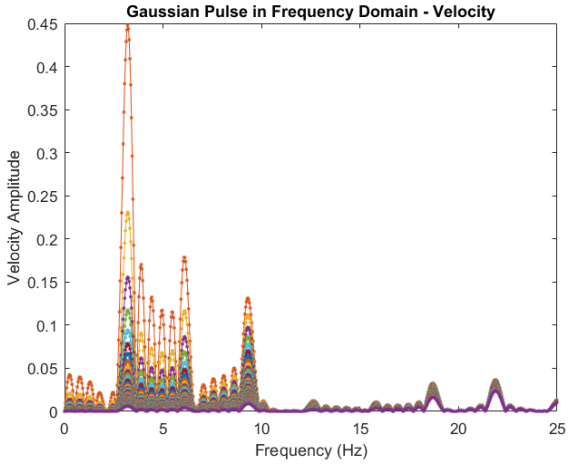

e)

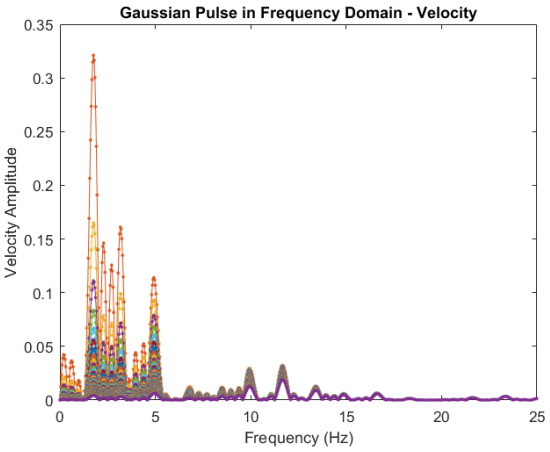

f)

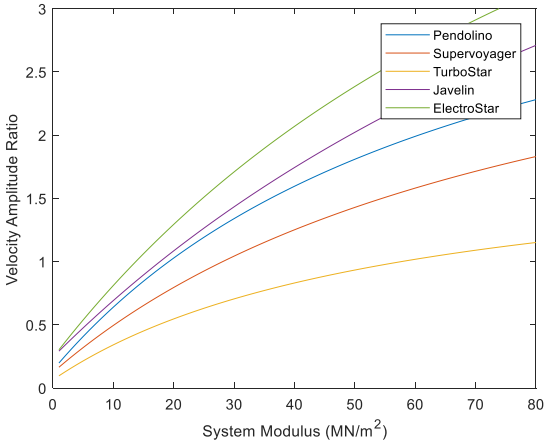

a) Pendolino; b) Supervoyager; c) Turbostar; d) Javelin; e) Electrostar; CC

Examples of the data recorded in the first case study for different trains, please contact the author for further information

a)

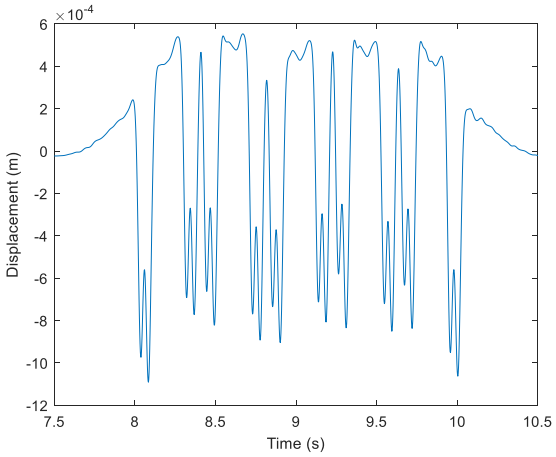

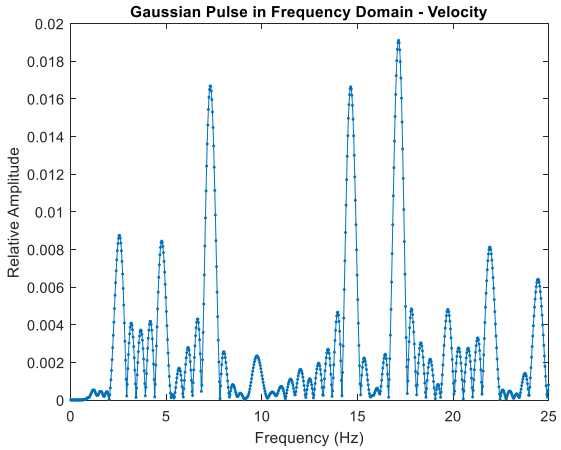

b)

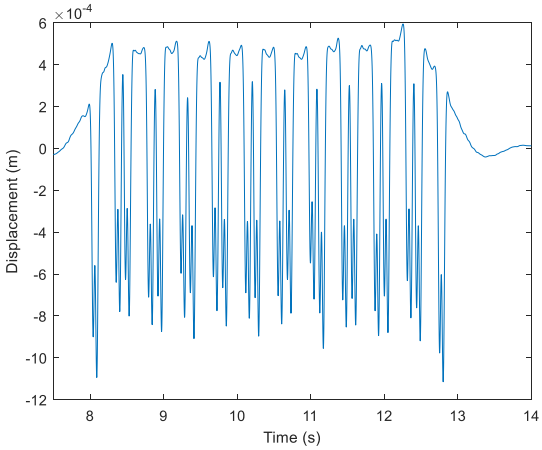

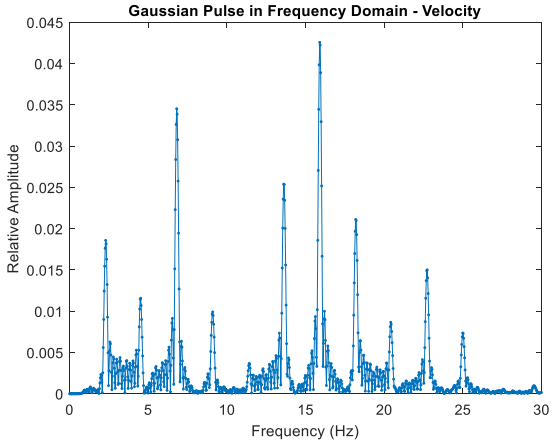

c)

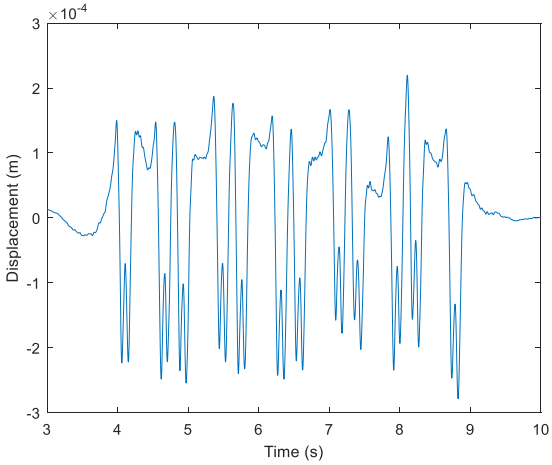

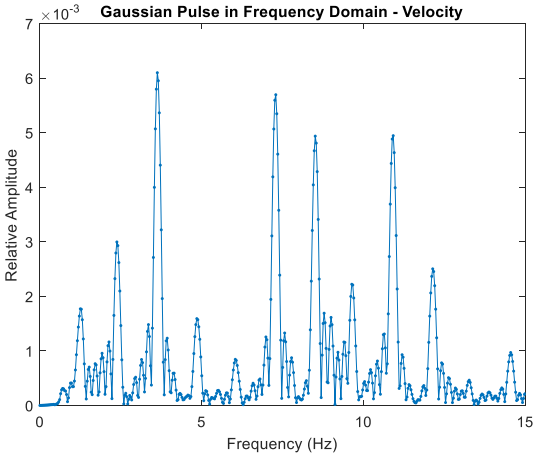

d)

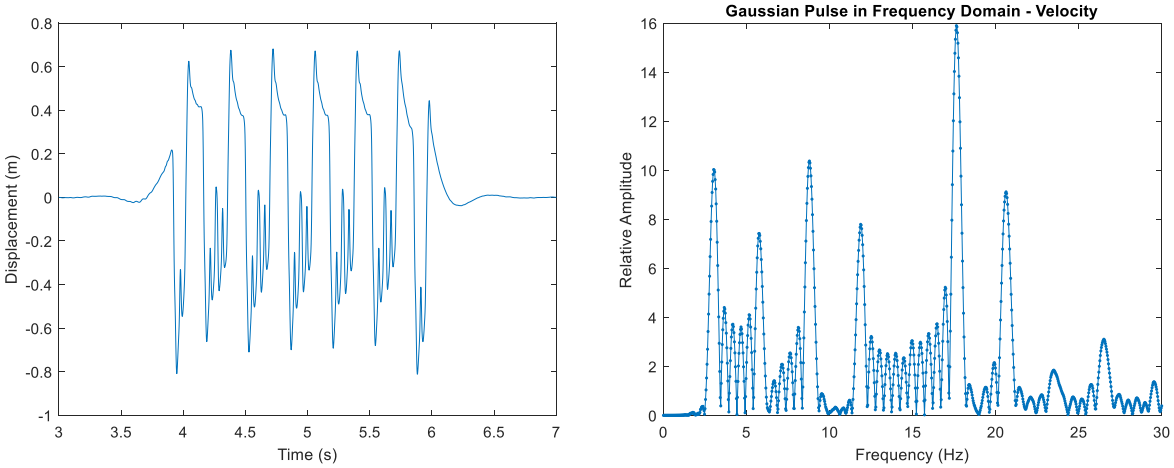

e)

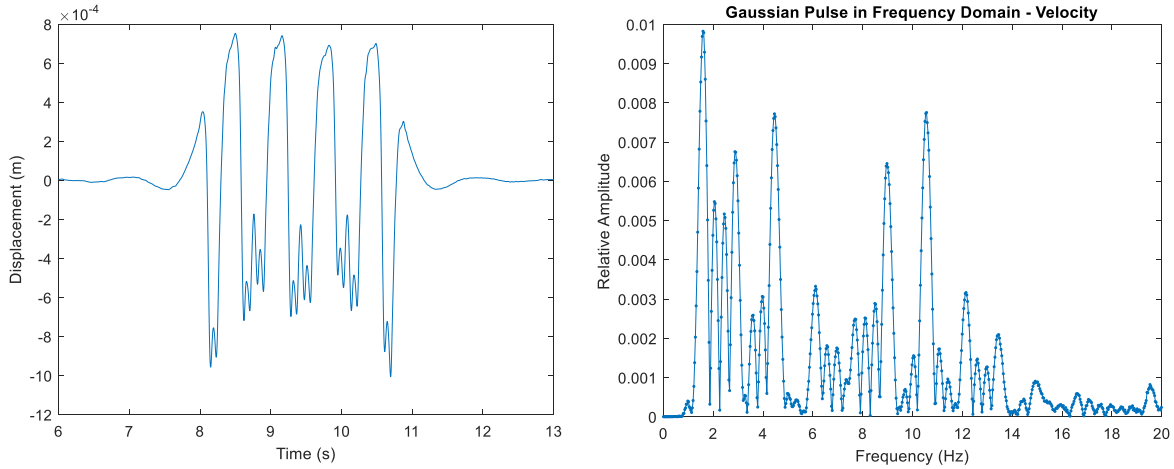

a) Supervoyager; b) Pendolino; c) Turbostar; d) Javelin e) Electrostar – Velocity data recorded during the train passage and correpondance of the data in the frequency spectrum

Calibration Curves Construction with acceleration ratios – second case study (dt=1/500 and multiplication of the number of bins by 4 to improve discretization)

a)

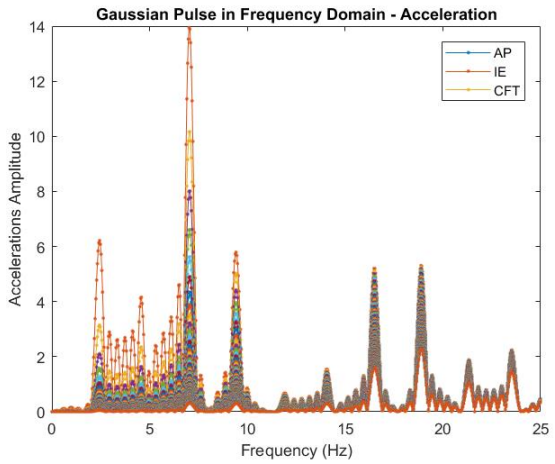

b)

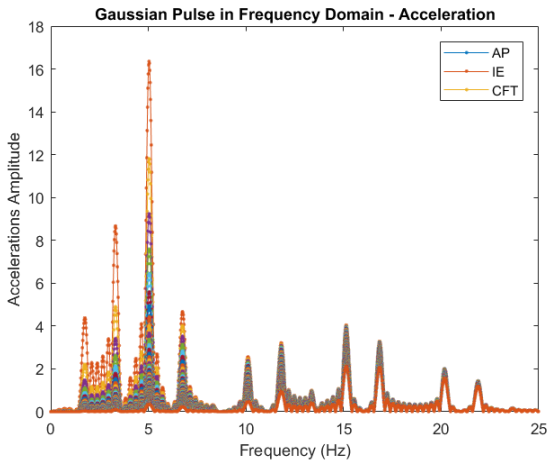

c) d)

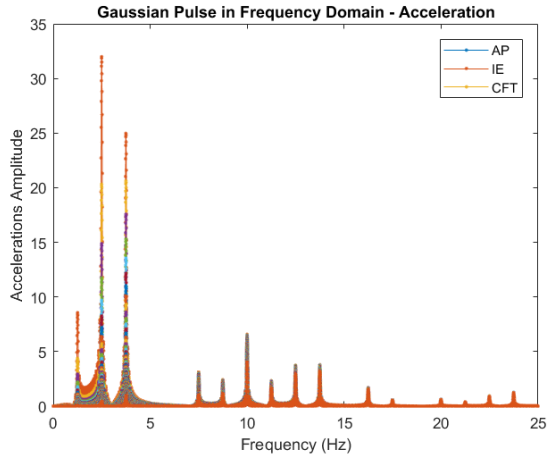

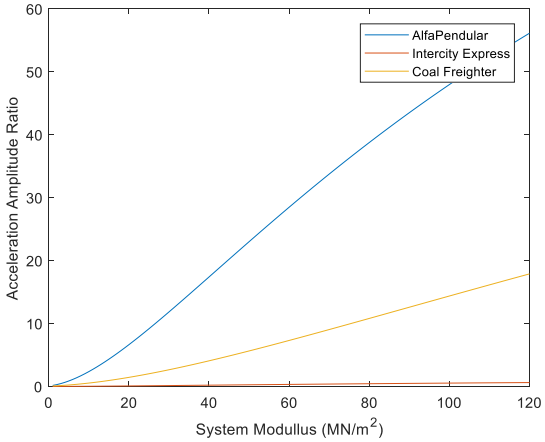

a) *Alfa Pendular* Express (6 cars); b) Intercity Express (6 cars); c) Coal Freigh Trains (20 cars); d) CC

Calibration Curves Construction for displacement ratios – second case study (dt=1/5000)

a) b)

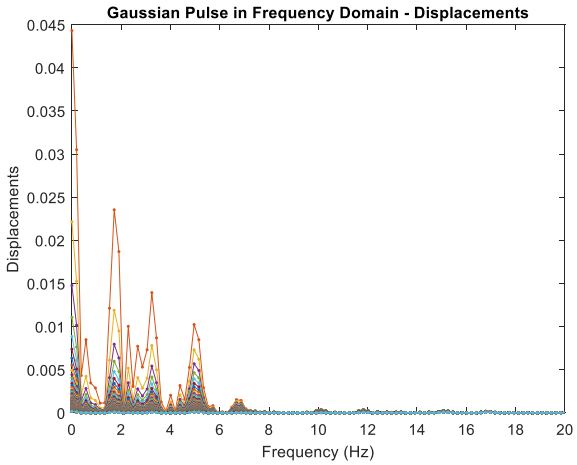

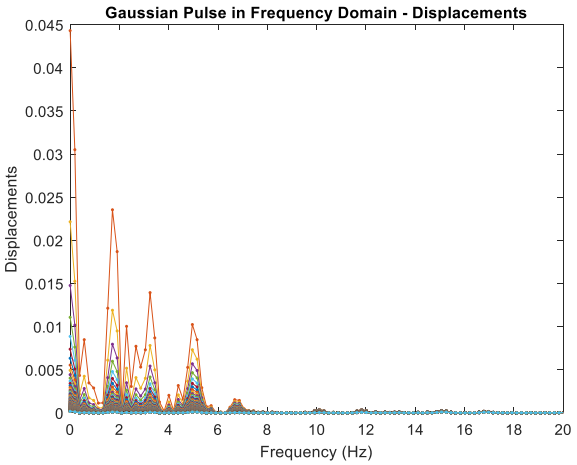

c) d)

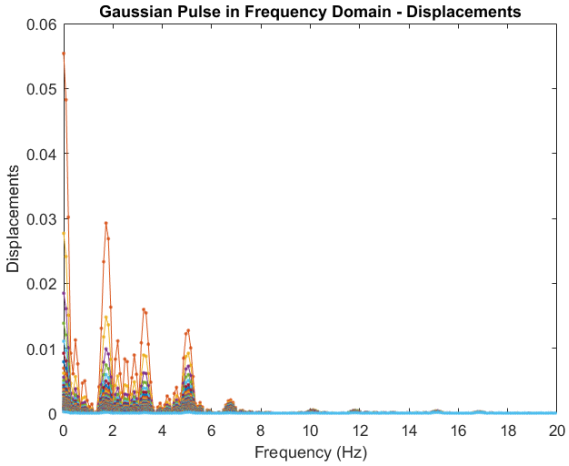

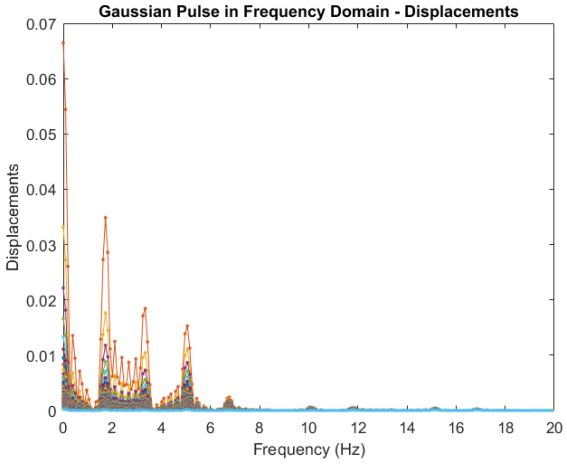

e)

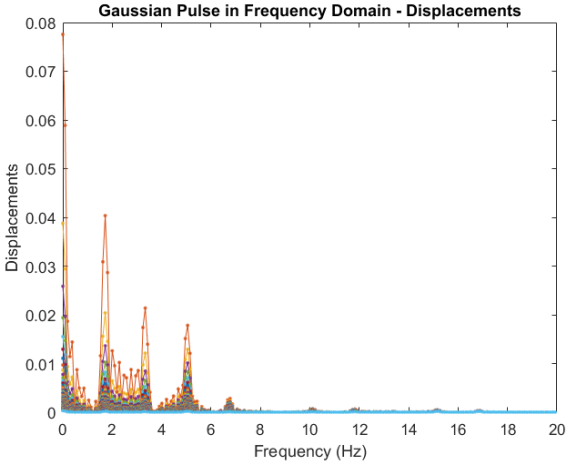

f)

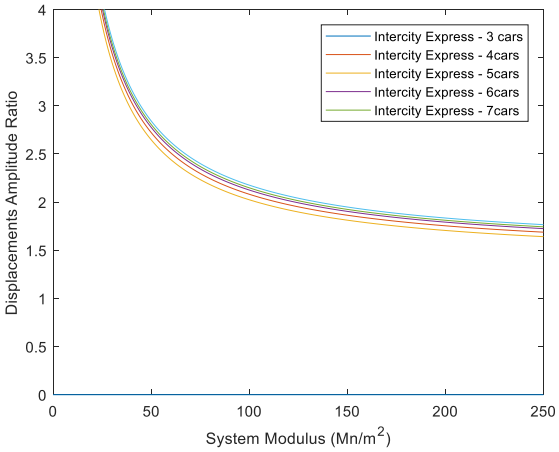

a) Intercity Express – 3 cars; b) Intercity Express (4cars); c) Intercity Express – 5 cars; d) Intercity Express – 6 cars; e) Intercity Express – 7 cars; f) CC

Calibration Curves Construction for displacement ratios – second case study (dt=500 and four times the base number bins to increase the discretization)

a)

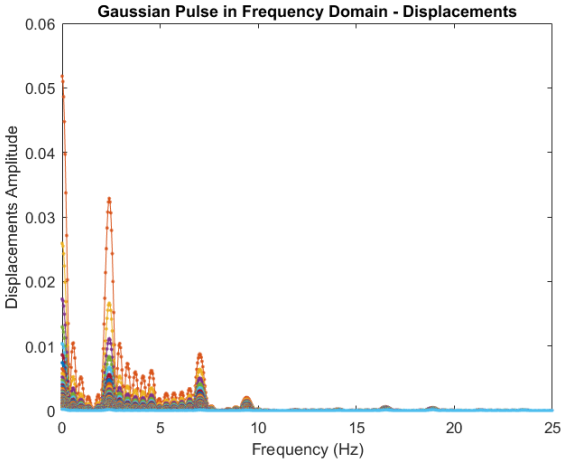

b)

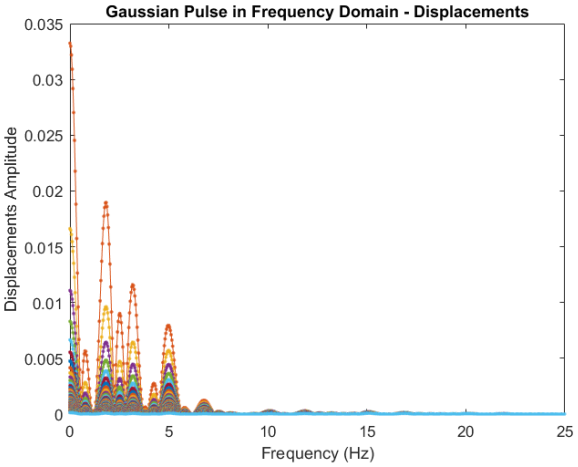

c)

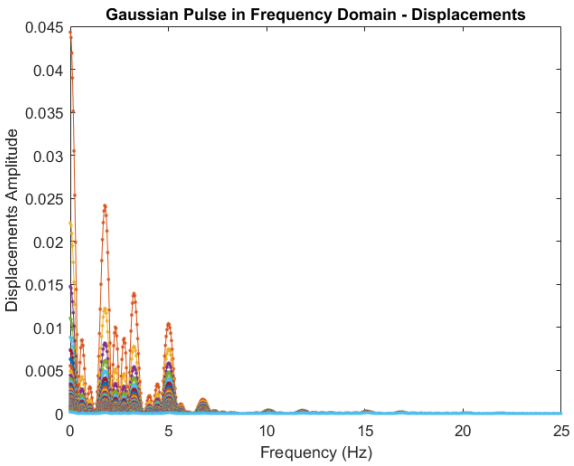

d)

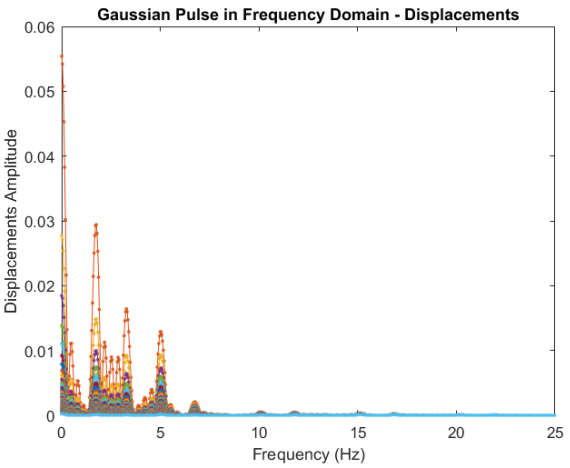

e)

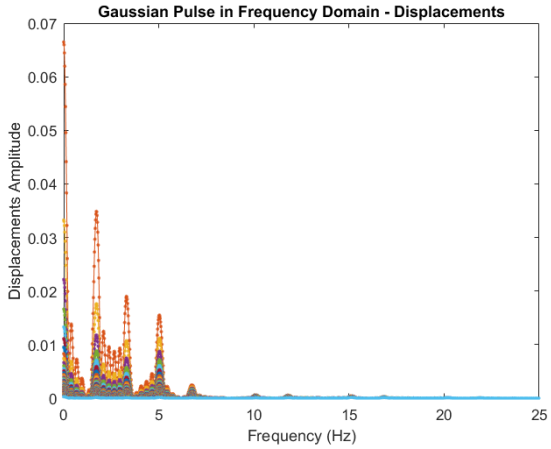

f)

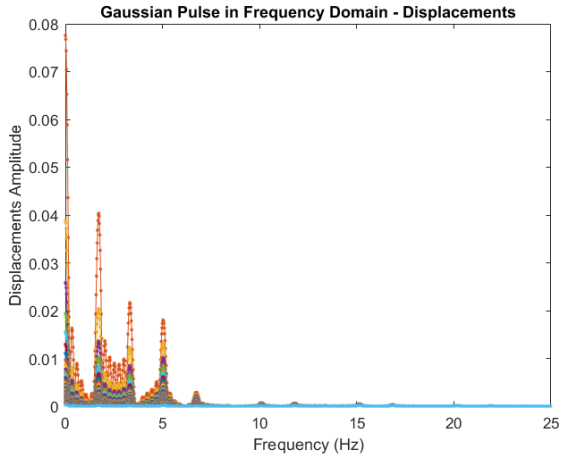

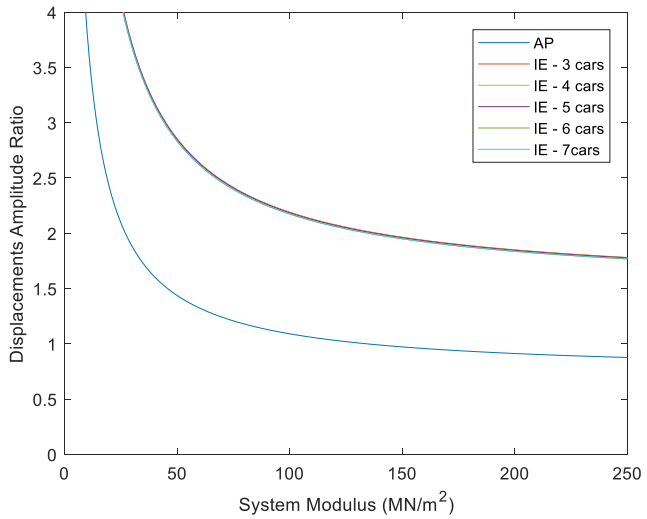

g)

a) *Alfa Pendular*; b) Intercity Express – 3 cars; c) Intercity Express (4cars); d) Intercity Express – 5 cars; e) Intercity Express – 6 cars; f) Intercity Express – 7 cars; g) CC

a) b)

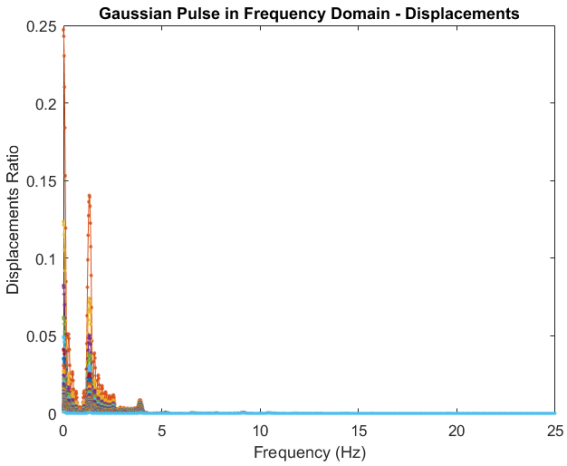

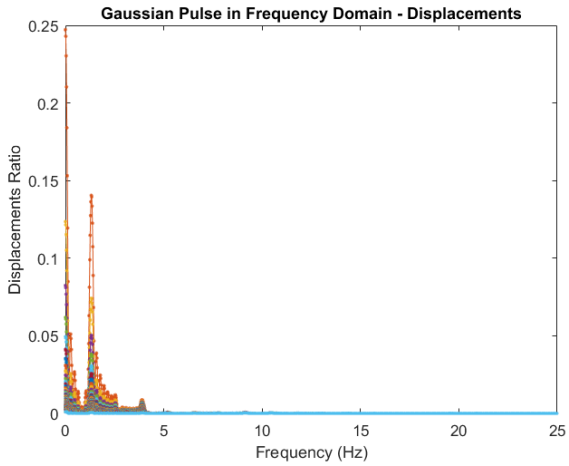

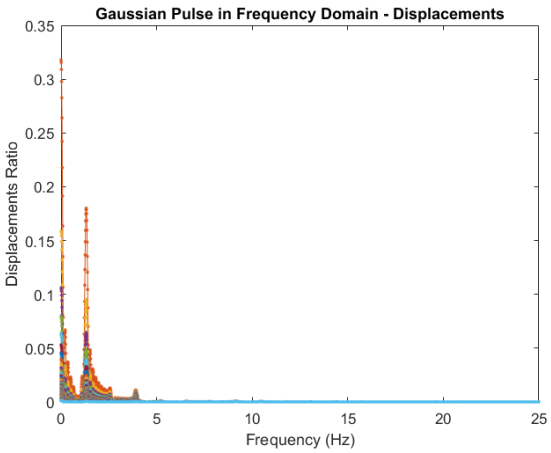

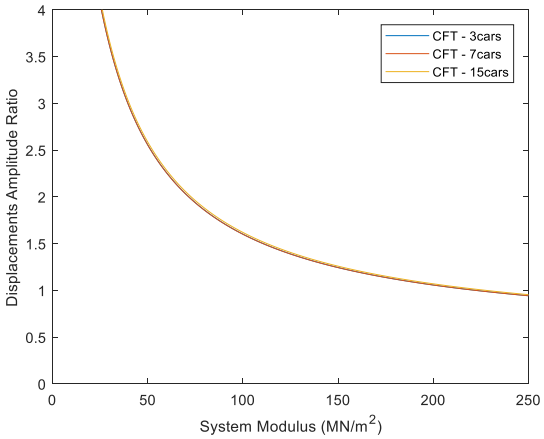

a) CFT – 3cars; b) CFT – 7cars; c) 15 cars; d) - CC

Examples of the data recorded in the second case study for different trains, please contact the author for further information

a)

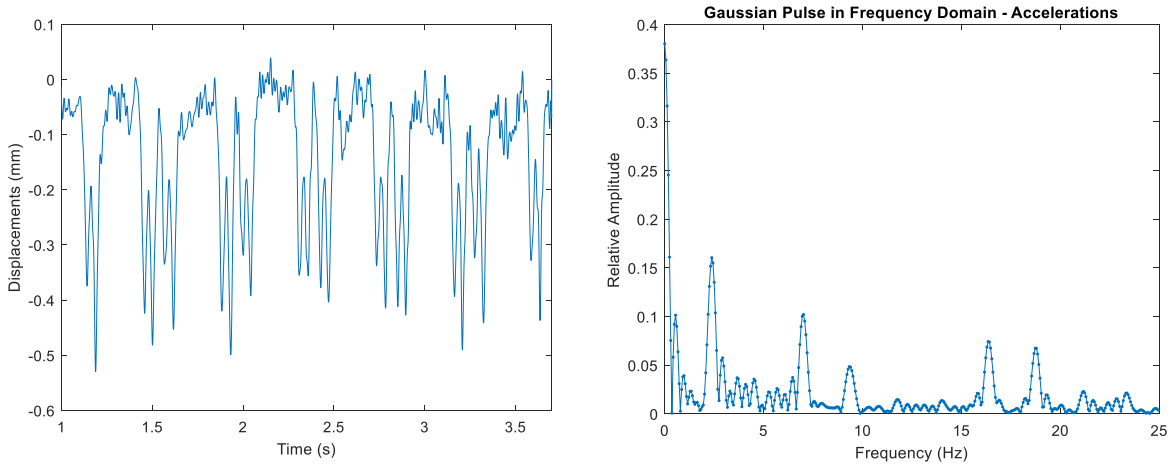

b)

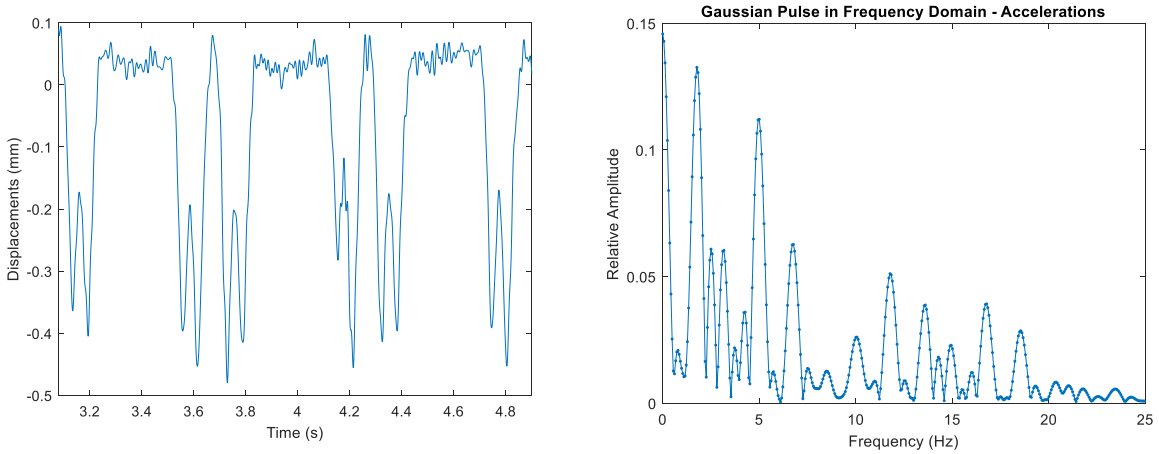

c)

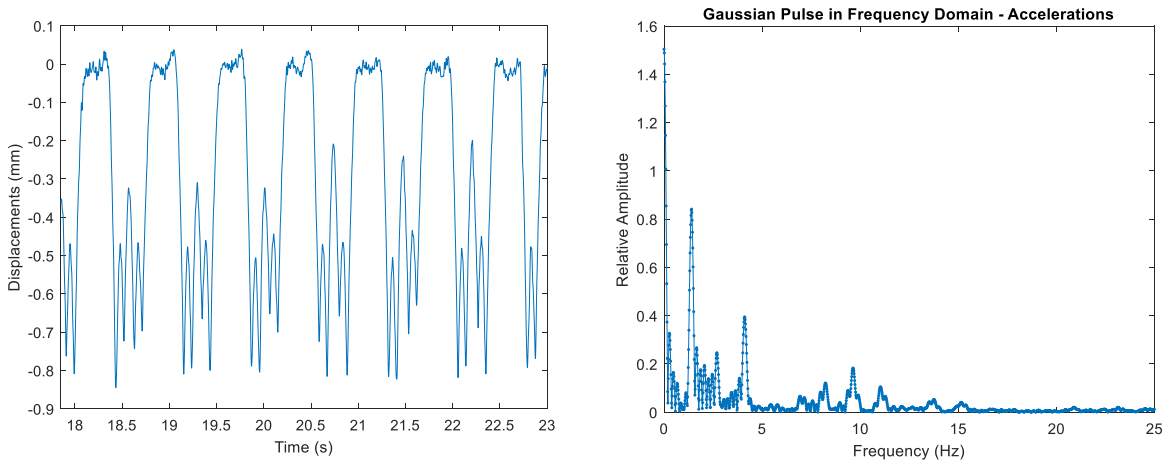

Data transformation to the frequency spectrum in UP1 a) *Alfa Pendular*; b) Intercity Express – 3 cars; c) Coal Freigth Train – 7 cars

a)

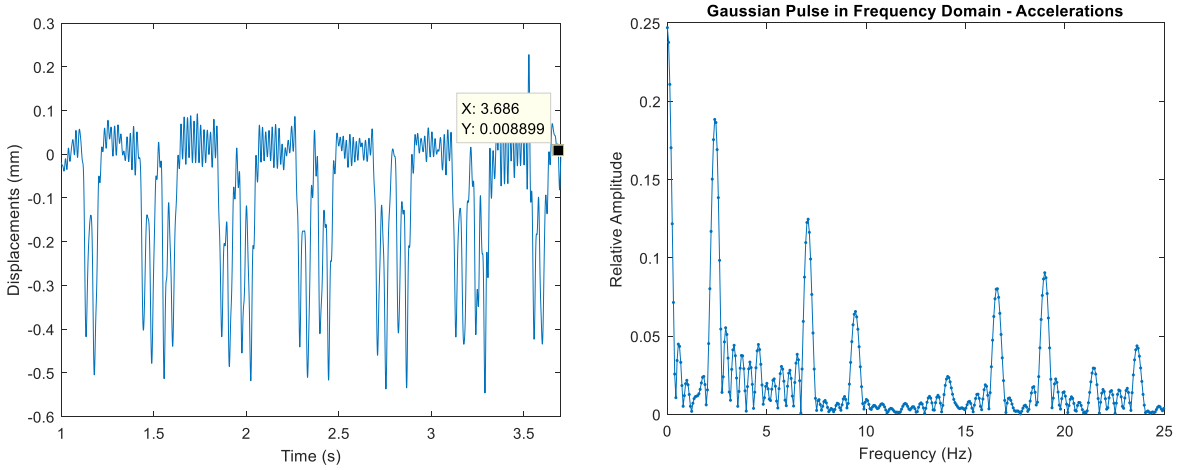

b)

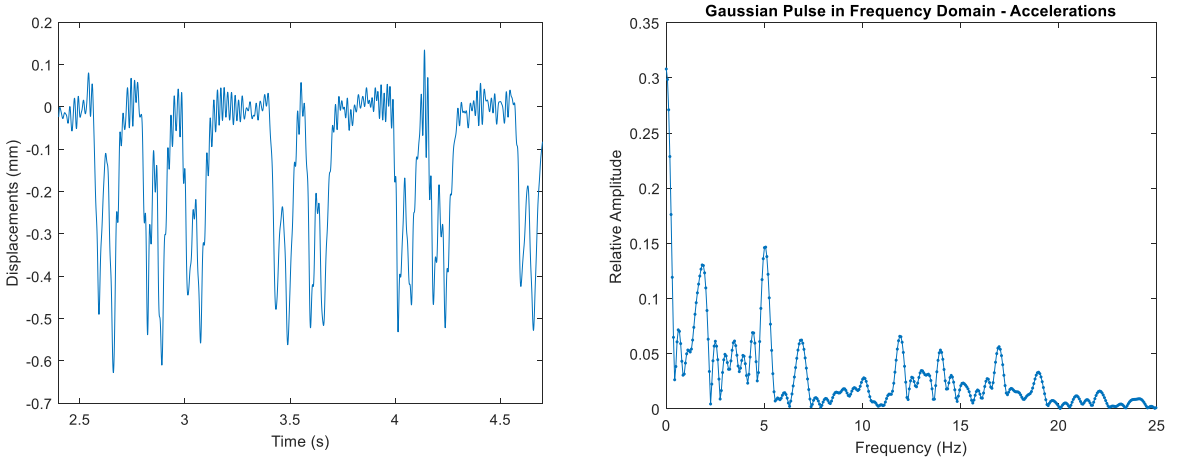

Data transformation to the frequency spectrum in UP2: a)*Alfa Pendular*; b) Intercity Express – 3 cars

Results obtained in the second study case

UP1

Alfa Pendular

***Alfa Pendular* 1**							
Site			**Harmonics**		**Interval: 3s**		**k**
	PSD	D. ratio	3rd	7th	t. min	t. max	Curves
1	PSD1D4	-	-	-	-	-	-
2	PSD1D3	1.376253298	0.1304	0.09475	1.4	4.4	55
3	PSD1D2	2.150537634	0.38	0.1767	1.4	4.4	24
4	PSD1D1	-	-	-	-	-	-
5	PSD2D2	2.345659164	0.2918	0.1244	1.5	4.5	21

***Alfa Pendular* 2**							
Site			**Harmonics**		**Interval: 3s**		**k**
		D. ratio	3rd	7th	t. min	t. max	Curves
1	PSD1D4	-	-	-	-	-	-
2	PSD1D3	1.516908213	0.1413	0.09315	0.8	3.8	45
3	PSD1D2	2.080617496	0.3639	0.1749	0.5	3.5	25
4	PSD1D1	-	-	-	-	-	-
5	PSD2D2	2.196721311	0.2546	0.1159	0.5	3.5	23

***Alfa Pendular* 5**							
Site			**Harmonics**		**Interval: 3s**		**k**
		D. ratio	3rd	7th	t. min	t. max	Curves
1	PSD1D4	1.935358255	0.2485	0.1284	1.4	4.4	29
2	PSD1D3	1.542372881	0.1911	0.1239	1	4	43
3	PSD1D2	-	-	-	-	-	-
4	PSD1D1	2.25995086	0.4599	0.2035	0.8	3.8	22
5	PSD2D2	2.320402299	0.323	0.1392	0.8	3.8	21

Alfa Pendular 3							
Site			**Harmonics**		**Interval: 3s**		**k**
		D. ratio	3rd	7th	t. min	t. max	Curves
1	PSD1D4	2	0.2412	0.1206	1.2	4.2	27
2	PSD1D3	1.380351262	0.1006	0.07288	0.7	3.7	55
3	PSD1D2	1.989665354	0.4043	0.2032	0.6	3.6	28
4	PSD1D1	2.010731053	0.2998	0.1491	0.6	3.6	27
5	PSD2D2	2.390095569	0.2751	0.1151	0.6	3.6	20

Alfa Pendular 4						
Site	**Harmonics**		**Interval: 3s**		**k**	
	D. ratio	3rd	7th	t. min	t. max	Curves
PSD1D4	1.850340136	0.2448	0.1323	0.8	3.8	31
PSD1D3	1.633363886	0.1782	0.1091	1.3	4.3	39
PSD1D2	-	-	-	-	-	-
PSD1D1	2.09106985	0.473	0.2262	1.4	4.4	25
PSD2D2	2.247058824	0.3056	0.136	1.5	4.5	23

Alfa Pendular						
Track bed System Modulus [MN/m^2]						
Distance	**Site**	**Trains**				
		1	2	3	4	5
40.5	1	-	-	29.9	34.9	32.4
14.1	2	68.8	53.8	68.8	45.4	51.0
8.7	3	26.3	27.5	31.2	-	-
1.5	4	-	-	29.9	27.5	23.9
-0.3	5	25.1	25.1	21.6	25.1	22.7

Note: In red are the results which data had considerable interferences.

Note: The hyphen appears when it was impossible to calculate the values due to major interferences.

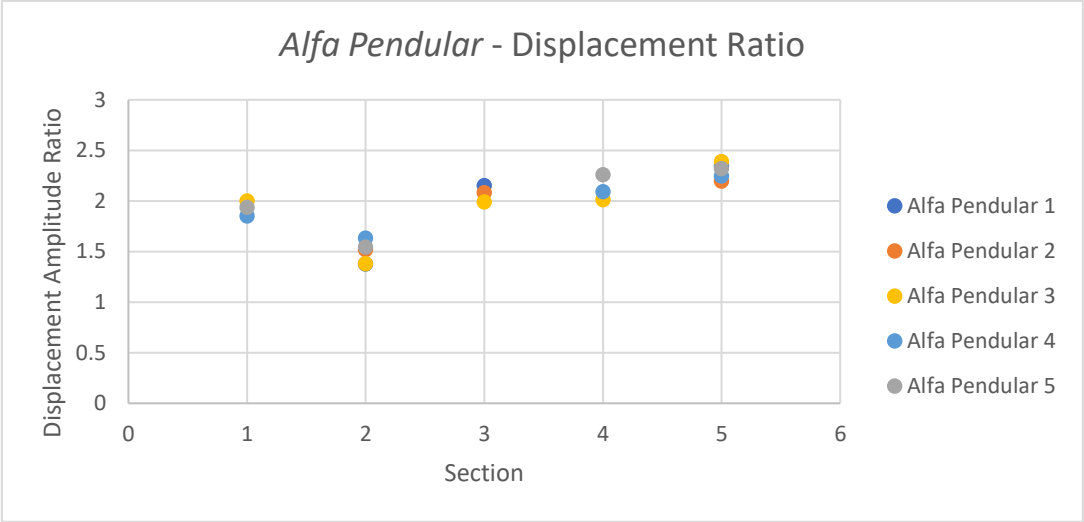
Alfa Pendular - Displacement Ratio
Displacement Amplitude Ratio
3
2.5
2
1.5
1
0.5
0
0
1
2
3
4
5
6
Section
Alfa Pendular 1
Alfa Pendular 2
Alfa Pendular 3
Alfa Pendular 4
Alfa Pendular 5

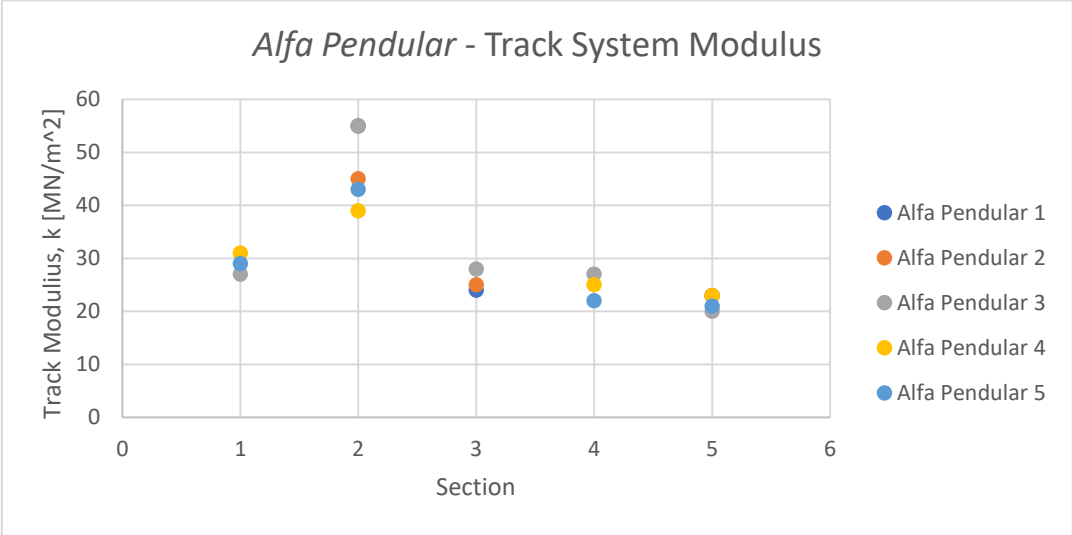
Alfa Pendular - Track System Modulus
Track Modulius, k [MN/m^2]
60
50
40
30
20
10
0
0
1
2
3
4
5
6
Section
Alfa Pendular 1
Alfa Pendular 2
Alfa Pendular 3
Alfa Pendular 4
Alfa Pendular 5

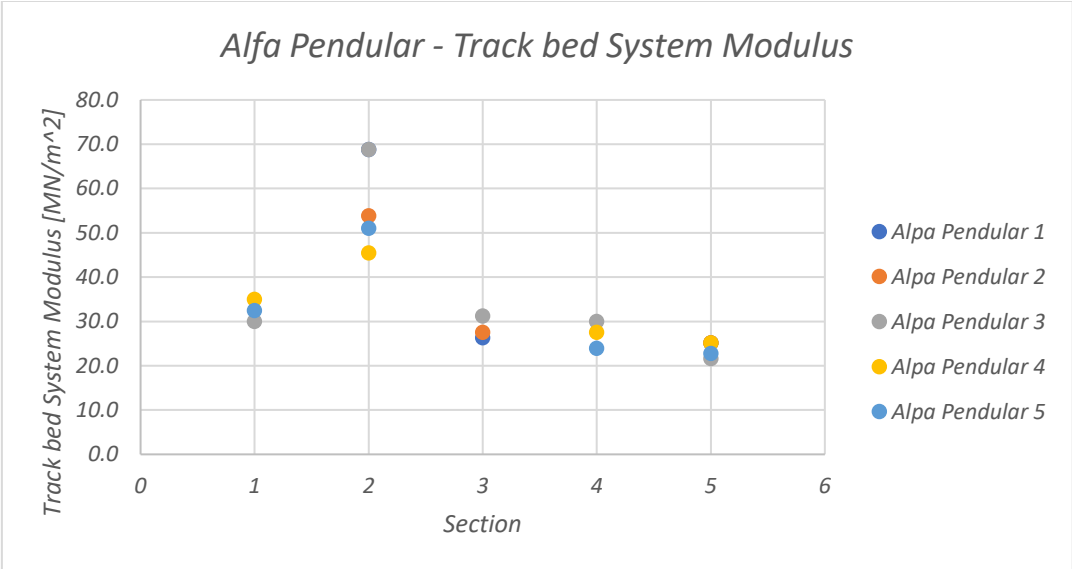
Alfa Pendular - Track bed System Modulus
Track bed System Modulus [MN/m^2]
80.0
70.0
60.0
50.0
40.0
30.0
20.0
10.0
0.0
0
1
2
3
4
5
6
Section
Alpa Pendular 1
Alpa Pendular 2
Alpa Pendular 3
Alpa Pendular 4
Alpa Pendular 5

Intercity Express

Intercity Express 1							
	3 passenger cars		Harmonics		Interval: 2s		K
Site		D. ratio	3rd	7th	t. min	t. max	Curves
1	PSD1D4	2.541755889	0.1187	0.0467	2.7	4.7	65
2	PSD1D3	1.736899963	0.0474	0.02729	3.3	5.3	*
3	PSD1D2	-	-	-	-	-	-
4	PSD1D1	-	-	-	-	-	-
5	PSD2D2	3.085176626	0.1869	0.06058	3.635	5.635	42

Intercity Express 2							
	3 passenger cars		Harmonics		Interval: 2s		K
Site		D. ratio	3rd	7th	t. min	t. max	Curves
1	PSD1D4	2.893226177	0.1764	0.06097	2.5	4.5	48
2	PSD1D3	2.168791039	0.1123	0.05178	3.07	5.07	101
3	PSD1D2	3.00170503	0.3521	0.1173	3.2	5.2	44
4	PSD1D1	2.909166667	0.3491	0.12	3.35	5.35	47
5	PSD2D2	3.161351965	0.2647	0.08373	3.4	5.4	40

Intecity Express 3							
Site	3 passenger cars		Harmonics		Interval: 2s		K
		D. ratio	3rd	7th	t. min	t. max	Curves
1	PSD1D4	2.70694752	0.1465	0.05412	4.05	6.05	56
2	PSD1D3	1.80452426	0.1045	0.05791	3.45	5.45	224
3	PSD1D2	2.61601455	0.2875	0.1099	3.32	5.32	60
4	PSD1D1	3.00271739	0.3315	0.1104	3.165	5.165	44
5	PSD2D2	3.0145787	0.244	0.08094	3.13	5.13	44

Intecity Express 4							
Site	4 passenger cars		Harmonics		Interval: 2.5s		K
		D. ratio	3rd	7th	t. min	t. max	Curves
1	PSD1D4	2.306926999	0.1855	0.08041	1.75	4.25	84
2	PSD1D3	1.799270566	0.1332	0.07403	2.35	4.85	225
3	PSD1D2	2.8438949	0.368	0.1294	2.47	4.97	50
4	PSD1D1	2.841374752	0.4299	0.1513	2.62	5.12	50
5	PSD2D2	3.014766202	0.294	0.09752	2.65	5.5	44

Intecity Express 5							
Site	5 passenger cars		Harmonics		Interval: 3.3s		k
		D. ratio	3rd	7th	t. min	t. max	Curves
1	PSD1D4	2.2354085	0.2298	0.1028	3.85	6.85	92
2	PSD1D3	1.74462309	0.1671	0.09578	3.25	6.55	*
3	PSD1D2	2.70316027	0.479	0.1772	3.125	6.425	56
4	PSD1D1	2.804511278	0.5222	0.1862	2.95	6.25	51
5	PSD2D2	3.303116147	0.3498	0.1059	2.9	6.2	37

Intecity Express 6							
Site	3 passenger cars		Harmonics		Interval: 2s		k
		D. ratio	3rd	7th	t. min	t. max	Curves
1	PSD1D4	2.748002339	0.141	0.05131	1.55	3.55	54
2	PSD1D3	2.145154805	0.1067	0.04974	2.1	4.1	105
3	PSD1D2	2.960615193	0.2849	0.09623	2.24	4.24	45
4	PSD1D1	2.860892388	0.327	0.1143	2.4	4.4	49
5	PSD2D2	3.237616655	0.2255	0.06965	2.42	4.42	38

Intecity Express 7							
Site	7 passenger cars		Harmonics		Interval: 5s		k
		D. ratio	3rd	7th	t. min	t. max	Curves
1	PSD1D4	2.659807956	0.3878	0.1458	3.32	7.62	58
2	PSD1D3	1.8832021	0.287	0.1524	2.74	7.04	176
3	PSD1D2	-	-	-	-	-	-
4	PSD1D1	2.920015308	0.763	0.2613	2.49	6.79	47
5	PSD2D2	3.046563193	0.5496	0.1804	2.45	6.75	43

Intercity Express							
Track bed System Modulus [MN/m^2]							
Site	Trains						
	1	2	3	4	5	6	7
1	85.1	58.1	70.3	120.9	138.3	67.2	73.5
2	*	159.6	*	*	*	169.9	*
3	-	52.4	76.7	61.1	70.3	53.8	-
4	-	56.7	52.4	61.1	62.6	53.8	56.7
5	49.6	46.8	52.4	52.4	42.8	59.6	51.0

Note: In red are the results which data had big interferences.

Note: The hyphen appears when it was impossible to calculate the values.

Note: * for values that get out of the range (0~250MN/m^2) or for track bed system modulus for high values of stiffness, as already explained.

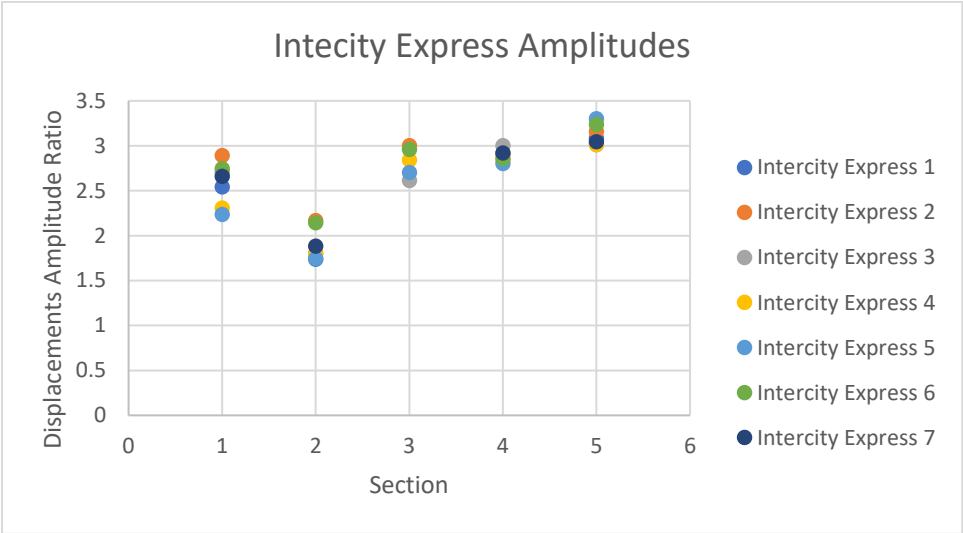

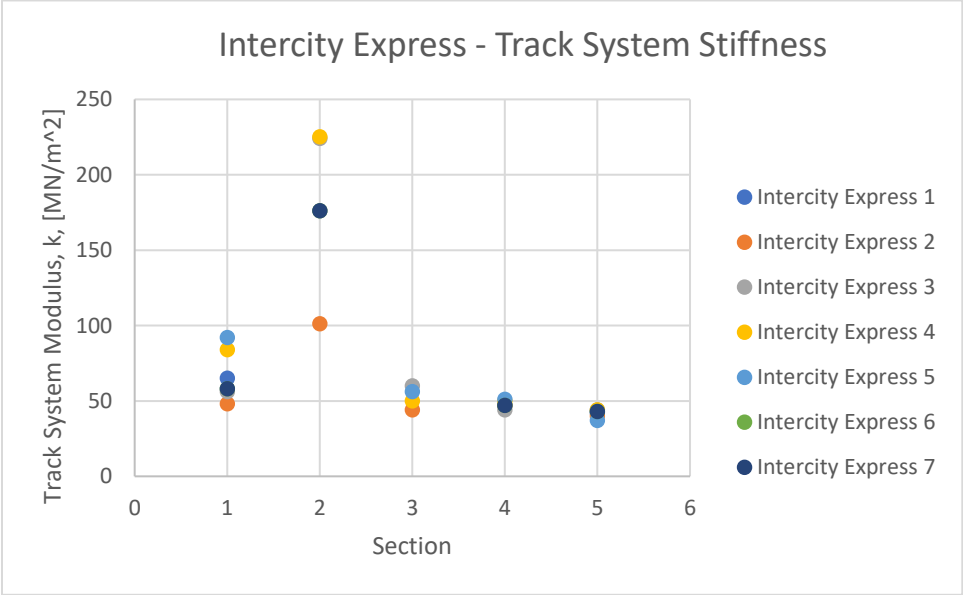

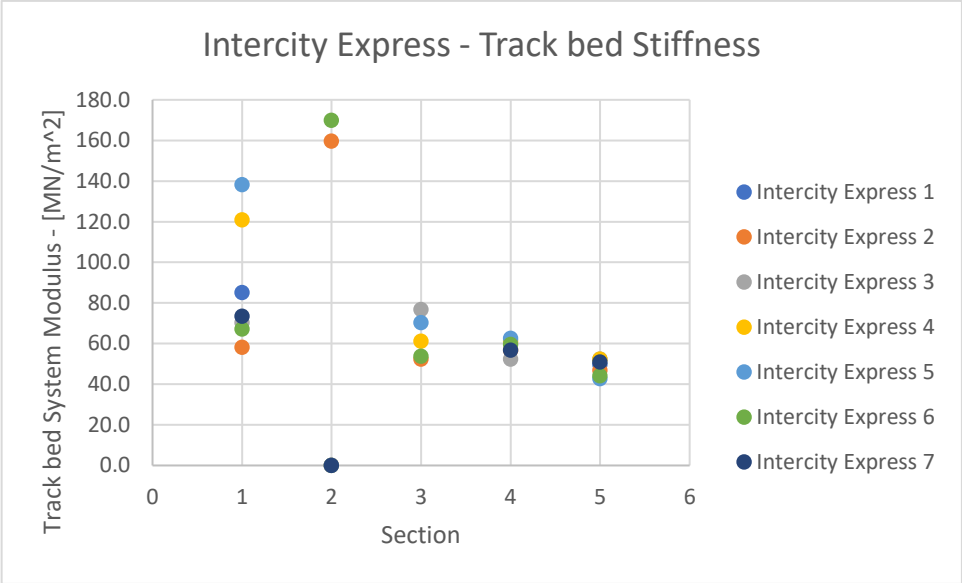

Coal Freight Trains

Coal freight Train 1							
Site	7 cars considered		Harmonics		Interval: 17.3s		k
		D. ratio	3rd	7th	t. min	t. max	Curves
1	PSD1D4	2.42745098	0.619	0.255	16.75	22.15	55
2	PSD1D3	2.164398476	0.3976	0.1837	17.86	23.26	65
3	PSD1D2	3.352752694	1.151	0.3433	18.1	23.5	34
4	PSD1D1	3.844784621	1.08	0.2809	18.4	23.8	28
5	PSD2D2	3.324579832	0.9495	0.2856	18.56	23.86	35

Coal freight Train 2							
Site	23 cars considered		Harmonics		Interval: 20s		k
		D. ratio	3rd	7th	t. min	t. max	Curves
1	PSD1D4	2.133780445	1.209	0.5666	1.1	20.1	67
2	PSD1D3	1.724659607	1.026	0.5949	2.3	21.3	92
3	PSD1D2	3.23388721	2.569	0.7944	2.54	21.54	36
4	PSD1D1	3.711120579	2.613	0.7041	2.88	21.88	30
5	PSD2D2	3.171671752	1.975	0.6227	2.95	21.95	37

Coal freight Train 3							
Site	7 cars considered		Harmonics		Interval: 4.13s		k
		D. ratio	3rd	7th	t. min	t. max	Curves
1	PSD1D4	2.544774957	0.1634	0.06421	13.65	17.78	52
2	PSD1D3	1.767554479	0.146	0.0826	12.8	16.93	88
3	PSD1D2	3.697072072	0.3283	0.0888	12.6	16.73	30
4	PSD2D2	3.365436788	0.2481	0.07372	12.3	16.43	34
5	PSD1D1	3.855225312	0.4021	0.1043	12.37	16.5	28

Coal freight Train			
Track bed System Modulus [MN/m^2]			
Site	Trains		
	1	2	3
1.0	68.8	88.6	64.1
2.0	85.1	138.3	129.4
3.0	38.8	41.4	33.7
4.0	31.2	33.7	31.2
5.0	40.1	42.8	38.8

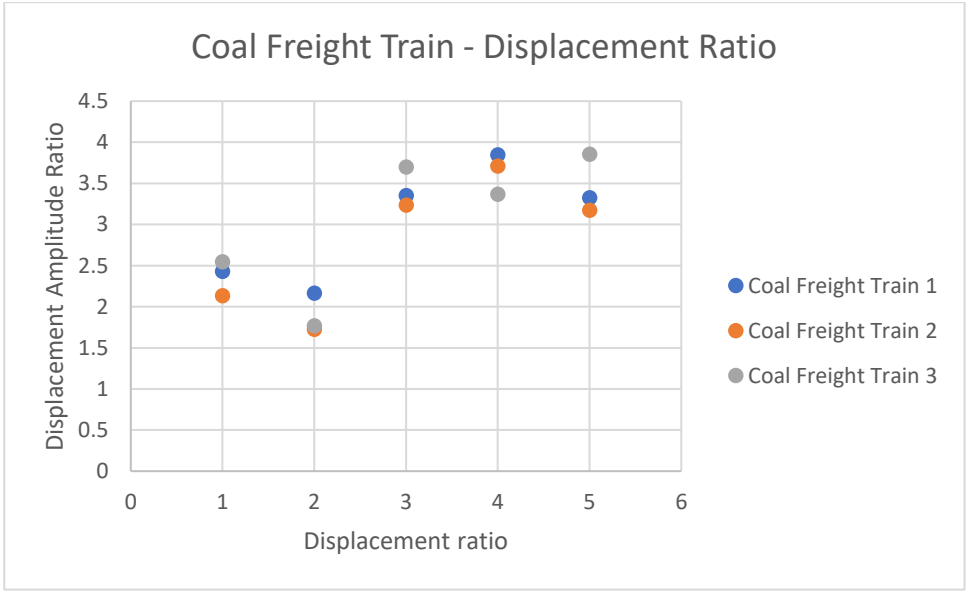

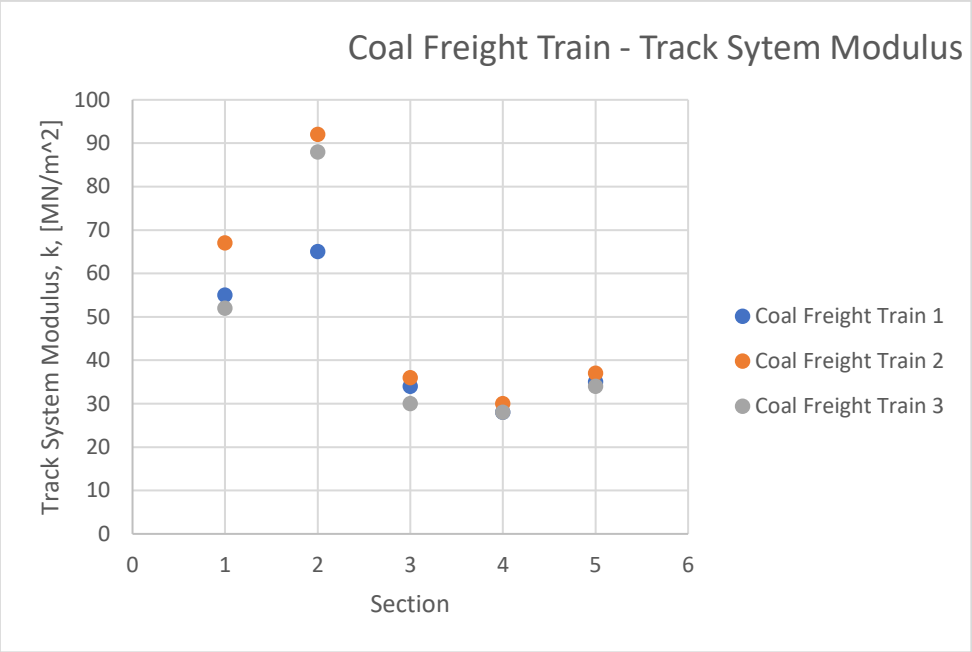
Coal Freight Train - Track Sytem Modulus
Track System Modulus, k, [MN/m^2]
100
90
80
70
60
50
40
30
20
10
0
0
1
2
3
4
5
6
Section
Coal Freight Train 1
Coal Freight Train 2
Coal Freight Train 3

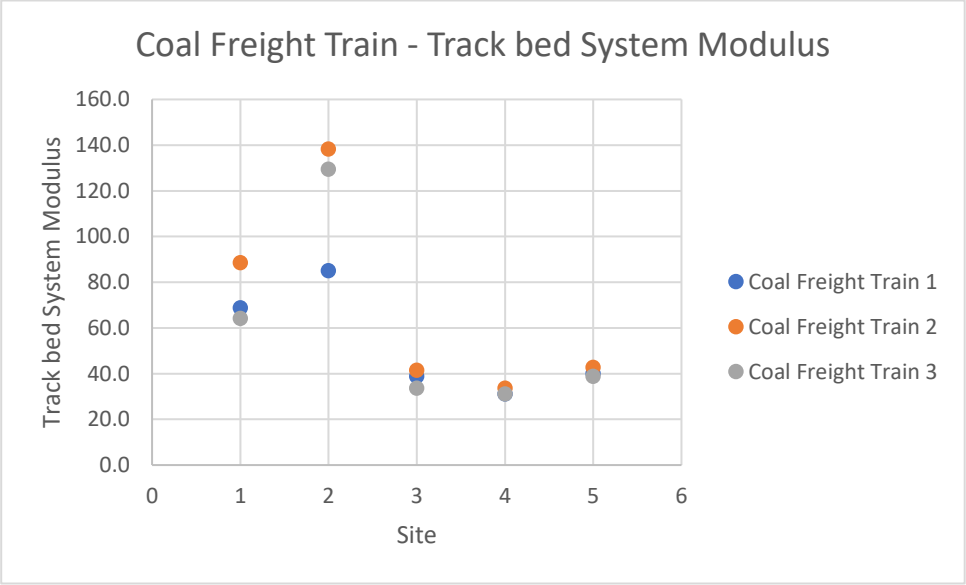
Coal Freight Train - Track bed System Modulus
Track bed System Modulus
160.0
140.0
120.0
100.0
80.0
60.0
40.0
20.0
0.0
0
1
2
3
4
5
6
Site
Coal Freight Train 1
Coal Freight Train 2
Coal Freight Train 3

UP2

Alfa Pendular

***Alfa Pendular* 1**							
Site			Harmonics		Interval: 3s		k
	PSD	D. ratio	3rd	7th	t. min	t. max	Curves
1	PSD2D2	1.937869822	0.1834	0.09464	0.3	3.3	29
2	PSD1D3	1.633710647	0.09237	0.05654	0.8	3.8	39
3	PSD1D2	1.536448598	0.1233	0.08025	1	4	44
4	PSD2D1	1.338836265	0.09894	0.0739	1	4	59
5	PSD1D1	1.271450858	0.1141	0.08974	1	4	66

***Alfa Pendular* 2**							
Site			Harmonics		Interval: 3s		ks
	PSD	D. ratio	3rd	7th	t. min	t. max	Curves
1	PSD2D2	1.955684008	0.1827	0.09342	1.5	4.5	28
2	PSD1D3	1.616056301	0.124	0.07673	1.2	4.2	40
3	PSD1D2	1.469608181	0.1279	0.08703	1.1	4.1	48
4	PSD2D1	1.218477057	0.09905	0.08129	1	4	75
5	PSD1D1	1.340229624	0.1179	0.08797	0.9	3.8	58

***Alfa Pendular* 3**							
Site			Harmonics		Interval: 3s		k
	PSD	D. ratio	3rd	7th	t. min	t. max	Curves
1	PSD2D2	2.027219175	0.1996	0.09846	1.4	4.4	27
2	PSD1D3	1.510901591	0.1282	0.08485	1	4	45
3	PSD1D2	1.574591351	0.1522	0.09666	0.8	3.8	42
4	PSD2D1	1.503879507	0.1318	0.08764	0.8	3.8	46
5	PSD1D1	1.643404345	0.1566	0.09529	0.6	3.6	38

Alfa Pendular 4							
Site			Harmonics		Interval: 3s		k
	PSD	D. ratio	3rd	7th	t. min	t. max	Curves
1	PSD2D2	1.748033462	0.14	0.08009	0.5	3.5	34
2	PSD1D3	-	-	-	-	-	-
3	PSD1D2	1.650134048	0.1231	0.0746	1	4	38
4	PSD2D1	1.252722323	0.08283	0.06612	1.1	4.1	68
5	PSD1D1	1.41356256	0.1332	0.09423	1.2	4.2	52

Alfa Pendular 5							
Site			Harmonics		Interval: 3s		k
	PSD	D. ratio	3rd	7th	t. min	t. max	Curves
1	PSD2D2	1.987724268	0.2105	0.1059	1.3	4.3	28
2	PSD1D3	-	-	-	-	-	-
3	PSD1D2	1.728462977	0.1571	0.09089	0.8	3.8	35
4	PSD2D1	1.473927902	0.1337	0.09071	0.7	3.7	48
5	PSD1D1	-	-	-	-	-	-

Note: The hyphen appears when it was impossible to calculate the values.

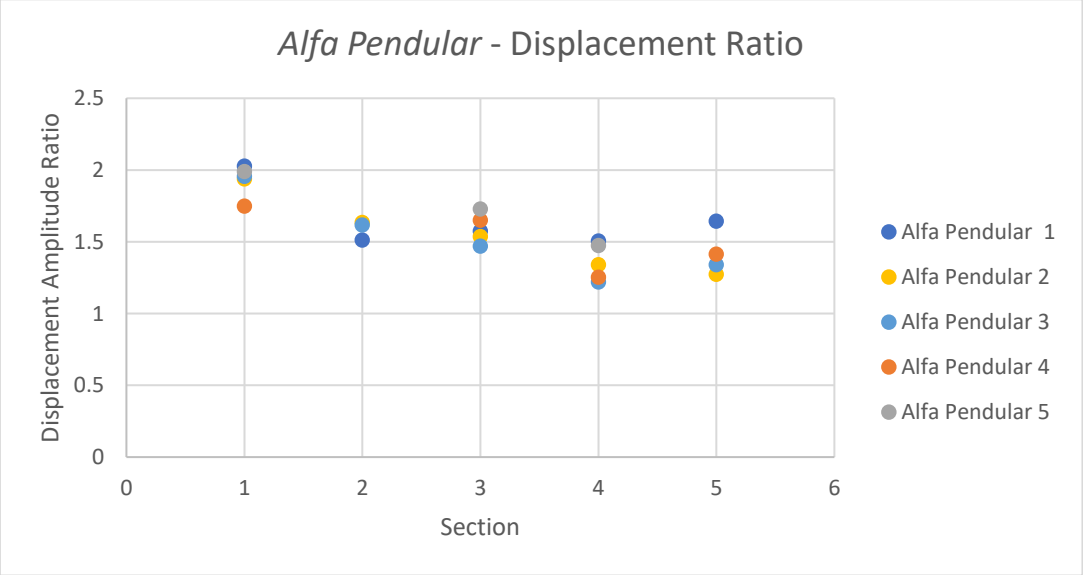

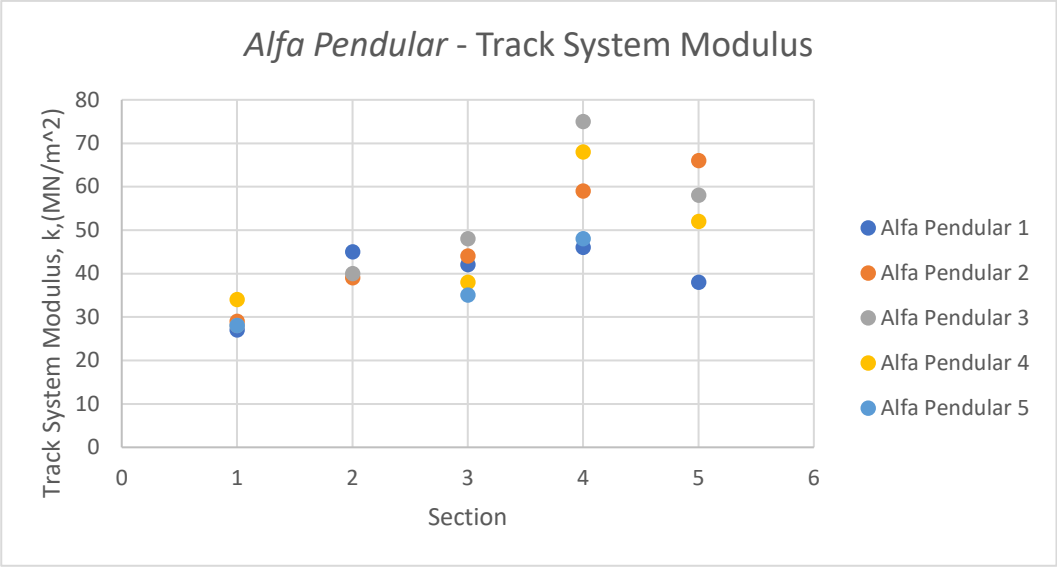

Intercity Express

Intercity Express 1							
	4 passenger cars		Harmonics		Interval: 2.5s		k
Site		D. ratio	3rd	7th	t. min	t. max	Curves
1	PSD2D2	2.344	0.162	0.069	3.3	5.8	80
2	PSD1D3	-	-	-	-	-	-
3	PSD1D2	1.999	0.120	0.060	2.55	5.05	135
4	PSD2D1	1.624	0.082	0.051	2.4	4.9	-
5	PSD1D1	1.959	0.122	0.062	2.35	4.85	150

Intercity Express 2							
	3 passenger cars		Harmonics		Interval: 2s		k
Site		D. ratio	3rd	7th	t. min	t. max	Curves
1	PSD2D2	3.165	0.143	0.045	2.26	4.26	50
2	PSD1D3	2.128	0.087	0.041	2.84	4.84	109
3	PSD1D2	2.194	0.110	0.050	2.95	3.95	98
4	PSD2D1	1.716	0.089	0.052	3.12	5.12	*
5	PSD1D1	2.024	0.108	0.054	3.15	5.15	129

Intercity Express 3							
	4 passenger cars		Harmonics		Interval: 2.5s		k
Site		D.ratio	3rd	7th	t. min	t. max	Curves
1	PSD2D2	2.630	0.183	0.070	3.6	6.1	59
2	PSD1D3	2.330	0.109	0.047	3	5.5	81
3	PSD1D2	1.683	0.101	0.060	2.85	5.35	*
4	PSD2D1	1.848	0.096	0.052	2.7	5.2	193
5	PSD1D1	1.805	0.108	0.060	2.65	5.15	220

Intercity Express 4							
	5 passenger cars		Harmonics		Interval: 3.3s		k
Site		D.ratio	3rd	7th	t. min	t. max	Curves
1	PSD2D2	2.791	0.186	0.067	1.8	5.1	52
2	PSD1D3	-	-	-	-	-	-
3	PSD1D2	1.817	0.109	0.060	2.5	5.8	212
4	PSD2D1	1.753	0.114	0.065	2.67	5.97	*
5	PSD1D1	1.782	0.127	0.071	2.7	6	*

Intercity Express 5							
	6 passenger cars		Harmonics		Interval: 3.9s		k
Site		D. ratio	3rd	7th	t. min	t. max	Curves
1	PSD2D2	2.202	0.161	0.073	3.60	7.00	96
2	PSD1D3	-	-	-	-	-	-
3	PSD1D2	1.515	0.159	0.105	2.9	6.8	*
4	PSD2D1	1.878	0.120	0.064	2.7	6.6	182
5	PSD1D1	1.913	0.158	0.082	2.71	6.61	168

Intercity Express 6							
	4 passenger cars		Harmonics		Interval: 2.5s		k
Site		D. ratio	3rd	7th	t. min	t. max	Curves
1	PSD2D2	2.526	0.111	0.044	1.50	4.00	66
2	PSD1D3	-	-	-	-	-	-
3	PSD1D2	1.749	0.104	0.059	2.24	4.74	*
4	PSD2D1	1.697	0.075	0.044	2.4	4.9	*
5	PSD1D1	1.949	0.101	0.052	2.45	4.95	150

Intercity Express 7							
	6 passenger cars		Harmonics		Interval: 3.9s		k
Site		D.ratio	3rd	7th	tmin	tmax	Curves
1	PSD2D2	2.289	0.220	0.096	3.55	7.00	86
2	PSD1D3	-	-	-	-	-	-
3	PSD1D2	2.015	0.187	0.093	2.85	6.75	131
4	PSD2D1	1.756	0.144	0.082	2.68	6.58	*
5	PSD1D1	1.987	0.182	0.092	2.68	6.58	138

Note: In red are the results which data had interferences.

Note: The hyphen appears when it was impossible to calculate the values, due to major interferences.

Note: * for values that get out of the range (0~250MN/m^2).

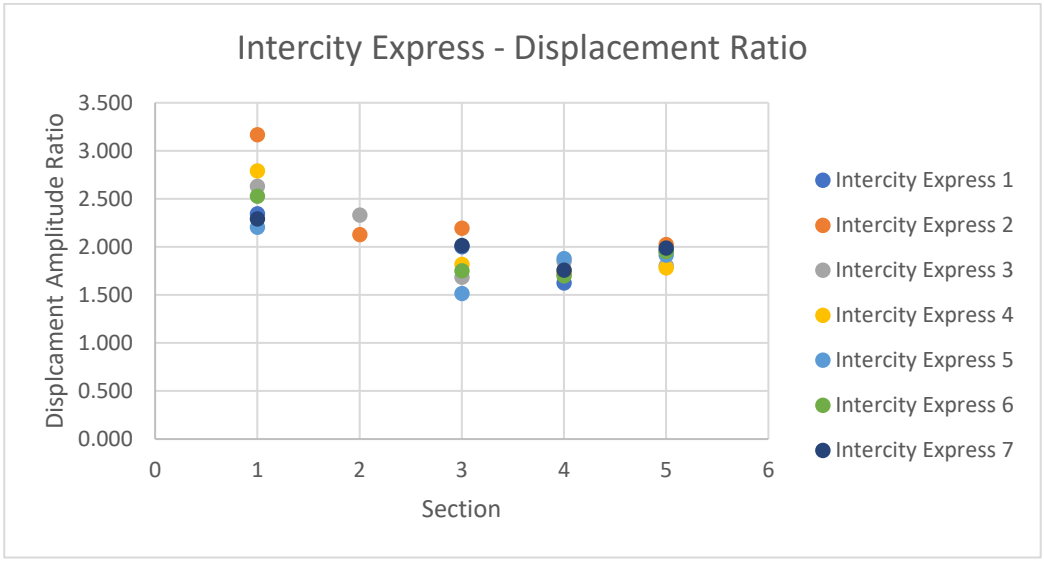

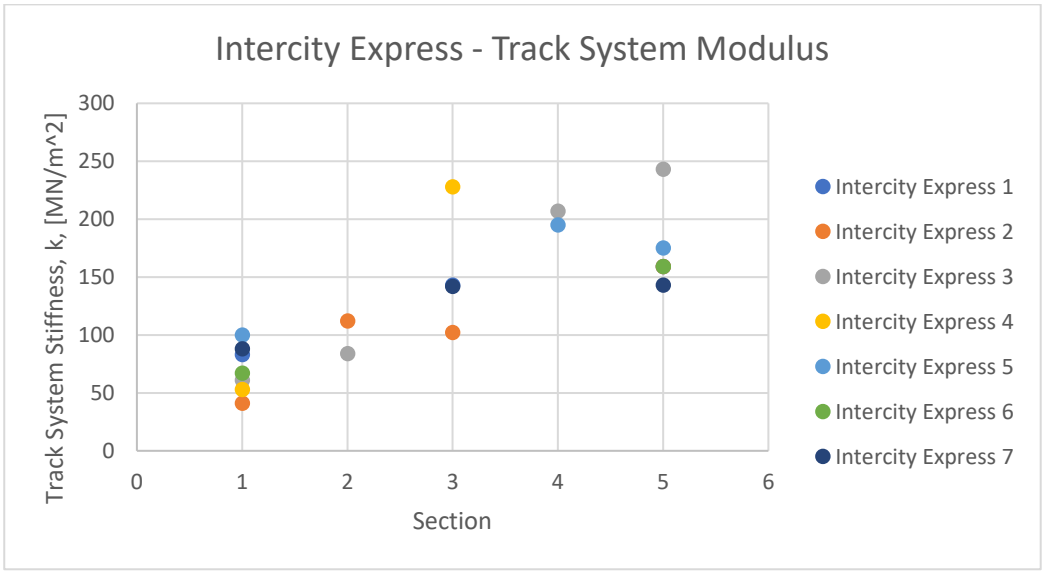

Coal Freight Train

Coal Freight Train							
		Harmonics					k
Site		D.ratio	3rd	7th	tmin	tmax	Curves
1	PSD2D2	1.77058	0.2732	0.1543	17.81	23	88
2	PSD1D3	-	-	-	-	-	-
3	PSD1D2	1.34703	0.2482	0.2492	19.16	25	136
4	PSD2D1	1.65856	0.1841	0.1841	19.46	25	98
5	PSD1D1	1.42346	0.2427	0.1705	19.54	25	123

Note: The hyphen appears when it was impossible to calculate the values, due to major interferences.

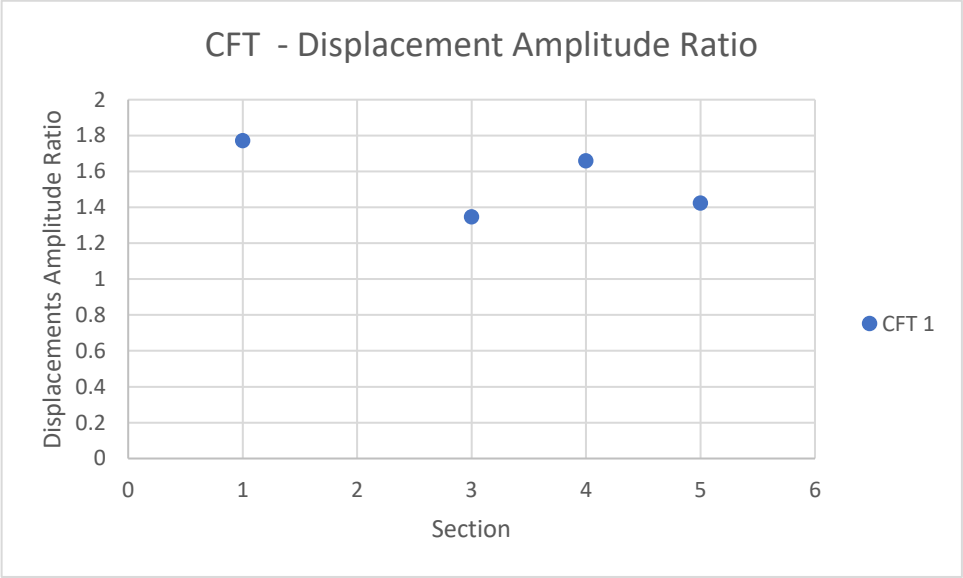

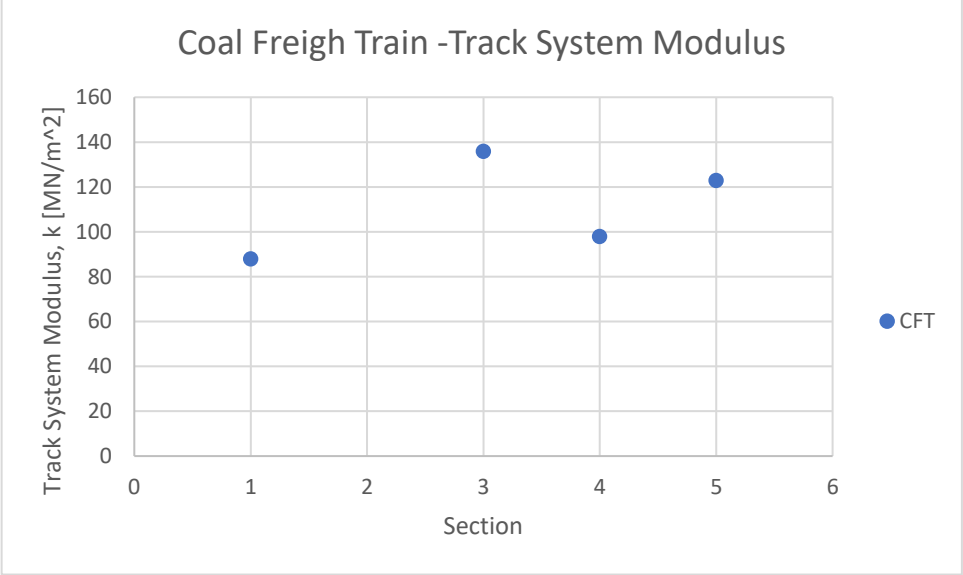

Accelerations data

a)

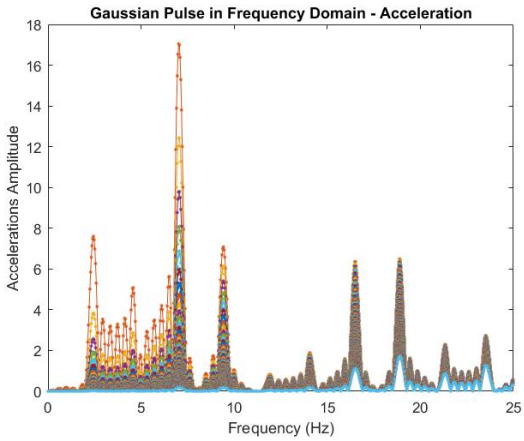

b)

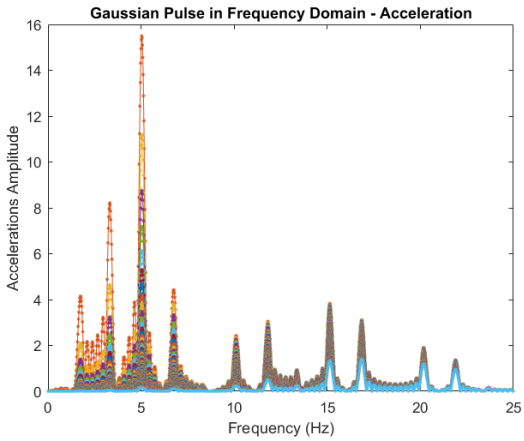

c)

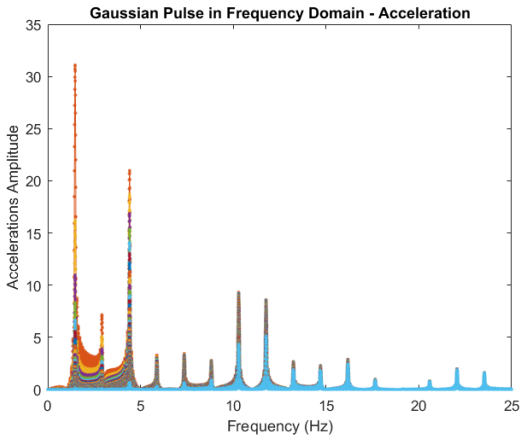

d)

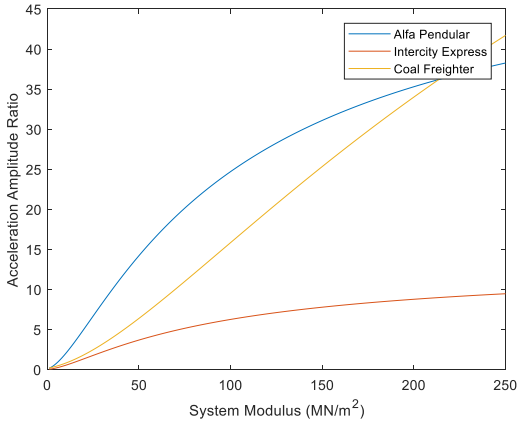

CC for acceleration data: a) AP, b) IE, c) CFT, d) CC